UNIVERSITY OF CALIFORNIA, SAN DIEGO

Population data is complex: the relationship between burst firing, spike adaptation, and attentional modulation in macaque Area V4

A dissertation submitted in partial satisfaction of the
requirements for the degree
Doctor of Philosophy

in

Neurosciences with a specialization in Computational Neuroscience

by

Emily B. Anderson

Committee in charge:

Professor John H. Reynolds, Chair
Professor Andrea Chiba, Co-Chair
Professor Karen Dobkins
Professor Massimo Scanziani
Professor Charles Stevens

2011

The dissertation of Emily B. Anderson is approved, and it is acceptable in quality and form for publication on microfilm and electronically:

_____

_____

_____

_____
Co-Chair

_____
Chair

University of California, San Diego

2011

DEDICATION

To my parents.

TABLE OF CONTENTS

LIST OF FIGURES

LIST OF ABBREVIATIONS

AHP	afterhyperpolarization
AI	Attention Modulation Index, (A-U)/(A+U)
BAI1	Burstiness Attention Index for adapted spikes
BAI2	Burstiness Attention Index for less adapted spikes
BRI	Burstiness-Refractoriness Index
FEF	Frontal Eye Fields
FRB	Fast Rhythmic Bursting neuron
FS	Fast Spiking Inhibitory neuron
IB	Intrinsically Bursting neuron
ISI	Interspike Interval
Kv7/KCNQ/M	voltage-dependent K^+ channel mediating I_M
LGN	Lateral Geniculate Nucleus
LIP	Lateral Intraparietal Area
mAHP	medium timescale afterhyperpolarization
MT	Mediotemporal area of visual cortex
MTRI	Microsaccade Triggered Response Index
NIH	National Institutes of Health
postISI	time between a spike and the subsequent spike
preISI	preceding interspike interval
RF	Receptive Field
RS	Regular Spiking neuron
TEO	cytoarchitectonic area TEO
	in posterior inferior temporal cortex

ACKNOWLEDGEMENTS

Chapter 2, in full, is a reprint of the following article in press: Emily B. Anderson, Jude F. Mitchell, John H. Reynolds (2011) Attentional modulation of firing rate varies with burstiness across putative pyramidal neurons in macaque visual Area V4. Journal of Neuroscience, *in press*. The article was reformatted to meet the style requirements for inclusion in the dissertation. The dissertation author was the principle researcher and author of this work.

Some of the material presented in Chapters 3 and 4 may be prepared for submission for publication. Anderson EB, Mitchell JF, Reynolds JH. The dissertation author was the primary investigator and author of this material.

In addition, I would like to express my gratitude to the many people who have supported me throughout my graduate career, both personally and scientifically. In particular, I would like to acknowledge my advisor, John Reynolds, and the members of the Reynolds lab, past and present, for their guidance and enthusiasm. I would also like to acknowledge the important role played by Jude Mitchell, who played a critical role in my scientific development and training, and on a personal level has proved a reliable friend. Jude Mitchell and Kristy Sundberg also helped with data collection for the work presented here. I would also like to thank Katie Williams for her very personal investment in the care of our animal colony, and to acknowledge the very professional support that has been provided by Jaclyn Reyes and members of the Salk Institute animal resources and facility services departments. I would also like to mention my appreciation for the excellent support provided by the UCSD Neurosciences graduate program coordinators, especially Christa Ludeking, which I believe has resulted in an unusually well run graduate program.

Finally, I would like acknowledge the UCSD Neurosciences graduate program for providing an unusually supportive, collegial, and exciting scientific environment. I owe a great deal of my scientific and personal development from interactions with the students, scientific staff, and faculty within the program. In particular, I would especially like to acknowledge the members of my dissertation committee, the members of the Callaway, Chiba, Krauzlis, and Senjowski laboratories, Lee Lovejoy, and my many classmates. During my stay here in San Diego,

I have forged many friendships through the Neurosciences graduate program, the mathematics department ultimate frisbee club, the UCSD archery club, the Okinawa computational neuroscience course, and craft night. These friendships have supported me through many difficult times. I would like to give a special shout out to Corinne Teeter, Claire Discenza, Jude Mitchell, Felice Friedman, and Nicholas Reid Wall.

And lastly, but most importantly, I would like to thank Nick and my entire family for their continuous support, trust, and general awesomeness.

VITA

2002	Diplôme d'Etudes Françaises, Second Degrée (Advanced French Studies) Université Stendhal, Grenoble, France
2002	Diplôme d'Etudes en Langue Françaises (French National Language Diploma)
2003	National Science Foundation Undergraduate Research Fellow Cold Spring Harbor Laboratory, New York
2004	B.A. in Biocomputation *with Honors* Grinnell College, Iowa
2004-2006	National Science Foundation Integrative Graduate Education and Research Traineeship Program (IGERT) Fellow
2006-2009	National Science Foundation Graduate Research Fellow
2011	Ph.D. in Neurosciences *with a specialization in Computational Neuroscience* University of California, San Diego

PUBLICATIONS

Emily B. Anderson, Jude F. Mitchell, John H. Reynolds (2011) Attentional modulation of firing rate varies with burstiness across putative pyramidal neurons in macaque visual Area V4. Journal of Neuroscience, *in press*.

David B. Anderson, Emily B. Anderson, Barry Perlman (2007) Voice-operated two-way asynchronous radio. Assignee: Mitsubishi Electric Research Laboratories, Inc. US Patent 7,158,499.

David B. Anderson, Emily B. Anderson, Neal Lesh, Joe Marks, Brian Mirtich, David Ratajczak, Kathy Ryall (2000) Human-guided simple search. Proceedings of AAAI 2000, Austin, Texas.

David B. Anderson, Emily B. Anderson, Neal Lesh, Joe Marks, Ken Perlin, David Ratajczak, Kathy Ryall (1999) Human-guided greedy search: combining information visualization and heuristic search. Workshop on New Paradigms in Information Visualization and Manipulation 1999:21-25.

ABSTRACT OF THE DISSERTATION

Population data is complex: the relationship between burst firing, spike adaptation, and attentional modulation in macaque Area V4

by

Emily B. Anderson

Doctor of Philosophy in Neurosciences with a specialization in Computational Neuroscience

University of California, San Diego, 2011

Professor John H. Reynolds, Chair
Professor Andrea Chiba, Co-Chair

Distinguishing between different neural cell classes can provide value insight into circuit mechanisms, but remains a challenge in extracellular recordings. One approach has been to characterize differences in the physiological properties of identified neuronal cell types, and then apply these physiological distinctions towards inferring neuronal identity in extracellular recordings. For example, intracellular studies have shown that the ability to fire action potentials of short duration is restricted to classes of neurons that express specific ion channels. This difference in action potential shape has allowed numerous studies to distinguish between narrow spiking (putative interneurons) and broad spiking (putative pyra-

midal) neurons.

Here, I extend this approach by considering how burst firing and spike adaptation can provide additional insight into neural identity, and use these metrics to account for heterogeneity in the electrophysiological correlates of attention across individual neurons in macaque Area V4. I begin by characterizing spike amplitude, duration, and frequency adaptation. I find that when I divide the population into broad and narrow spiking groups, there is significantly greater action potential amplitude and frequency adaptation among broad spiking neurons. This finding provides further validation of the use of spike waveform duration as a method to distinguish between cortical cell classes, and as discussed in the final chapter, may provide a glimpse into the depolarization state of neurons across different attention conditions.

In addition to characterizing spike adaptation, I characterize the burst spiking behavior of V4 neurons. I find that burstiness varies considerably across the population, but did not find evidence for distinct classes of burst behavior. Burstiness did, however, vary more widely across the class of neurons that show the greatest heterogeneity in attentional modulation, and within that class, burstiness helped account for differences in attentional modulation. Among these broad spiking neurons, rate modulation was largely restricted to bursty neurons, which as a group showed a highly significant increase in firing rate with attention. Further work will need to determine whether this relationship between attentional modulation and burstiness reflects a difference in the intrinsic excitability of these neurons or whether it reflects differences in the inputs they receive.

Chapter 1

Introduction

The nervous system is a network of neurons that direct behavior in response to sensory signals about the local environment and the internal state of an animal. As an animal interacts with the environment, it must decide which signals are best suited to govern its behavior. In many cases, it may prove advantageous for the animal to devote a greater percentage of resources to processing these selected signals[1]. Loosely defined, attention compromises both the selection of a sensory signal as behaviorally-relevant, as well as the subsequent privileged processing that can increase the speed and accuracy of perceptual decisions.

1.1 Neuron identification

Most electrophysiological studies of "high-level" cognitive processes such as attention are descriptive in nature. Typically, these studies manipulate the stimulus conditions or behavioral state of an animal, and then correlate these manipulations with changes in the firing patterns of a subset of individual, unidentified

[1]Since we are talking about biological systems, it almost goes without saying that there are strong evolutionary constraints on the processing strategies and resources devoted to perceptual processing and decision making. Perhaps the most important constraint is the need for the animal to be able to respond rapidly to changes in the environment. Other factors, such as the high metabolic cost of neuronal signaling (thought to favor sparse neuronal codes), the metabolic cost of neuronal maintenance and development, and (for humans) the size of the human birth canal, are also thought to provide important constraints on the number of individual neurons, connectivity, and processing strategies. For a review of some of these constraints and their consequences, see Sejnowski and Laughlin (2003).

neurons in a particular brain region. Ultimately, to understand how manipulations of stimuli or changes in neural firing patterns influence perception and behavior, we will need to link changes in the firing patterns of individual neurons to the larger context of how information "flows" through processing loops throughout the entire organism. An important component of this effort will be to identify the participants in these circuits, and to link changes in signaling patterns to specific participants.

A primary goal of this dissertation is to take an incremental step towards linking description of electrophysiological changes with attentional state to understanding mechanisms within circuits. Many of the challenges we face in linking circuit mechanisms with "high-level" cognitive states are technical; robust behavioral control requires months or even years of behavioral training of primate subjects, while most methods used to study circuit mechanisms are in their infancy or remain acute preparations. Here, the main approach will be to use under-appreciated aspects of the available electrophysiological signals (e.g., waveform shape, spiking statistics) to infer the identity of individual neurons recorded during an attention-dependent tracking task. In particular, I will use the shape of the action potentials of individual neurons in cortical area V4 to divide neurons into two superclasses of neurons: narrow spiking neurons, which are largely comprised of fast-spiking (FS) inhibitory interneurons, and broad spiking neurons, which include most pyramidal neurons and some interneuron classes.

There is substantial evidence in support of dividing neurons into different classes based on action potential waveform shape. Studies in brain slices, intracellular studies in vivo, and extracellular studies in several mammalian species including the macaque have found that narrow and broad spiking neurons represent distinct groups of neurons. Intracellular studies have demonstrated that the ability to fire action potentials of short duration is restricted to classes of neurons that express specific ion channels, including in particular the Kv3 class of potassium channel (for reviews, see Rudy and McBain, 2001, and Bean, 2007).[2] It has also

[2]There are a great deal of differences in the expression of ion channels among different neuronal classes. Some of these differences are discussed in more detail in Chapter 3. One difference of interest in the context of this dissertation is the evidence for differences in the ion channel expression that are thought to contribute to burst firing in intrinsically bursting neurons (which

been shown that the duration of the extracellular spike waveform is directly related to the duration of the intracellular waveform (Henze et al., 2000; Gonzàlez-Burgos et al., 2005; Gold et al., 2006). This relationship between extracellular waveform duration and ion channel expression has allowed an extensive number of extracellular studies to draw conclusions regarding the differences in neuronal activity across these two classes of cortical neurons. In recent years, researchers studying brain activity in the awake non-human primate have increasingly begun to apply this technique, and in several cases have observed important differences between these classes (Constantinidis and Goldman-Rakic, 2002; Mitchell, et al., 2007; Chen et al., 2008; Cohen et al., 2008; Diester and Nieder, 2008; Hussar and Pasternak, 2009; Johnston et al., 2009; Kaufman et al., 2010; Reimer and Hatsopoulous 2010; Song and McPeek 2010; Yokoi and Komatsu, 2010).

Although it is important to acknowledge that broad and narrow spiking neurons can be further subdivided into subclasses, they clearly represent different populations of neurons. In the data presented within this dissertation, I find a clearly bimodal distribution of spike waveform duration (see Figure 2.3), indicating that I can divide my population of neurons into these groups. Previously, members within my dissertation laboratory have documented differences in attentional modulation between the broad and narrow spiking neurons (Mitchell et al., 2007), as well as differences in their mean firing rates. In **chapter 3**, I will provide further evidence in support of this distinction, by comparing spike height, duration, and frequency adaptation across narrow and broad spiking neurons. I will then show that the differences in adaptation between these classes is consistent with the hypothesis that most narrow spiking neurons correspond to FS interneurons, and suggest a refinement of our classification based on these adaptation metrics. In **chapter 2**, I will extend this spike waveform classification by considering burst firing. First, I will describe differences in the burstiness of broad and narrow spiking neurons. I will then expand on the differences in attentional modulation between narrow and broad spiking neurons reported by Mitchell et al. (2007), by showing that the relationship between burst firing and attentional modulation differs

have broad action potentials) and chattering neurons (which have narrow action potentials), as reviewed by Krahe and Gabbiani, 2004.

between these two neuronal classes.

1.2 Evidence of a role for V4 in spatially-selective visual attention

This dissertation attempts to link electrophysiological correlates of attention with circuit mechanisms. The data used in this effort was obtained from single-unit electrophysiological recordings from neurons located with macaque Area V4.

Area V4 is a region in the primate occipital cortex located within and adjacent to the prelunate gyrus (Gattass et al. 1988, 2005). Anatomically, Area V4 seems well positioned to integrate information regarding the visual scene with information regarding salience and behavioral relevance. The region receives extensive feedforward visual inputs from primary and secondary visual cortex (V1 and V2), and also receives visual inputs from the LGN, MT, TEO, and area V3 (Weller et al., 2002; Ungerleider et al., 2008). Area V4 also has reciprocal connections with structures thought to have a role in attentive processes, including FEF, LIP, and the pulvinar, and sends projections to the superior colliculus (Weller et al., 2002; Ungerleider et al., 2008). Interestingly from the standpoint of spatially-selective visual attention, all of these regions have been shown to possess some degree of retinotopic organization. In addition, Area V4 also receives input from areas of the brain that are thought to be involved in arousal, behavioral state, and assessing the valence of stimuli, including the basal amygdala, dorsal raphe, locus coeruleus, and the basal forebrain (Weller et al., 2002).

Neurons within area V4 have been proposed to play an important role in processing the color (Zeki, 1973) and form (especially contours, Pasupathy and Connor, 1999) of visual stimuli (Kobatake and Tanaka, 1994; Conway et al., 2007; Tanigawa et al., 2010). New evidence suggests that the processing of these features within area V4 is largely segregated into intermingled regions of color and form selectivity (Conway et al., 2007; Tanigawa et al., 2010). In addition to its role in visual processing, V4 is thought to play a pivotal role in attending to spatial

locations (Moran and Desimone, 1985), visual features (McAdams and Maunsell, 2000), and visual objects (reviewed by Reynolds and Chelazzi, 2004; Bisley, 2011). In the remainder of this section, I will review the two main lines of evidence in support for a role of Area V4 in spatially-selective visual attention.

1.2.1 Neural correlates

In Principles of Psychology (1890), William James famously wrote:

> Everyone knows what attention is. It is the taking possession by the mind, in clear and vivid form, of one out of what seem several simultaneously possible objects or trains of thought. Focalization, concentration, of consciousness are of its essence. It implies withdrawal from some things in order to deal effectively with others...

Despite the fact that "everybody knows what attention is", attention has often been difficult to rigorously define in a scientific setting. Many researchers resort to an operational definition of attention, where attention is defined as a behaviorally-induced state, usually corresponding to a reduction in response times or improvements in accuracy. A typical experimental paradigm is the spatial-cueing task, where subjects are instructed to fixate a central fixation point while voluntarily and covertly attending to a region of space defined by a brief visual cue. After the cue is extinguished, subjects perform a detection or discrimination task on a target stimulus. A large body of human psychophysical literature has demonstrated that when subjects are directed to attend to the target, their performance dramatically improves compared to when they are instructed to attend to a different location.

Currently, the gold standard for investigating the neural mechanisms of attention is to record from single-units in attentionally-modulated visual areas (such as macaque Area V4) while a non-human primate simultaneously performs an attention-demanding task. The neural activity is then correlated with the behavioral state of the animal. Typically, when an animal is instructed to attend towards an individual neuron's receptive field (RF), the firing rate of the neuron increases. The degree of this increase can depend on many variables, including

the difficulty of the task performed and the specific visual features of the stimuli presented.

A major hypothesis within the field is that this increase in firing rate with attention enhances visual processing, and that this enhancement in turn allows subjects to improve their behavioral performance. McAdams and Maunsell (1999) demonstrated that the increase in firing rate in V4 improves the discriminability of the signals carried by individual neurons. To show this, they estimated the minimum orientation difference that would allow an ideal observer to distinguish between the neural responses elicited by two different stimuli. One method they used to calculate this threshold was to use a d' measure based on the difference in the orientation tuning curves and response variability between the two attention conditions. They found that the orientation difference required was smaller when the animal attended to a stimulus then when the animal attend away from the stimulus. In this model, improvement with attention was enhanced when individual neurons were pooled.

In addition to increases in firing rate, our laboratory recently found that directing attention to a stimulus can also reduce the response variability of individual neurons, as measured by the Fano factor across trials (Mitchell et al., 2007). Further, Mitchell et al. (2009) and Cohen and Maunsell (2009) have shown that directing attention towards the receptive field can reduce correlated activity shared among nearby neurons. This reduction in correlated activity and increase in the reliability of individual neurons could potentially have an even bigger impact on signal quality than increases in firing rate.

Despite the evidence for attention-depdendent improvements in signal quality in Area V4, it is unclear whether this improvement in signal quality underlies attention-dependent improvements in behavior. Probably the best evidence in support of this relationship comes from a recent study Cohen and Maunsell (2010). They found that fluctuations in the population response of simultaneously recorded V4 neurons could be used (via a method analogous with choice probability) to predict performance on a trial-to-trial basis.

In addition to the evidence for attention-dependent improvements in signal quality and is potential causal role in improvements in perceptual judgements

with attention, several electrophysiological studies studies implicate Area V4 in competitive processes involved in the attentional selection of stimuli (Reynolds and Chelazzi, 2004; Reynolds and Heeger, 2009). In one such study, Reynolds et al. (1999) compared the response of V4 neurons to pairs of stimuli in the RF when attention was directed away from the RF to the response when attention was directed to one of the two stimuli. When attention was directed away from the RF, the responses of neurons to the pair was similar to the weighted average of the responses to the individual stimuli. However, when the animal was instructed to attend to one of the two stimuli, the responses of these neurons shifted towards the response elicited when the attended stimulus was presented alone. Recent work by Sundberg et al. (2009) suggests that attention-dependent modulation of V4 center-surround interactions plays a role in this competitive selection.

1.2.2 Lesions of Area V4

One of the limitations of the Cohen and Maunsell study is that it is correlative in nature. The changes they report in V4 might, in principle, simply be an epiphenomenon resulting from activation in other areas, such as the frontal eye fields (FEF), that project to V4. The improvement in behavior at an attended location might depend on activity in these other areas, without involvement of V4.

The strongest line of evidence against such an interpretation comes from lesion studies showing that when V4 is removed, monkeys show a strong impairment in their ability to select an attended stimulus from among distracters (Schiller 1993; De Weerd et al., 1999, 2003). An interesting aspect of the De Weerd studies is that they did not find much of a deficit in the discrimination ability of animals with V4 or V4+TEO lesions when only one stimulus was presented in the lesioned quadrant.[3] However, they found a large deficit when task-irrelevant distracters were placed near the discriminandum. Interestingly, as the contrast of the distracter stimuli was raised, the deficit increased. This suggests that the signals in V4 may not be important for the discrimination of simple features but for filtering

[3]However, it is possible that the Schiller and De Weerd studies underestimate the importance of V4 neurons in the visual perception of normal animals, as the studies occur after the lesioned animals may have developed compensation strategies.

out distracting stimuli.

While these studies implicate V4 in attentional selection, lesions studies can often be difficult to interpret because lesions can cause non-selective damage, e.g., in areas that project to the site of the lesion, and they are long lasting, raising the possibility that observed deficits may result from changes in behavioral strategy that the animal has adopted to accommodate for the effects of the lesion itself. Nevertheless, the results of these studies, combined with the electrophysiological evidence, provides a reasonably compelling picture in favor of a role of Area V4 in attentional selection and attention-dependent improvements in visual processing. However, very little is known about the specific circuit mechanisms within V4 that could underlie either of these components of spatially-selective visual attention. Further work is needed to elucidate the specific circuit mechanisms within area V4, as well as how specific components of the V4 circuit participate in concert with neurons in other brain areas to control perception and behavior. The primary approach of this dissertation is to exploit understudied components of extracellular signals, such as waveform shape and spiking statistics, with the aim to further link extracellular correlates of attentional mechanisms to specific circuit mechanisms.

1.3 References

Bean BP (2007) The action potential in mammalian central neurons. Nature Rev Neurosci 8:451-465.

Bisley JW (2011) The neural basis of visual attention. J Physiol 589:29-57.

Chen Y, Martinez-Conde S, Macknik SL, Bereshpolova Y, Swadlow HA, Alonso J-M (2008) Task difficulty modulates the activity of specific neuronal populations in primary visual cortex. Nat Neurosci 11:974-982.

Cohen JY, Pouget P, Heitz RP, Woodman GF, Schall JD (2008) Biophysical support for functionally distinct cell types in frontal eye field. J Neurophysiol 101:912-916.

Cohen MR, Maunsell JHR (2009) Attention improves performance primarily by reducing interneuronal correlations. Nat Neurosci 12:1594-1600.

Cohen MR, Maunsell JHR (2010) A neuronal population measure of attention predicts behavioral performance on individual trials. J Neurosci 30(45):15241-15253.

Constantinidis C, Goldman-Rakic PS (2002) Correlated discharges among putative pyramidal neurons and interneurons in primate prefrontal cortex. J Neurophysiol 88:3487-3497.

Conway BR, Moeller S, Taso DY (2007) Specialized color modules in macaque extrastriate cortex. Neuron 560-573.

De Weerd P, Desimone R, Ungerleider LG (2003) Generalized deficits in visual selective attention after V4 and TEO lesions in macaques. Eur J Neurosci 18:1671-1691.

De Weerd P, Peralta MR, Desimone R, Ungerleider LG (1999). Loss of attentional stimulus selection after extrastriate cortical lesions in macaques. Nat Neurosci 2:753-758.

Diester I, Nieder A (2008) Complementary contributions of prefrontal neuron classes in abstract numerical categorization. J Neurosci 28:7737-7747.

Gattass R, Sousa APB, Gross CG (1988) VIsuotopic organization and extent of V3 and V4 of the macaque. J Neurosci 8(6):1831-1845.

Gattass R, Nascimento-Silva S, Soares JGM, Lima Bruss, Jansen AK, Diogo ACM, Farias MF, Marcondes M, Botelho E, Mariani O, Azzi J, Fiorani M (2005) Cortical visual areas in monkeys: location, topography, connections, columns, plasticity and cortical dynamics. Phil Trans R Soc B 360:709-731.

Gold C, Henze DA, Koch C, Buzsáki G (2006) On the origin of the extracellular action potential waveform: a modeling study. J Neurophysiol 95:3113-3128.

Gonzàlez-Burgos G, Krimer LS, Povysheva NV, Barrionuevo G, Lewis DA (2005) Functional properties of fast spiking interneurons and their synaptic connections with pyramidal cells in primate dorsolateral prefrontal cortex. J Neurophysiol 93(2):942-953.

Henze DA, Borhegyi Z, Csicsvari J, Mamiya A, Harris KD, Buzsáki G (2000) Intracellular features predicted by extracellular recordings in the hippocampus in vivo. J Neurophysiol 84:390-400.

Hussar CR, Pasternak T (2009) Flexibility of sensory representations in prefrontal cortex depends on cell type. Neuron 64:730-743.

James W (1890) The Principles of Psychology. Holt, New York.

Johnston K, DeSouza JFX, Everling S (2009) Monkey prefrontal cortical pyramidal and putative interneurons exhibit differential patterns of activity between prosaccade and antisaccade tasks. J Neurosci 29: 5516-5524.

Kaufman MT, Churchland MM, Santhanam G, Yu BM, Afshar A, Tyu SI, Shenoy KV (2010) Roles of monkey premotor neuron classes in movement preparation and execution. J Neurophysiol 104:799-810.

Kobatake E, Tanaka K (1994) Neuronal selectivities to complex object features in the ventral visual pathway of the macaque cerebral cortex. J Neurophysiol 71:856-867.

Krahe R, Gabbiani F (2004) Burst firing in sensory systems. Nature Rev Neurosci 5:12-23.

Laughlin SB, Sejnowski TJ (2003) Communication in neuronal networks. Science 26(301):1870-1874.

McAdams CJ, Maunsell JHR (1999) Effects of attention on the reliability of individual neurons in the monkey visual cortex. Neuron 23:765-773.

McAdams CJ, Maunsell JHR (2000) Attention to both space and feature modulates neuronal responses in macaque area V4. J Neurophysiol 83:1751-1755.

Mitchell JF, Sundberg KA, Reynolds JH (2007) Differential attention-dependent response modulation across cell classes in macaque visual area V4. Neuron 55:131Ð141.

Mitchell JF, Sundberg KA, Reynolds JH (2009) Spatial attention decorrelates intrinsic activity fluctuations in macaque area V4. Neuron 63:879-888.

Moran J, Desimone R (1985) Selective attention gates visual processing in the extrastriate cortex. Science 229:782-784.

Pasupathy A, Connor CE (1999) Responses to contour features in macaque area V4. J Neurophysiol 82:2490-2502.

Reimer J, Hatsopoulos NG (2010) Periodicity and evoked responses in motor cortex. J Neurosci 30:11506-11515.

Reynolds JH, Chelazzi L, Desimone R (1999) Competitive mechanisms subserve attention in macaque areas V2 and V4. J Neurosci 19:1736-1753.

Reynolds JH, Chelazzi L (2004) Attentional modulation of visual processing. Ann Rev of Neurosci 27:611-647.

Reynolds JH, Heeger DJ (2009) The normalization model of attention. Neuron 61:168-185.

Rudy B, McBain CJ (2001) Kv3 channels: voltage-gated K+ channels designed for high-frequency repetitive firing. Trends Neurosci 24:517-526.

Schiller, PH (1993) The effects of V4 and middle temporal (MT) area lesions on visual performance in the rhesus monkey. Vis Neurosci 10:717-746.

Song J-H, McPeek RM (2010) Roles of narrow- and broad-spiking dorsal premotor area neurons in reach target selection and movement production. J Neurophysiol 103: 2124-2138.

Sundberg KA, Mitchell JF, Reynolds JH (2009) Spatial attention modulates center-surround interactions in macaque visual area V4. Neuron 61:952-963.

Tanigawa, H, Lu HD, Roe AW (2010) Functional organization for color and orientation in macaque V4. Nat Neurosci 13:1542-1548.

Ungerleider LG, Galkin TW, Desimone R, Gattass R (2008) Cortical connections of area V4 in the macaque. Cerb Cortex 18:477-499.

Weller ER, Steele GE, Kaas JH (2002) Pulvinar and other subcortical connections of dorsolateral visual cortex in monkeys. J Comp Neurol 450:215-240.

Yokoi I, Komatsu H (2010) Putative pyramidal neurons and interneurons in the monkey parietal cortex make different contributions to the performance of a visual grouping task. J Neurophysiol 104: 1603-1611

Zeki SM (1973) Colour coding in rhesus monkey prestriate cortex. Brain Res 53:422-427.

Chapter 2

Attentional modulation of firing rate varies with burstiness across putative pyramidal neurons in macaque visual Area V4

2.1 Abstract

One of the most well established forms of attentional modulation is an increase in firing rate when attention is directed into a neuron's receptive field. The degree of rate modulation, however, can vary considerably across individual neurons, especially among broad spiking neurons (putative pyramids). We asked whether this heterogeneity might be correlated with a neuronal response property that is used in intracellular recording studies to distinguish among distinct neuronal classes: the burstiness of the neuronal spike train. We first characterized the burst spiking behavior of V4 neurons and found that this varies considerably across the population, but did not find evidence for distinct classes of burst behavior. Burstiness did, however, vary more widely across the class of neurons that show the greatest heterogeneity in attentional modulation, and within that class, burstiness helped account for differences in attentional modulation. Among these broad spiking neurons, rate modulation was largely restricted to bursty neurons,

which as a group showed a highly significant increase in firing rate with attention. Further, every bursty broad spiking neuron whose firing rate was significantly modulated by attention exhibited an increase in firing rate. In contrast, non-bursty broad spiking neurons exhibited no net attentional modulation, and while some individual neurons did show significant rate modulation, these were divided among neurons showing increases and decreases. These findings show that macaque Area V4 shows a range of bursting behavior, and that the heterogeneity of attentional modulation can be explained, in part, by variation in burstiness.

2.2 Introduction

The longest studied form of attention-dependent neuronal response modulation is a change in mean firing rate, which typically increases when attention is directed to a stimulus within a neuron's receptive field (Treue, 2003; Reynolds and Chelazzi, 2004; Knudsen, 2007). However, the degree of attention-dependent firing rate modulation across individual neurons can vary considerably, with some neurons even showing statistically significant reductions in firing rate with attention. Recently, Mitchell et al. (2007) found that in Area V4, an intermediate stage of visual processing that is strongly modulated by attentional state, two classes of neurons can be distinguishe*D:* narrow spiking neurons (putative interneurons) and broad spiking neurons (putative pyramidal neurons). Much of the heterogeneity in attentional modulation was restricted to broad spiking neurons. We wondered whether other properties of the neurons' responses, such as variation in their spiking statistics, could help account for this heterogeneity.

Several early studies concluded that the spiking of cortical neurons can, to a first approximation be described as Poisson, with spike count variance proportional to the mean rate and spike timing that is nearly independent of preceding spike history (Tolhurst et al, 1983; Softky and Koch, 1993; Shadlen and Newsome, 1998). However, recent studies in the awake primate that have examined spiking statistics in more detail have revealed a diversity of firing patterns across neocortical regions (Maimon and Assad, 2009) as well as across neurons recorded within individual cortical areas (Bair et al., 1994; Friedman-Hill et al., 2000;Compte et

al., 2003; Joelving et al., 2007; Katai et al., 2010). Indeed, many intracellular recording studies have used discharge patterns such as bursting to distinguish among different neocortical neuronal classes (McCormick et al., 1985; Nowak et al., 2003). These findings underscore the importance of examining the spiking statistics within a brain area of interest. They also raise the possibility that we may gain valuable insights from characterizing deviations from Poisson spiking within an area, and examining whether these deviations correlate with other neuronal response properties.

With this motivation, we asked whether neurons in macaque Area V4 exhibit deviations from Poisson-like behavior. We find that V4 neurons exhibit a broad continuum of spiking statistics, with some responding much like Poisson processes, while others exhibited strikingly bursty behavior. We next considered whether this diversity of discharge patterns might correspond with different patterns of attentional modulation. We find that, among broad spiking neurons, differences in burstiness predict attentional rate modulation, with bursty broad spiking neurons showing more consistent increases in firing rate with attention than non-bursty broad spiking neurons.

2.3 Methods

2.3.1 Electrophysiology and receptive field characterization

All procedures were approved by the Salk Institute Institutional Animal Care and Use Committee (IACUC) and conformed to NIH guidelines for the humane care and use of animals in research. Monkeys were prepared for neuronal recording following procedures described by Mitchell et al. (2007). After training each animal on the behavioral task described below, recordings were made from two to five tungsten electrodes (FHC, 1201 Main Street, Bowdoin, ME 04287) that were advanced until action potentials of single neurons could be isolated based on action potential waveform shape. Neuronal signals were recorded extracellularly, filtered (Butterworth filter, 6-pole, 3db cutoff at 154 Hz and 8.8 kHz), and stored

using the Multichannel Acquisition Processor system (Plexon, Inc., Houston, TX). Spike waveforms crossing a negative threshold, which was set to exclude noise, were stored for later off-line analysis. Units were identified as isolated in offline analysis (Offline Sorter, Plexon, Inc., Houston, TX) if the first three principle components of their waveform shape formed a clearly separable cluster from noise and other units. After isolating one or more neurons, receptive fields were mapped using a subspace reverse correlation procedure (Ringach et al., 1997; Mitchell et al., 2007). In this procedure, colored Gabor stimuli (eight orientations, six colors, 80% luminance contrast, 1.2 cycles per degree, Gabor Gaussian half-width 2°) were flashed at random locations (chosen from a grid with 3° spacing) to determine a single stimulus location that would elicit a robust visual response. When multiple neurons were recorded simultaneously, the features and location of the stimulus were selected to excite the best isolated units.

2.3.2 Stimulus presentation and eye movement monitoring

Stimuli were presented on a computer monitor (Sony Trinitron Multiscan, TC, 640 x 480 pixel resolution, 120Hz) placed 57 cm from the eye. Experimental control was handled by NIMH Cortex software (http://www.cortex.salk.edu).

Eye position was continuously monitored with an infrared eye tracking system (240 Hz, ETL-400; ISCAN, Inc.). We detected microsaccades as described in Mitchell et al. (2007). Matlab source code and example data are available online at (http://www.snl.salk.edu/ jude). Briefly, saccades were defined as points in the eye position traces where a 400 ms window around the time point was better fit with a model with a saccade-like discontinuity than with a smooth polynomial spline function. After determining model parameters by minimizing the mean squared error, saccades were identified as points in time when the variance explained by the saccade model was more than 30% greater than for the spline model, with additional constraint that the instantaneous velocity at that point exceeded 10 deg/s, and the instantaneous acceleration exceeded 1000 deg/s^2. Figure 2.5A provides an example trial with raw eye position traces, model fits, and detected microsaccades.

2.3.3 Task and stimuli

Two monkeys performed a multiple-object tracking task (Figure 2.1) that has been used to study attention in humans (Pylyshyn and Storm, 1988; Sears and Pylyshyn, 2000; Cavanagh and Alvarez, 2005) and non-human primates (Mitchell et al., 2007, 2009; Sundberg et al., 2009). The animals began each trial by fixating a central point and maintained fixation until the end of the trial. After 200 ms, four identical Gabor stimuli appeared (40% luminance contrast). The color and orientation of these stimuli were chosen based on the subspace reverse correlation map to produce a strong response. The positions of the stimuli were selected to fall at regular intervals along an invisible ring of equal eccentricity, selected such that all of the stimuli fell outside of the neurons' receptive fields. One or two stimuli were then cued as targets by a brief elevation in luminance. All four stimuli then moved along independent, randomly-generated trajectories that positioned the stimuli at four new, equally-eccentric positions. This placed one of the stimuli at the center of the neuron's receptive field and the others outside the receptive field. The trajectories were designed to match stimulation history across the two attention conditions, by using the identical trajectories in the attended and unattended trials, and by preventing all but one stimulus from entering the receptive field. The stimuli then paused for 1000 ms before moving to a final set of equally-eccentric positions and stopping. At this point, the fixation point disappeared, signaling the animal to make a saccade to each cued target. To minimize the development of spatial biases, the starting and ending positions for the target and non-target stimuli were symmetrically balanced. Correct identification of the targets resulted in a liquid reward. Only correctly completed trials with two of four stimuli tracked were analyzed.

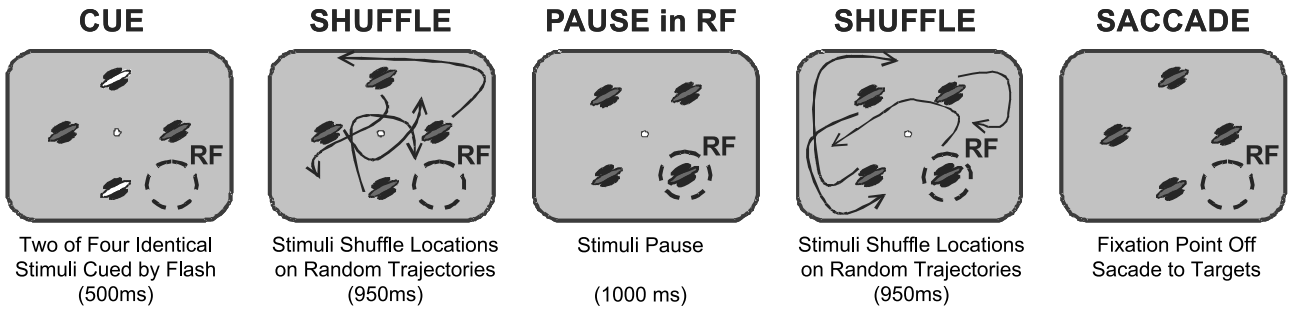

Figure 2.1: Behavioral paradigm

Attentional state was controlled with a multi-object tracking task. Animals initiated trials by fixating a central point. Four identical Gabor stimuli then appeared, and one or two of them were cued as targets with a brief elevation in luminance. The monkey then maintained fixation while attentively tracking the targets as they moved along independent randomized trajectories that brought one of the stimuli into the receptive field, at which point all four stimuli paused for 1000 ms. The stimuli then shuffled position a second time, with randomized trajectories that placed them at equally eccentric positions outside the receptive field. The fixation point then disappeared, indicating that the monkey should saccade to the previously cued targets. Juice reward was delivered if the monkey correctly made a saccade to each cued stimulus and none of the distracter stimuli.

2.3.4 Inclusion criteria

We recorded from 206 well-isolated neurons from two male monkeys (N = 53 Monkey B, N = 153 Monkey M). We restricted our discharge pattern analyses to units whose response on trials when attention was directed away from the RF exceeded 5 Hz, averaged over the final 500 ms of the stimulus pause period, and was significantly greater than the mean spontaneous firing rate averaged over the 250 ms preceding the onset of the Gabor stimuli (Mann-Whitney U test, $p < 0.05$). This resulted in 84 neurons being excluded. In addition, four units were excluded because their waveforms did not have the typical biphasic shape, with a trough followed by a clearly defined peak, and they could not therefore be classified as narrow or broad-spiking. In total, 118 neurons met these selection criteria. Unless otherwise specified, analysis of spiking statistics was restricted to the final 800 ms of the pause period (the "sustained period") which excluded periods of transient response as stimuli entered or exited the receptive field, and thus the mean firing rate was relatively stationary.

2.3.5 Broad and narrow spiking classification

As described previously (Mitchell et al., 2007), we divided neurons into narrow and broad spiking subpopulations based on waveform duration (Figure 2.3). We defined waveform duration to be the time from the trough to the peak of the average waveform (Mitchell et al., 2007). We selected this metric on the basis of studies showing that this measure best distinguishes putative pyramidal neurons from putative fast-spiking interneurons in the neocortex (Barthò et al., 2004). The distribution of spike waveform duration was significantly bimodal across all isolated cells with biphasic spike waveforms (N = 202, Hartigan's dip test, $p < 0.0001$), and also across the subset of these cells with significant visual responses (N = 118, Hartigan's dip test, $p < 0.01$). Narrow and broad spiking neurons were separated based on the trough between the two modes of the waveform duration distribution, with narrow spiking neurons defined as those ranging in duration from 100 to 224 μs and broad-spiking neurons defined as those ranging in duration from 225 to 500 μs.

2.3.6 Burst analysis

To assess the degree of burstiness of a given neuron, we computed the burstiness/refractoriness index (B.R.I.), as defined by Compte et al. (2003), over the 800ms sustained period. First, we calculated the autocorrelation function of the neuron separately for each attention condition. We then subtracted the shuffle predictor for that condition. The shuffle predictor is defined as the mean cross-correlation across all pairs of trials of an individual neuron, and corresponds to the autocorrelation of a Poisson process with the same mean time course as the cell. By subtracting the predictor, we remove any trial-locked fluctuations in spiking that result from repeated presentation of the stimulus. After this subtraction, we normalized the result to the standard deviation of the shuffle predictor at each time lag. This results in a shuffle-corrected autocorrelation function that has been normalized for the standard deviation in the shuffle predictor, for the attended and unattended conditions. The B.R.I. is defined to be the average height of the unattended shuffle-predictor-normalized autocorrelation function over the interval corresponding to 1-4 ms. This measure is expressed in units of the shuffle-predictor standard deviations. The logic of this metric is analogous to a z-transformation. The z-score indicates how many standard deviations an observation is from the population mean. By assuming a normal distribution with a given mean and standard deviation, one can determine whether the observation falls outside the range expected by chance. The metric used here to assess burstiness assumes a Poisson distribution, which, by definition, is not bursty, as the occurrence of each spike is independent of spiking history. For analyses where we divided the units into bursty and non-bursty populations (Figure 2.4A-D), we define neurons as bursty if their B.R.I. exceeded two (central autocorrelation peak more than two standard deviations above the shuffle predictor).Values greater than two indicate that the neuron exhibits more short-duration inter-spike-intervals than would be expected by chance from a rate-matched Poisson process, indicating that the neuron is bursty. Large negative values indicate an extended period of refractoriness.

Since we observe a continuum of discharge patterns across our data (Figure 2.3), this division is not intended to imply that these are intrinsic subclasses of neurons, but rather to illustrate the differences we observe between significantly

bursty and non-significantly bursty neurons. We obtained similar results when we used a B.R.I. threshold of one standard deviation to define bursty and non-bursty cells.

2.4 Results

We characterized the discharge patterns of 118 visually-driven neurons in area V4, in two macaques as they performed the attention demanding tracking task depicted in Figure 2.1. This task allowed us to direct attention toward or away from a stimulus that we positioned within the neurons' receptive fields. We then asked whether there was a relationship between attentional modulation and the discharge patterns we observed in broad and narrow spiking neurons.

2.4.1 Assessment of discharge patterns

The population of V4 neurons exhibited a wide range of discharge patterns in response to sustained stimuli, ranging from highly bursty neurons that frequently fired doublets and triplets to neurons with long relative refractory periods that rarely, if ever, exhibited bursts. Example neurons are presented in Figure 2.2, which also serves to illustrate several different ways of visualizing burstiness. The neuron in Figure 2.2A is a broad spiking neuron (see mean waveform in upper right panel) that frequently fired in bursts. The upper left panel shows 100 ms samples of this neuron's spiking behavior, taken from unattended trials. In this spike raster, it can be seen the neuron often fired several spikes in close succession. Another way to visualize the bursting behavior of neurons is through their inter-spike interval (ISI) return map, which plots each spike according to the ISI before and after each spike. As shown in the middle panel, the ISI return map reveals clusters of spikes. Points in the lower right-hand corner correspond to spikes at the beginning of bursts, while points in the upper left-hand corner correspond to spikes at the end of a burst. Points in the lower left-hand corner correspond to spikes in the middle of bursts. Burstiness can also be revealed by looking at the ISI distribution, shown in the upper right panel. For a unit with Poisson firing, the ISI distribution would appear as an exponential distribution decaying from the

shortest ISI. Here we can see a strong peak in the ISI distribution at short intervals of 2-4 ms indicating bursting behavior. The lower right panel shows the neuron's normalized spike autocorrelation function in the unattended condition, which is arguably a simpler way of looking at how spiking deviates from Poisson behavior. It plots the probability of firing at a given delay, normalized by its deviation from the expectation of a rate-matched Poisson process (see Methods). For a Poisson processes, this normalized autocorrelation function would appear as a flat line fixed at zero. Similar to the early peak seen in the ISI distribution, we see once again that this neuron exhibits a strong early peak centered near 2-4 ms. Unlike the ISI distribution, however, this normalized autocorrelation function makes it clear that this peak deviates significantly from the Poisson expectation, indicating that the spikes following at short delays are occurring much more frequently than would be expected for a rate matched Poisson process.

The degree of burst spiking varied considerably over the population, as can be seen by comparing the example neurons in Figure 2.2. The neurons in Figures 2.2B (broad spiking) and 2.2D (narrow spiking) showed relatively modest deviations from Poisson spiking. This can be seen by a lack of clustering in the ISI return map (middle panels) and a normalized autocorrelation function that deviated only modestly from the Poisson expectation (horizontal dashed line), with a dip at short ISIs corresponding to a period of relative refractoriness. Some narrow spiking neurons also exhibited burst firing, as seen for the example neuron in Figure 2.2C, although this was less common.

Figure 2.2: Examples of four individual neurons with varying degrees of burstiness

(facing page)

A: Example of a bursty broad spiking neuron. *B:* Example of non-bursty broad spiking neuron. *C:* Example of a bursty narrow spiking neuron. *D:* Example of a non-bursty narrow spiking neuron. For each neuron, top left panels show spike raster plots of a 100ms window within the sustained period for the first 40 correct unattended trials. Bottom left panels show the neuronal response (spikes per second) averaged across trials, to targets (gray) and distracters (black) as they entered the receptive field, paused, and exited the receptive field. These response time courses were smoothed by convolving each with a Gaussian kernel (σ = 25ms). Middle panels show interspike interval return maps for the unattended condition. Each point corresponds to one action potential, plotted to indicate its interspike interval relative to the previous and subsequent spikes. Top right panels show interspike interval histograms (bin width, 4ms). Insets in the top right panels are normalized mean action potential waveforms, with peak to trough duration indicated by horizontal bars. Bottom right panels show the normalized autocorrelation functions (autocorrelation minus the shuffle predictor divided by the standard deviation of the shuffle predictor; see Methods) for the unattended condition. Dashed line at 0 indicates the normalized autocorrelation function of a rate-matched Poisson process.

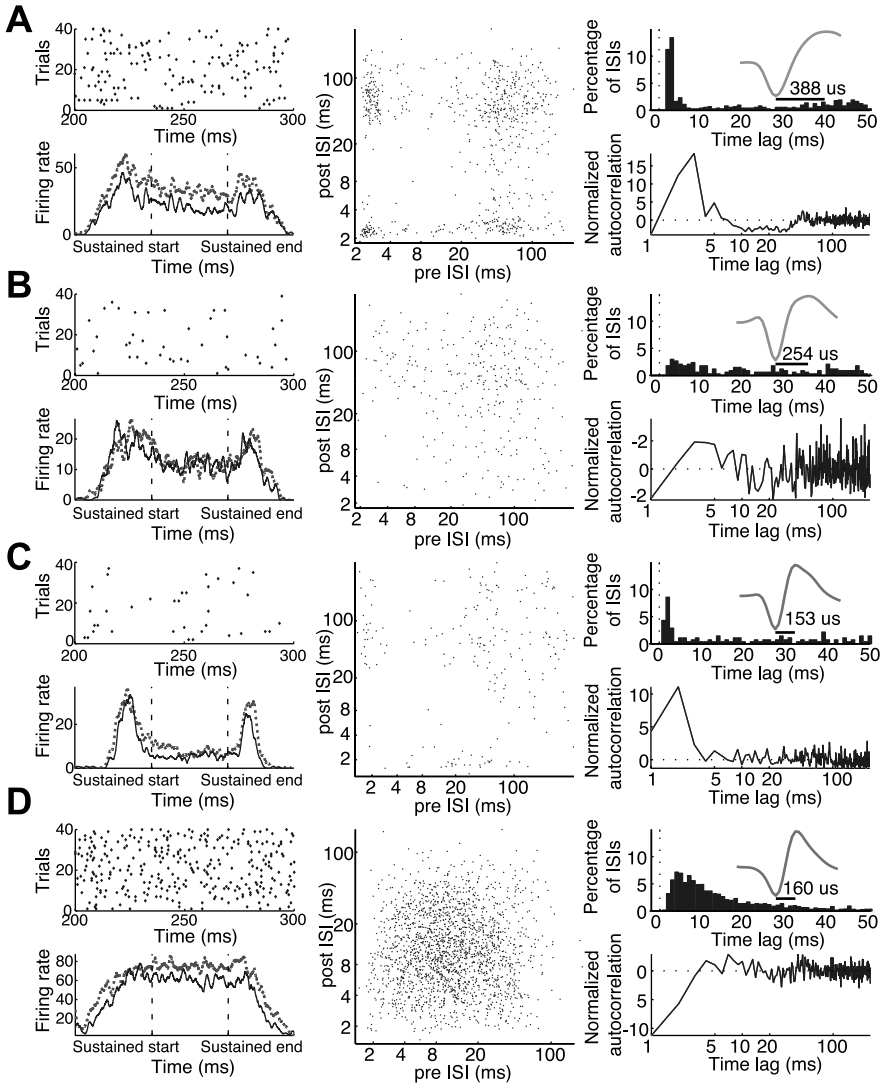
A
B
C
D
Trials
Time (ms)
Firing rate
Sustained start
Sustained end
post ISI (ms)
pre ISI (ms)
Percentage of ISIs
Time lag (ms)
388 us
254 us
153 us
160 us
Normalized autocorrelation

We used the burstiness/refractoriness index (B.R.I.) introduced by Compte et al., 2003, to quantify the distribution of burst firing behavior across the population. This metric examines the deviation of the first four milliseconds of a unit's autocorrelation function from that of its shuffle-predictor (see Methods). A positive B.R.I. indicates the neuron tended to fire spikes in bursts, as indicated by a larger number of closely spaced spikes than would be expected from a rate-matched Poisson process. In contrast, a negative value indicates an extended relative refractory period. Using this metric, we find that both narrow and broad spiking cells exhibit a continuum of discharge patterns, though broad spiking neurons exhibit more extreme burstiness. Figure 2.3 displays the distribution of B.R.I. as a function of spike waveform duration across the entire population. Those neurons with statistically significant burst firing (B.R.I. > 2; see Methods) are indicated by dark gray circles and non-bursty neurons are indicated by light gray circles. There was a wide distribution of burst firing across the population, but it was not clearly bimodal (Hartigan's dip test, $p > 0.5$, histogram not shown). However, as shown previously (Mitchell et al., 2007), there was a bimodal distribution of spike waveforms as indicated by the histogram at the bottom of the figure (Hartigan's dip test, $p < 0.001$). We therefore divided neurons into narrow and broad spiking categories based on this histogram, with narrow spiking defined as those units with waveform durations less than 225 μs (vertical line), and examined burstiness separately for each class. Narrow spiking neurons tended to have lower B.R.I.s, indicating a more modest tendency to fire action potentials in bursts. The broad spiking population showed a wider range of values, including some neurons that were extremely bursty. This difference in burstiness across narrow and broad spiking neurons was highly significant (Mann-Whitney U test, $p < 0.000005$; narrow median B.R.I. -0.87, broad median B.R.I. 2.67).

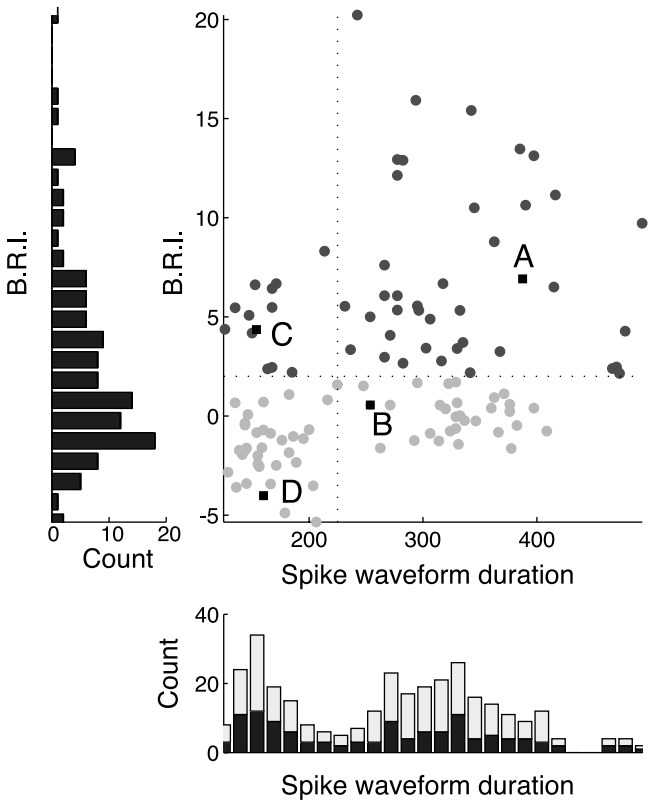

Figure 2.3: Population scatter plot of spike waveform duration (μs) vs. burstiness/refractoriness index (B.R.I.)
Labels (A-D) indicate example units from Figure 2.2. Dark gray circles correspond to bursty neurons, defined as neurons whose burstiness exceeded two standard deviations of a rate-matched Poisson process (B.R.I. > 2). Light gray circles correspond to non-bursty cells. The left panel shows the distribution of the B.R.I. across the population, which was not significantly bimodal. The bottom panel shows the distribution of spike waveform durations, which is significantly bimodal both for visually driven cells (dark bars, Hartigan's dip test, $p < 0.01$) and the entire population (light bars indicate non-visually driven neurons, Hartigan's dip test, $p < 0.0001$).

2.4.2 Relationship between burst firing and attention-dependent rate modulation

Broad spiking neurons exhibit more heterogeneous attentional rate modulation than narrow spiking neurons (Mitchell et al., 2007). The present finding, that they also show more variability in their spiking statistics, led us to wonder whether the two phenomena could be related. To examine this, we asked whether the degree of burstiness corresponds to the magnitude of attentional modulation. We first subdivided the narrow and broad spiking populations into bursty and non-bursty groups according to whether the neurons' burstiness/refractoriness indices (B.R.I.) exceeded two standard deviations of the B.R.I.s of Poisson processes matched in mean firing rate (see Methods). The left panels of Figure 4 show mean population responses of these groups to attended (red) and unattended stimuli (blue). Remarkably, one group of neurons, non-bursty broad spiking neurons, exhibited nearly identical mean firing rates across attention conditions, indicating that, on average, these neurons are not modulated by attention (median unattended median unattended 11.80Hz, median attended 11.95Hz, median 2.80% increase in absolute firing rate, Wilcoxon signed rank test $p > 0.3$). The other three groups of neurons exhibited significant attention-dependent increases in firing rate (broad spiking bursty neurons: median unattended 10.26Hz, median attended 13.79Hz, a median 21.72% increase, Wilcoxon signed rank test $p < 0.00001$; narrow spiking bursty neurons, median unattended 18.05Hz, median attended 27.81Hz, 25.40%, $p < 0.01$; narrow spiking non-bursty neurons, median unattended 18.00Hz, median attended 24.80Hz, 26.72%, $p < 0.000005$).

To examine the distribution of attentional modulation of firing rate across neurons in each subpopulation, we computed a normalized attention index (rate A.I.) for each neuron (attended mean rate - unattended mean rate) / (attended mean rate + unattended mean rate). Positive values of this index correspond to neurons showing attention-dependent increases in rate, and negative values correspond to decreases. The distribution of this index, for each group, appears in Figure 2.4, middle column. Black bars indicate individual neurons that showed statistically significant modulation of firing rate (Mann-Whitney U test, $p < 0.001$).

Consistent with the above population median and mean modulation, we find that among broad spiking neurons, attention-dependent increases in rate are largely restricted to bursty cells. Among broad spiking bursty neurons, all neurons with significant attention-dependent rate modulation showed increases in firing rate when attention is directed into the neuron's receptive field (N = 12 of 40 neurons, 30.0%). Similarly, all narrow spiking neurons with significant attentional rate modulation showed increases in firing rate (bursty narrow N = 7 of 13 neurons, 53.9%; non-bursty narrow N = 15 of 34 neurons, 44.1%). For all three of these groups, the distributions of A.I. indices showed significant increases, according to a Wilcoxon signed rank test (bursty broad $p < 0.00005$; bursty narrow $p < 0.005$; non-bursty narrow $p < 0.00001$). The distributions of the rate A.I. did not differ significantly among these three groups. This contrasts markedly with the non-bursty broad spiking group, where attentional modulation was less common and more heterogeneous, with similar numbers of increases and decreases in firing rate observed (3 decreases and 5 increases, out of 31 neurons, 9.7,%, 16.1%). Further, the distribution of A.I. indices for the non-bursty broad spiking group differed significantly from each of the other three groups (Mann-Whitney U test, bursty broad $p < 0.006$; bursty narrow $p < 0.05$; non-bursty narrow $p < 0.0005$).

Since the degree of burstiness appears to fall along a continuum, and not into a bimodal distribution, one possible concern is that the above findings depended on the threshold we set to divide neurons into bursty and non-bursty groups (B.R.I. > 2). Therefore, we also asked whether there was a correlation between the degree of burstiness and the strength of attentional mean rate modulation. We computed the correlation between the B.R.I. and the rate A.I. The results are shown in Figure 2.4, panels E-F, which show population scatter plots of B.R.I. vs. rate A.I. for the narrow (Panel E) and broad spiking populations (Panel F). Within the narrow spiking subpopulation, we observe increases in firing rate with attention regardless of the degree of burstiness, with all significantly modulated neurons showing increases in firing rate with attention. We also observe no correlation between rate A.I. and B.R.I. among narrow spiking neurons (Figure 2.4E, Spearman's non-parametric correlation, $p > 0.7$, $R_s = 0.\ 0490$). In contrast, we find that among broad spiking neurons there is a significant correlation between

greater degrees of burstiness and greater attention-dependent increases in firing rate (Figure 2.4F, Spearman's rank correlation, $p < 0.05$, $R_s = 0.2499$). This suggests that the differences in attentional modulation we observe between the bursty and non-bursty broad spiking groups are not an artifact of our choice of threshold, but rather reflect a relationship between burstiness and attention-dependent modulations of firing rate. A remaining concern was that this correlation could potentially be driven by outliers. To test this, we measured correlation among broad spiking neurons after excluding neurons with rate A.I. or B.R.I. values that exceeded 1.5 standard deviations of the broad spiking population mean. After excluding these neurons, the correlation remained (Figure 2.4F, filled circles within dashed orange region, $p < 0.01$, $R_s = 0.3583$). Thus, we conclude that among broad but not among narrow spiking neurons, attention-dependent increases in firing rate are observed primarily among bursty neurons.

Differences in firing rate do not explain attention differences among broad spiking neurons Another possible concern is that this difference in rate A.I. could be due to differences in firing rate across the broad spiking groups. If the non-bursty broad spiking group had lower firing rates than the bursty broad spiking group, this could reduce statistical power, impairing our ability to detect attentional modulation, rather than reflecting an actual difference in attentional rate modulation between these two groups. To test this, we compared the unattended firing rate distributions of the bursty and non-bursty broad spiking groups. We find that there is no significant difference in the unattended firing rates between the non-bursty and bursty broad spiking neurons (Mann-Whitney U test, $p > 0.8$; bursty broad median 10.26Hz, non-bursty broad median 11.80Hz), nor is there a significant difference in the absolute number of action potentials recorded in the unattended state for the two populations of neurons (Mann-Whitney U test, $p > 0.6$; bursty broad median 353.5 spikes/neuron, non-bursty broad median 378 spikes/neuron).

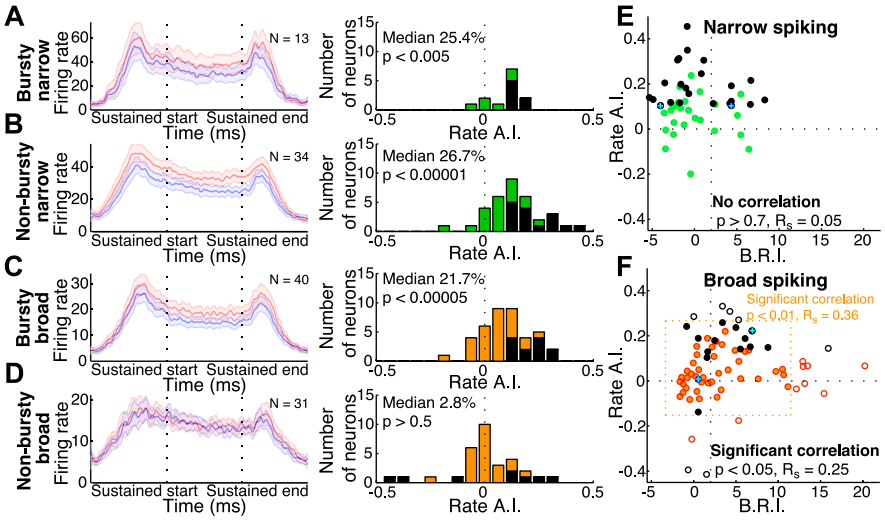

Figure 2.4: Relationship between burstiness/refractoriness index and attention-dependent rate modulation

A-D: Attention-dependent modulation of firing rate across four groups of V4 neurons: bursty narrow (*A*), non-bursty narrow (*B*), bursty broad (*C*), and non-bursty broad (*D*). Left panels show population mean stimulus-evoked responses for tracked (red traces) or ignored (blue traces) stimuli (data smoothed with a Gaussian filter where $\sigma = 25$ms; shaded regions indicate +/- 1 SEM). The middle column of panels shows the distributions of the firing rate attention index for each population, with individually significant units ($p < 0.001$) shaded black. *E-F:* Population scatter plots of burstiness/refractoriness index (B.R.I.) vs. firing rate attention index (rate A.I.). Narrow spiking cells are shown in panel E (green circles), broad spiking cells in panel *F* (orange circles). Individual units with significant attention-dependent rate modulation ($p < 0.001$) are shown in black. Points with blue crosses correspond to the example individual neurons in Figures 2.2 and 2.3. In *F*, filled circles indicate broad-spiking neurons with rate A.I. and B.R.I. values within 1.5 STD of the broad-spiking population mean (indicated by dashed orange box). There is a significant correlation between B.R.I. and rate A.I. across the entire broad spiking population (open and filled circles, Spearman's correlation, $p < 0.05$, $R_s = 0.25$), and for the subset within 1.5 STD of the mean (filled circles, Spearman's correlation, $p < 0.01$, $R_s = 0.36$).

To examine this further, we asked whether mean firing rate in the unattended condition correlated with attentional modulation. There is no correlation between mean unattended firing rate and rate A.I. for either the broad spiking neurons (Spearman's rank correlation $p > 0.4$, R_s = -0.0917) or across the entire population (Spearman's rank correlation $p > 0.9$, R_s = -0.0063). Thus, our normalized measure of attentional rate modulation is robust to differences in firing rate. As a final control, we compared the rate A.I. of the lower-firing rate bursty broad spiking neurons (mean unattended rate < 15Hz, N = 26) with the rate A.I. of the higher-firing rate non-bursty broad spiking neurons (mean unattended rate >= 10Hz, N = 17). As before, the bursty broad spiking neurons showed a significant increase in rate with attentional modulation (Wilcoxon signed rank test, $p < 0.001$), while the non-bursty broad spiking neurons did not. Further, the difference in attentional rate modulation between these groups remained significant (Mann-Whitney U test, $p < 0.01$).

We also repeated our analyses using an additional burstiness metric that was normalized by firing rate. Here, burstiness was measured as the mean of the autocorrelation function from 1-4 ms in unattended trials, divided by the mean firing rate in these trials. As before, we find that there is a significant correlation between burstiness and attention-dependent firing rate modulation among broad spiking (Spearman's rank correlation, $p < 0.05$, R_s = 0.2458) but not among narrow-spiking neurons ($p > 0.7$, R_s = -0.0458).

2.4.3 Session-to-session variability does not explain heterogeneity in attentional modulation or burstiness

We next considered whether the observed heterogeneity in attentional modulation could be accounted for by differences across sessions, perhaps reflecting differences in the internal state of the animal, rather than differences in the intrinsic properties of individual neurons. We reasoned that if the relationship between burstiness and attentional modulation stemmed from variation across sessions, then attentional modulation should be correlated across simultaneously recorded pairs of broad spiking neurons. However, we do not find a significant correlation in

the Rate A.I. pairs of broad spiking neurons (N = 52 pairs, p > 0.9, R_s = -0.01). In fact, we see examples of pairs in which one neuron exhibited attention-dependent increases in firing rate, while the other exhibited reductions in rate. This pattern of results supports the conclusion that attentional modulation varies as a function of spike wave form and burstiness.

We find a related pattern of results for burstiness, with substantial variability in the degree of burstiness within the same session. In particular, we do not observe a significant correlation in the B.R.I. values of simultaneously recorded broad spiking neurons (N = 52 pairs, p > 0.1, R_s = 0.12). We thus conclude that much of the heterogeneity we observe is due to differences in the neurons themselves, such as their intrinsic membrane properties or their place in the cortical circuit.

2.4.4 Spontaneous burst firing correlated with stimulus-evoked burst firing

A related question is whether the patterns we observed might perhaps reflect variations in stimulus conditions across experimental sessions. For example, neurons differ in contrast sensitivity, raising the possibility that differences in burstiness and attentional modulation might vary as a function of where the stimulus fell on a given neuron's contrast response function. Such stimulus-dependent differences would not be expected to hold in the absence of a stimulus. Therefore, to test this possibility, we asked if the burst firing properties observed during the stimulus-evoked response also held during the 250 ms spontaneous pre-stimulus period, when no stimulus of any kind was present. The low firing rates observed in this spontaneous period decreased our ability to accurately estimate the burst properties for some neurons. In particular, for a subset (N=6) of neurons with very low spontaneous firing rates the lack of action potentials led to artifactually high B.R.I values (B.R.I. » 100). We excluded these neurons from further analysis. However, among the remaining neurons (N=112), we found a strong correlation between the spontaneous period and sustained period B.R.I. estimates, both pooling across narrow and broad spiking neurons (Spearman's non-parametric correlation,

p « 0.0001, $R_s = 0.81$) as well as among the narrow and broad spiking subpopulations (broad, p « 0.0001, $R_s = 0.79$; narrow, p « 0.0001, $R_s = 0.70$). This suggests that the degree of burstiness in our neuronal population is not an artifact of the particular experimental conditions in an individual recording session, but instead reflects properties intrinsic to the neuron, either due to intrinsic neuronal properties such as membrane conductance, or perhaps due to the neuron's position within the cortical circuit.

If burstiness is a neuron property that predicts attentional modulation, we reasoned that we might see a systematic relationship between burstiness during the spontaneous period and attentional rate modulation during the stimulus evoked response period. To examine this, we first subdivided the broad spiking neurons, based on their spontaneous activity, into bursty and non-bursty groups using the same burst metric and definition of burstiness we previously applied the stimulus-evoked response. That is, we classified cells as bursty or non-bursty according to whether the B.R.I. derived from spontaneous activity exceeded the 2 STD threshold. As before, we found significant attentional modulation among bursty broad spiking neurons (Wilcoxon signed rank test, N=39, $p < 0.00005$) but not among non-bursty broad spiking neurons (N=27, $p > 0.2$). Further, the difference in attentional modulation between these two groups remained significant (Mann-Whitney U test, $p = 0.005$). We also tested whether there was a significant correlation between the spontaneous B.R.I. and the Rate A.I. of the sustained period. As before (see Figure 2.4F), we excluded outliers falling outside of a 1.5 standard deviation window around the population mean B.R.I. and Rate A.I. Despite the loss of statistical power inherent in the lower spike rates observed in the pre-stimulus period, there was, among broad spiking neurons, a significant correlation between the spontaneous level of burstiness and attentional modulation ($p < 0.02$, $R_s = 0.3351$).

2.4.5 Eye movements do not explain differences in attentional modulation

Previous studies have found that even small eye movements, such as fixational microsaccades, can influence neuronal responses (Gur et al., 1997; Martinez-Conde et al., 2004; Gur and Snodderly, 2006). We therefore examined whether differences in eye movements across the bursty and non-bursty broad and narrow spiking groups could underlie the differences in attention effects we observe. We used a saccade detection algorithm to identify microsaccades within the sustained response period (see Methods). Figure 2.5A shows microsaccades detected by the algorithm on a single trial. Green and blue lines show, respectively, fits to vertical and horizontal eye position, and three detected microsaccades are indicated by pink vertical bars.

To examine the impact of microsaccades on neural responses, we computed the mean microsaccade-triggered response, normalized on a neuron-by-neuron basis to the mean response evoked by the ignored stimulus. Figure 2.5B shows the mean microsaccade-triggered response across the entire population computed for attended (red) and unattended (blue) trials. As expected, the firing rates are higher, on average, in the attended condition, but there is no obvious difference in the deviations of the response that were induced by the microsaccade. In both conditions, the microsaccade-triggered response initially shows a transient reduction in firing rate followed by a brief increase in firing. This response is similar to that reported by Mitchell et al. (2007), but somewhat smaller in amplitude and delayed in time compared to the V4 responses observed by Leopold and Logothetis (1998). To quantify the saccade-induced response across the population, we computed a microsaccade-triggered response index (M.T.R.I.), which we define as the ratio between the mean normalized microsaccade-triggered response 200-300ms and 100-200ms following a detected microsaccade. We find that the M.T.R.I. during the presentation of an unattended stimulus in the receptive field is significantly greater than unity across the entire population and for each of bursty and non-bursty broad and narrow spiking groups, indicating that the responses of all four subclasses of neurons were modulated by microsaccades (Wilcoxon signed rank

test, entire population $p < 0.00000001$, bursty broad $p < 0.005$, non-bursty broad $p < 0.0005$, bursty-narrow $p < 0.05$, and non-bursty narrow $p < 0.005$).

Given that we see a significant modulation in the firing rate response following microsaccades, we next examined whether differences in eye movements could account for the differences we observe between the bursty and non-bursty broad and narrow spiking groups. First, we tested whether the number, size, direction or peak velocity of microsaccades varied between the non-bursty broad group and any of the other three groups in either attention condition. It did not differ significantly in any of these measures (Mann-Whitney U test, all p values > 0.1). We next examined whether there was a correlation between the B.R.I. and the number, size, direction, or peak velocity of microsaccades in either attention condition. We find no correlation, either across the entire population or across broad spiking cells (Spearman's rank correlation, all p values > 0.05). Finally, we tested whether there was a difference in the magnitude of the unattended M.T.R.I. across the four groups. There was no significant difference (Mann-Whitney U test, all p values > 0.5).

As an additional test, we repeated our burst and attention analyses after removing all action potentials that occurred within 400ms after each detected microsaccade. This did not significantly change any of our findings. This is shown in Figure 2.5C, which shows the distribution of the firing rate attention index among bursty (above) and non-bursty broad spiking neurons (below), calculated after removing the action potentials immediately following microsaccades. As was the case previously, we find that attention induced a significant attention-dependent increase in firing rate among the bursty broad spiking neurons (Wilcoxon signed rank test, $p < 0.00001$) and among the narrow spiking neurons (bursty narrow $p < 0.05$, non-bursty narrow $p < 0.00001$, not shown), but not among the non-bursty broad spiking neurons ($p > 0.8$). Further, attentional modulation among non-bursty broad spiking neurons remained significantly different from the increase in firing rate with attention seen among the bursty broad spiking group (Mann-Whitney U test, $p < 0.005$). We also found that the correlation between B.R.I. and rate A.I. among the broad spiking neurons remained significant (Spearman's non-parametric correlation, $p < 0.05$, $R_s == 0.2530$). Thus, the differences in

attentional modulation between bursty and non-bursty broad spiking neurons we see cannot be attributed to eye movements.

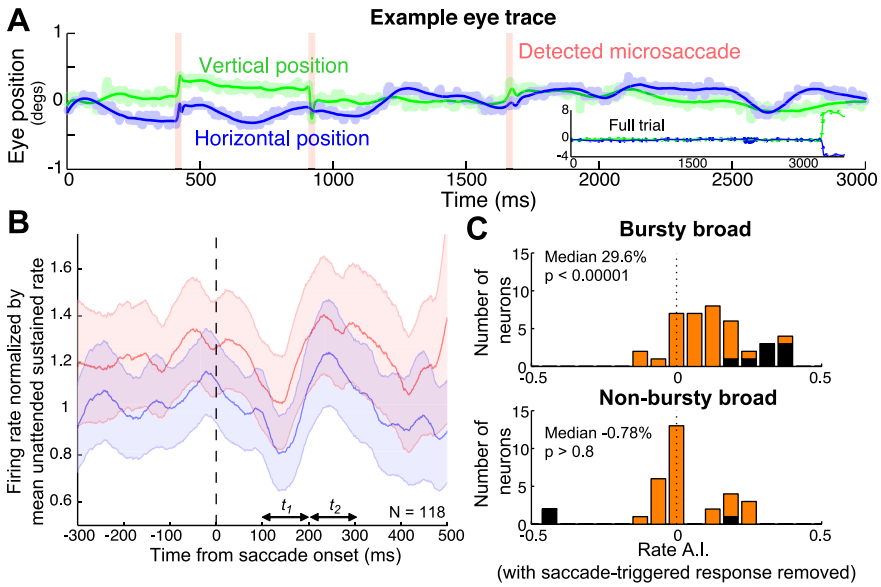

Figure 2.5: Microsaccade-triggered response modulation
A: Single trial example of the saccade detection algorithm (see Methods). Blue and green curves correspond to the model fits of the horizontal and vertical eye position, with shaded lines indicating the raw position traces. Detected microsaccades are indicated by pink vertical bars. Inset shows eye position across the entire trial (including the saccade to the cued stimulus at the end of the trial). *B:* Microsaccade-triggered responses averaged across the entire population. Curves show the population mean of normalized microsaccade-triggered responses to when the stimulus was tracked (red traces) or ignored (blue). Data are smoothed with a Gaussian filter where $\sigma = 25$ms; Shaded regions indicate +/- 1 SEM). *C:* Distribution of the firing rate attention index for the bursty and non-bursty broad spiking groups, calculated after removing all action potentials that occurred within 400 ms after a detected microsaccade. Individually significant units ($p < 0.001$) are shaded black.

2.5 Discussion

The primary goals of this study were to better characterize an aspect of response heterogeneity in macaque Area V4 – burst firing – and determine whether this heterogeneity could help account for variability in attention-dependent rate modulation. We observed considerable variability in burst firing across the population, spanning the gamut from neurons that fire in a manner consistent with a refractory-limited Poisson process to neurons that fire numerous bursts of action potentials. The range of burstiness was particularly pronounced among broad spiking neurons, which were, on average, more bursty than narrow spiking neurons, and which included the most bursty neurons in our population. This is similar to observations in prefrontal and parietal areas by Compte et al. (2003) and Constantinidis and Goldman-Rakic (2002), who report that many of their narrow spiking cells had pronounced relative refractory periods, and found that almost all of their highly bursty cells were broad spiking cells.

Our second main finding is that attentional modulation varied as function of burstiness. Here, we found a clear difference between narrow and broad spiking neurons. There was no evidence for a correlation between burstiness and attentional modulation among narrow spiking neurons, and no significant difference in attentional modulation for narrow spiking neurons classified as bursty versus non-bursty. In contrast, among broad spiking neurons, there is a significant positive correlation between the degree of burstiness and the magnitude of attention-dependent rate modulation. Further, among bursty broad spiking neurons, attention caused a significant median increase in firing rate of (21.7%), as compared to a non-significant change (2.8%) among non-bursty broad spiking neurons. Among bursty broad spiking neurons, all neurons showing individually significant rate modulation with attention showed increases in mean rate, while among non-bursty broad spiking neurons, attention caused both increases and decreases in mean rate. Across our population, significant decreases in firing rate with attention were thus restricted to non-bursty broad spiking neurons. These results therefore lead to the conclusion that variation in the degree of burstiness helps account for the wider range of attentional modulation among broad-spiking neurons, as compared to

narrow-spiking neurons (Mitchell et al., 2007).

2.5.1 Firing rates

There are several potential confounds which could have contributed to the differences in attention-dependent rate modulation we observe between the bursty and non-bursty broad spiking neurons. In particular, if the bursty broad spiking neurons had higher firing rates than the non-bursty broad spiking neurons, our ability to detect attentional modulation among the non-bursty broad spiking neurons could have been impaired relative to the bursty broad spiking neurons. We ruled this out by conducting control analyses in which we compared responses evoked by unattended stimuli. We found no significant difference in median firing rate between these two groups. Further, when we compare high firing rate non-bursty neurons with low firing rate bursty neurons, we continued to see significant differences in attentional modulation between these groups. Thus, we conclude that the differences we observe are not a rate artifact.

2.5.2 Threshold for burstiness

A second potential concern was that the differences we see between bursty and non-bursty broad spiking cells might potentially have depended on the particular threshold we used to define the boundary between these two groups. We addressed this by examining the data without dividing neurons into bursty and non-bursty groups. In this analysis we tested whether there is a significant correlation between the degree of burstiness and attention-dependent firing rate modulation. We found that among broad spiking neurons, there was a significant positive correlation between burstiness and attention-dependent increases in firing rate. Thus, attentional modulation increased as a function of burstiness, independent of the boundary we set between bursty and non-bursty neurons. We also validated this by repeating the analysis using a different burstiness metric that was normalized by mean firing rate. Again, there was a significant correlation for broad spiking neurons, but not for narrow spiking neurons.

2.5.3 Eye movements

The final possible confound we ruled out was whether there were differences in eye movements or in eye-movement-triggered responses that could underlie the differences in attentional modulation we observed. These possibilities struck us as unlikely in light of the fact that many of the bursty and non-bursty neurons were recorded simultaneously, and were therefore subject to identical eye movements. However, to address this directly, we determined that there were no differences in the number, direction, or velocity of microsaccades across broad-spiking and narrow-spiking neurons. As a final control, we re-analyzed the data after removing spikes recorded after microsaccades. The relationship between burst firing and attention-dependent rate modulation remained significant.

The relationship between attentional modulation and burstiness reflects intrinsic cell properties Previous studies have found that attentional modulation can vary markedly as a function of stimulus conditions such as where the stimulus falls along a neuron's contrast response function (Reynolds et al., 2000; Reynolds and Chelazzi, 2004; Williford and Maunsell, 2006; Reynolds and Heeger, 2009). Variation in these factors may have contributed to the heterogeneity of burst firing and attentional modulation we observed. However, the heterogeneity we observe is preserved across stimulus conditions, suggesting that it is due to intrinsic cell properties. In particular, we found that burstiness in the stimulus-evoked period was very strongly correlated with burstiness in the pre-stimulus period, when no stimuli were present. Further, the degree of burstiness during this pre-stimulus period was correlated with attentional modulation of firing rate during the later stimulus-evoked response period. Therefore, we conclude that differences in stimulus-evoked response properties cannot account for the present results.

We find a related pattern of results for burstiness, with substantial variability in the degree of burstiness within the same session. B.R.I. values of simultaneously recorded broad spiking neurons were not correlated with one another ($N = 52$ pairs, $p > 0.1$, $R_s = 0.12$). We thus conclude that much of the heterogeneity we observe is due to differences in the neurons themselves, such as their intrinsic membrane properties or their place in the cortical circuit.

2.5.4 Potential anatomical correlates

Given the differences in attentional modulation between bursty and non-bursty broad spiking neurons, it is tempting to speculate that these may correspond to anatomically distinct classes of neurons. Intracellular recording studies have used burstiness as one of the key metrics to distinguish among classes of neurons, including "intrinsically bursting" (IB) neurons, pyramidal neurons that emit short bursts of action potentials (McCormick et al., 1985; Connors and Gutnick, 1990). A substantial portion of these neurons occupy layer V and project to the superior colliculus and the pontine nucleus (Agmon and Connors, 1992; Wang and McCormick, 1993; Kasper et al., 1994). These can be distinguished from another class of bursting neurons, called "chattering cells" or "fast rhythmic bursting" cells, which have been found in layers II/III of ferret and cat cortex, and which exhibit narrow action potentials (Brumberg et al., 2000; Nowak et al., 2003). Though less common in our dataset, we did observe some narrow spiking neurons with significant burst firing. These should be distinguished from narrow spiking neurons that lack burst firing, which are instead likely to correspond to fast-spiking interneurons. One recent study (Katai et al., 2010) has used spiking statistics to distinguish among four different cell classes in the frontal cortex of the behaving primate. Their study identified these with classes previously defined in slice (intrinsically bursting (IB), regular spiking (RS), fast spiking (FS), and fast rhythmic bursting (FRB)). However, we do not find evidence, in V4, for distinct classes of bursting and non-bursting neurons. The range of bursting behavior in V4 appears to fall along a continuum, as has also been seen in Area MT (Bair et al., 1994). Therefore, while variability in burst firing can help account for variability in attentional modulation, our data do not allow us to conclude that the bursty broad spiking neurons we find modulated by attention constitute a distinct class of neurons.

Nonetheless, it would be of significant value to determine whether bursty and non-bursty broad spiking neurons recorded in the awake primate do, in fact, correspond to anatomically distinct classes of neurons. If they do, understanding where these neurons fit into the local cortical circuit could lead to major new insights into the role of attentional modulation of visual cortical neurons. If, for

example, the bursty broad spiking neurons that we find are modulated by attention correspond to layer V intrinsically bursty neurons this would, by virtue of their corticotectal projection patterns, implicate attentional modulation of Area V4 neurons as playing a role in modulating sensory input to the oculomotor system, rather than the more traditional view that attention serves to modulate ascending sensory signals as they progress from V4 to higher order visual areas. Further, since layer V corticotectal neurons correspond to tall-tufted pyramidal neurons, this would suggest that the laminar distribution of attentional feedback signals are directed toward the layers from which these pyramidal neurons receive input (Kasper et al., 1994; Larsen et al., 2008).

This chapter, in full, is a reprint of the following article in press: Emily B. Anderson, Jude F. Mitchell, John H. Reynolds (2011) Attentional modulation of firing rate varies with burstiness across putative pyramidal neurons in macaque visual Area V4. Journal of Neuroscience, *in press*. The article was reformatted to meet the style requirements for inclusion in the dissertation. The dissertation author was the principle researcher and author of this work.

2.6 References

Agmon A, Connors BW (1992) Correlation between intrinsic firing patterns and thalamocortical synaptic responses of neurons in mouse barrel cortex. J Neurosci 12:319-329.

Bair W, Koch C, Newsome W, Britten K (1994). Power spectrum analysis of bursting cells in are MT in the behaving monkey. J Neurosci 14:2870-92.

Barthò P, Hirase H, Monoconduit L, Zugaro M, Harris KD, Buzsáki G (2004) Characterization of neocortical principal cells and interneurons by network interactions and extracellular features. J Neurophysiol 92:600-608.

Brumberg JC, Nowak LG, McCormick DA (2000) Ionic mechanisms underlying repetitive high-frequency burst firing in supragranular cortical neurons. J Neurosci 20:4829-4843.

Cavanagh P, Alvarez GA (2005) Tracking multiple targets with multifocal attention. Trends Cogn Sci 9:349-354.

Compte A, Constantinidis C, Tegnér J, Raghavachari S, Chafee MV, Goldman-Rakic PS, Wang X-J (2003) Temporally irregular mnemonic persistent activity in prefrontal neurons of monkeys during a delayed response task. J Neurophysiol 90:3441-3454.

Connors BW, Gutnick MJ (1990) Intrinsic firing patterns of diverse neocortical neurons. Trends Neurosci 13:99-104.

Constantinidis C, Goldman-Rakic PS (2002) Correlated discharges among putative pyramidal neurons and interneurons in primate prefrontal cortex. J Neurophysiol 88:3487-3497.

Friedman-Hill S, Maldonado PE, Gray CM (2000) Dynamics of striate cortical activity in the alert macaqu*E:* I. Incidence and stimulus-dependence of gamma-band neuronal oscillations. Cereb Cortex 10:1105-1116.

Gur M, Snodderly DM (2006) High response reliability of neurons in primary visual cortex (V1) of alert, trained monkeys. Cereb Cortex 16:888-895.

Gur M, Beylin A, Snodderly DM (1997) Response variability of neurons in primary visual cortex (V1) of alert monkeys. J Neurosci 17:2914-2920.

Joelving FC, Compte A, Constantinidis C (2007) Temporal properties of posterior parietal neuron discharges during working memory and passive viewing. J Neurophysiol 97:2254-2266.

Kasper EM, Larkman AU, Lubke J, Blakemore C (1994) Pyramidal neurons in layer 5 of the rat visual cortex. I. Correlation among cell morphology, intrinsic electrophysiological properties, and axon targets. J Comp Neurol 339:459-474.

Katai S, Kato K, Unno S, Kang Y, Saruwatari M, Ishikawa N, Inoue M, Mikami A (2010) Classification of extracellularly recorded neurons by their discharge patterns and their correlates with intracellularly identified neuronal types in the frontal cortex of behaving monkeys. Eur J Neurosci 31:1322-1338.

Knudsen EI (2007) Fundamental components of attention. Annu Rev Neurosci 30:57-78.

Larsen DD, Wickersham IR, Callaway EM (2008) Retrograde tracing with recombinant rabies virus reveals correlations between projection targets and dendritic architecture in layer 5 of mouse barrel cortex. Front Neural Circuits 1:5.

Leopold DA, Logothetis NK (1998) Microsaccades differentially modulate neural activity in the striate and extrastriate visual cortex. Exp Brain Res 123:341-345.

Maimon G, Assad JA (2009) Beyond Poisson: increased spike-time regularity across primate parietal cortex. Neuron 62:426-440.

Martinez-Conde S, Macknik SL, Hubel DH (2004) The role of fixational eye movements in visual perception. Nature Rev Neurosci 5: 229-240.

McCormick DA, Connors BW, Lighthall JW, Prince DA (1985) Comparative electrophysiology of pyramidal and sparsely spiny neurons of the neocortex. J Neurophysiol 54:782-806.

Mitchell JF, Sundberg KA, Reynolds JH (2007) Differential attention-dependent response modulation across cell classes in macaque visual area V4. Neuron 55:131-141.

Mitchell JF, Sundberg KA, Reynolds JH (2009) Spatial attention decorrelates intrinsic activity fluctuations in macaque area V4. Neuron 63:879-888.

Nowak LG, Azouz R, Sanchez-Vives MV, Gray CM, McCormick DA (2003) Electrophysiological classes of cat primary visual cortical neurons in vivo as revealed by quantitative analyses. J Neurophysiol 89:1541-1566.

Pylyshyn ZW, Storm RW (1988) Tracking multiple independent targets: Evidence for a parallel tracking mechanism. Spat Vis 3:179-197.

Reynolds JH, Chelazzi L (2004) Attentional modulation of visual processing. Ann Rev of Neurosci 27:611-647.

Reynolds JH, Heeger DJ (2009) The normalization model of attention. Neuron 61(2):168-85.

Reynolds JH, Pasternak T, Desimone R (2000) Attention Increases Sensitivity of V4 Neurons. NeuronÊ 26:703-714

Ringach DL, Hawken MJ, Shapley R (1997) Dynamics of orientation tuning in macaque primary visual cortex. Nature 387:281-284.

Sears CR, Pylyshyn ZW (2000) Multiple object tracking and attentional processing. Can J Exp Psychol 54:1-14.

Shadlen MN, Newsome WT (1998) The variable discharge of cortical neurons: implications for connectivity, computation, and information coding. J Neurosci 18: 3870-96.

Softky WR, Koch C (1993) The highly irregular firing of cortical cells is inconsistent with temporal integration of random EPSPs. J Neurosci 13: 334-50.

Sundberg KA, Mitchell JF, Reynolds JH (2009) Spatial attention modulates center-surround interactions in macaque visual area V4. Neuron 61:952-963.

Tolhurst DJ, Movshon JA, Dean AF (1983) The statistical reliability of signals in single neurons in cat and monkey visual cortex. Vision Res 23: 775-85.

Treue S (2003) Visual attention: the where, what, how and why of saliency. Curr Opin Neurol 14:744-751.

Wang Z, McCormick DA (1993) Control of firing mode of corticotectal and corticopontine layer V burst-generating neurons by norepinephrine, acetylcholine, and 1S,3R-ACPD. J Neurosci 13:2199-2216.

Williford T, Maunsell JHR (2006) Effects of spatial attention on contrast response functions in macaque area V4. J Neurophysiol 96:40-54.

Chapter 3

Differences in action potential adaptation between broad and narrow spiking neurons in macaque Area V4

3.1 Abstract

In this chapter, I consider the hypothesis that if narrow spiking neurons correspond to fast-spiking inhibitory interneurons, then there should be limited action potential frequency and amplitude adaptation among this group compared to the broad spiking population. Here, I report the first evidence for spike frequency, height, and duration adaptation in the awake macaque, and find greater spike height and frequency adaptation among broad spiking neurons. I continued to see differences in adaptation between narrow and broad spiking neurons when I compared conditions matched in their preceding interspike intervals. This finding further validates the use of the narrow and broad spiking classification. In addition, this approach may provide a means for inferring the internal state of pyramidal neurons in the behaving animal, which could provide insight into how these neurons integrate synaptic inputs, generate bursts of action potentials, and influence their postsynaptic partners.

3.2 Introduction

Distinguishing between different neural cell classes can provide value insight into circuit mechanisms, but remains a challenge in extracellular recordings. One approach has been to characterize differences in the physiological properties of identified neuronal cell types, and then apply these physiological distinctions towards inferring neuronal identity in extracellular recordings (Nowak et al., 2003; Gonzàlez-Burgos et al., 2005.) A mainstay of this approach has been to exploit differences in action potential shape between different classes of neurons (Bean, 2007). For example, intracellular studies have shown that the ability to fire action potentials of short duration is restricted to classes of neurons that express specific ion channels, such as the parvalbumin positive fast-spiking inhibitory interneurons (Erisir et al, 1999). As discussed in section 1.1, this difference in action potential shape has allowed numerous studies to distinguish between narrow spiking (putative interneurons) and broad spiking (putative pyramidal) neurons.

Another difference in physiological responses among cortical cell classes is the degree to which their action potentials adapt in frequency, amplitude, and duration. While pyramidal neurons show consistent adaptation in response to sustained or repeated input, fast-spiking inhibitory interneurons exhibit little or no accommodation (McCormick et al., 1985; Martina and Jonas, 1997; Cauli et al., 1997; Nowak et al., 2003; Gonzàlez-Burgos et al., 2005). As described in greater detail in the discussion, this difference in adaptation has been shown to arise largely from differences in the dynamics of the potassium channels expressed by these classes of neurons (Colbert et al., 1997; Jung et al., 1997; Martina and Jonas, 1997; Remy et al., 2009). I wondered whether this difference in adaptation could further enhance our ability to distinguish between these neuronal populations. Here, I report significant spike waveform amplitude, duration, and frequency adaptation in extracellular recordings in area V4 of the awake macaque. Further, when I divide the population into broad spiking and narrow spiking, I find significantly greater action potential amplitude and frequency adaptation among the broad spiking neurons. I also find a significant correlation between waveform duration and the adaptation of spike amplitude. I continued to see differences in spike amplitude

adaptation between narrow and broad spiking neurons when I compared conditions matched in their preceding interspike intervals. Together, these findings provide further validation of the use of spike waveform duration as a method to distinguish between cortical cell classes, and may provide a glimpse into the internal state of these neurons.

3.3 Methods

3.3.1 Electrophysiology, receptive field characterization, task, and stimuli

All procedures were approved by the Salk Institute Institutional Animal Care and Use Committee (IACUC) and conformed to NIH guidelines for the humane care and use of animals in research. Monkeys were prepared for neuronal recording following procedures described in Chapter 2. After finding an isolated unit, a subspace reverse correlation procedure (described in section 2.3.1) was used to identify the receptive field location and stimulus features that would activate the neuron. After the completion of the receptive field mapping procedure, the animals performed an attention-demanding track task (depicted in Figure 2.1, and described in greater detail in sections 2.3.2 and 2.3.3). This task provided a means to direct attention toward or away from a stimulus positioned within the neurons' receptive fields, but data analyzed within this chapter will be averaged over both behavioral conditions. During the task, the animals foveated a central fixation point while a colored Gabor stimulus swept into the receptive field, paused for 1000 ms, and finally moved out of the receptive field. Unless otherwise specified, analysis of spiking statistics was restricted to the final 800 ms of the period when the stimulus paused within the receptive field (the "sustained period") corresponding to a period when the neurons had fairly stable firing activity above baseline levels.

3.3.2 Inclusion criteria

I analyzed 206 well-isolated neurons from two male monkeys (N = 53 Monkey B, N = 153 Monkey M). Analyses were restricted to units whose response on trials when attention was directed away from the receptive field exceeded 5 Hz, averaged over the final 500 ms of the stimulus pause period, and was significantly greater than the mean spontaneous firing rate averaged over the 250 ms preceding the onset of the Gabor stimuli (Mann-Whitney U test, $p < 0.05$). This resulted in 84 neurons being excluded. In addition, four units were excluded because their waveforms did not have the typical biphasic shape, with a trough followed by a clearly defined peak, and they could not therefore be classified as narrow or broad-spiking. Finally, three units were excluded because only the mean waveform data was available. In total, 115 neurons met these selection criteria.

3.3.3 Broad and narrow spiking classification

As described previously (Mitchell et al., 2007, and chapter 2), I divided neurons into narrow and broad spiking subpopulations based on waveform duration (Figure 2.3). Waveform duration was defined to be the time from the trough to the peak of the average waveform (Mitchell et al., 2007). The distribution of spike waveform duration was significantly bimodal across all isolated cells with biphasic spike waveforms (N = 202, Hartigan's dip test, $p < 0.0001$), and also across the subset of these cells with significant visual responses (N = 115, Hartigan's dip test, $p < 0.01$). Narrow and broad spiking neurons were separated based on the trough between the two modes of the waveform duration distribution, with narrow spiking neurons defined as those ranging in duration from 100 to 224 μs and broad-spiking neurons defined as those ranging in duration from 225 to 500 μs.

3.4 Results

I characterized the action potential waveforms of 115 visually-driven neurons in area V4, in two macaques as they performed the multi-object tracking task depicted in Figure 2.1. I then examined the activity-dependence of action potential

shape and timing of these neurons.

3.4.1 Action potential height and duration depends on preceding interspike interval

Many neurons in our population elicit action potentials with waveform shapes that depend on the preceding interspike interval. An example of this history dependence is shown in Figure 3.1. Here, the action potential waveforms of an individual highly bursty broad spiking neuron are divided into five groups depending on their preceding interspike interval (preISI). The most prominent difference between these groups of action potentials is a change in the depth of the trough of the waveform, with action potentials immediately following an action potential showing a reduction in trough depth relative to action potentials following a long period of quiescence. The differences in action potential waveform troughs of between each of these five groups are highly significant (Mann-Whitney U test, all p values « 0.0001), with the exception of the comparison between group 1 (preISI 0-2ms) and group 2 (preISI 2-4ms). I also computed the height of the action potentials (defined as the difference between the peak and the trough). As before, I found significant differences between all of the five groups (Mann-Whitney U test, all p values < 0.0001), with the exception of the comparison between groups 1 and 2, where I found a marginally significant difference ($p < 0.05$).

In addition to the history-dependent changes in spike height, the example neuron in Figure 3.1 also exhibited a history-dependent change in the duration of action potentials: action potentials with short preISIs had broader waveforms compared to action potentials with longer preISIs. This difference in duration was significant between group 1 and groups 4 and 5, group 2 and groups 4 and 5, and group 3 and groups 4 and 5 (Mann-Whitney U test, all p values < 0.01).

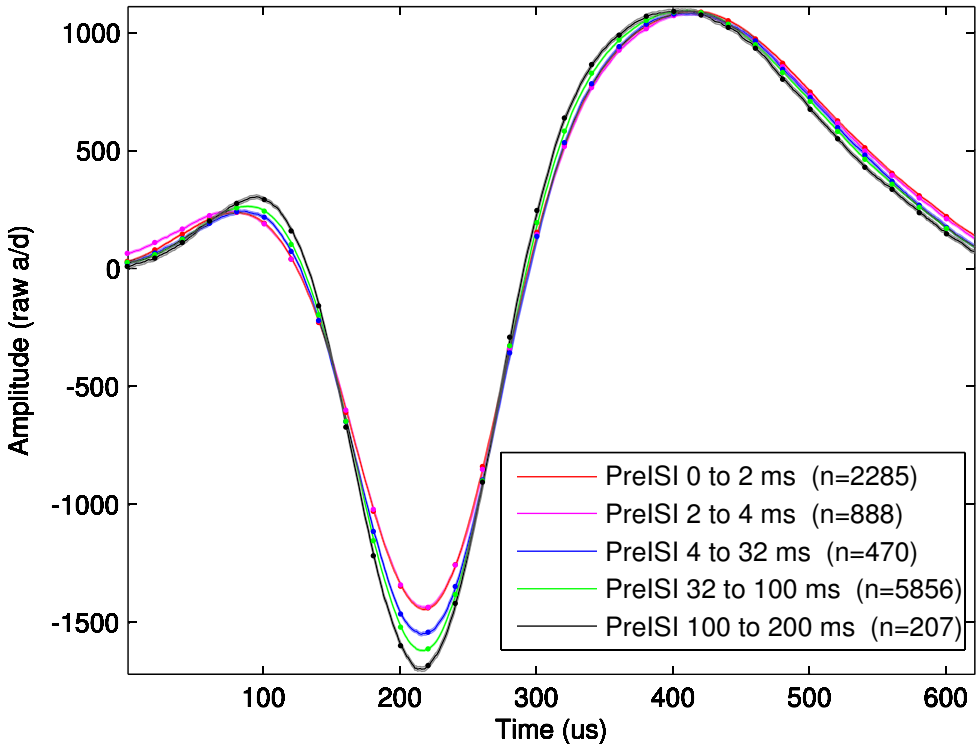

Figure 3.1: The shape of the action potential waveforms of example neuron mbbag52_u1 depends on preceding interspike interval
Each trace corresponds to the mean waveform of the action potentials in the sustained stimulus period with a preceding interspike interval with the range specified by the table legend. The waveforms were spline-interpolated from 25 μs to a resolution of 0.05 μs; dots correspond to the mean of the raw waveform a/d. Thin shaded regions correspond to +/- 1 SEM of the interpolated waveform traces.

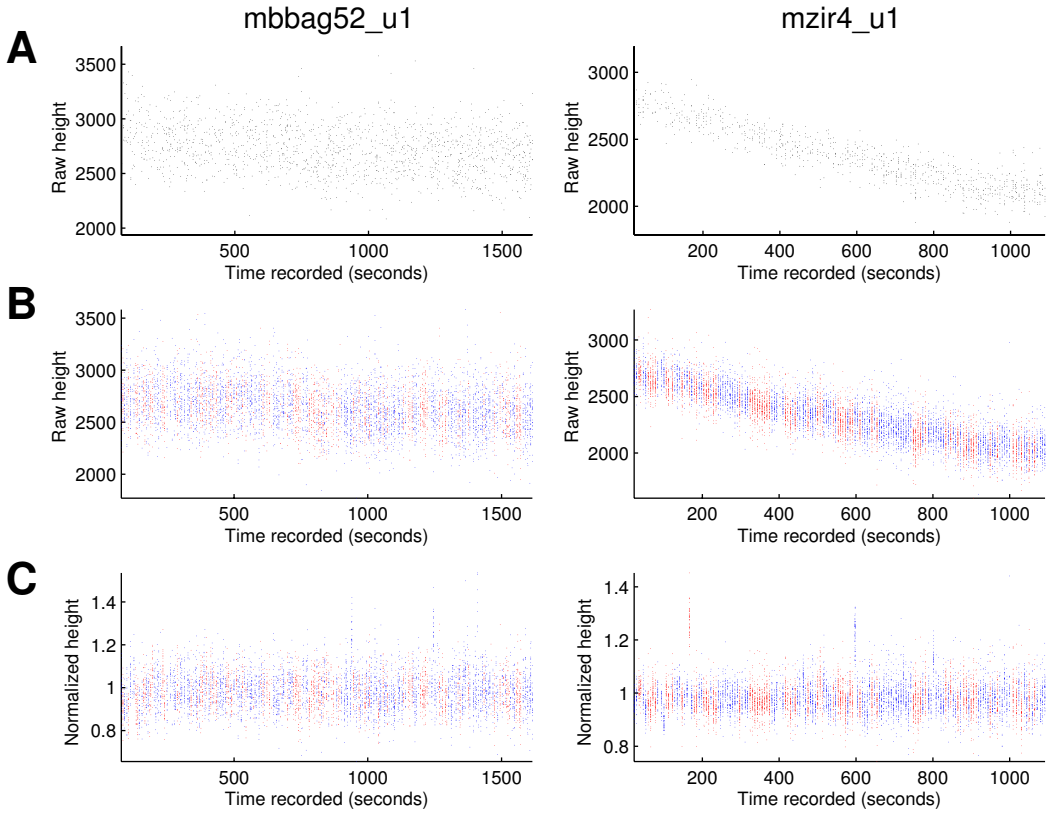

Figure 3.2: Long timescale drift in extracellular amplitude
First column corresponds to example neuron mbbag52_u1, second column corresponds to example neuron mzir4_u1. *A:* Raw height of action potentials in the pre-stimulus spontaneous period. *B:* Raw height of action potentials in stimulus sustained period. *C:* Raw height of action potentials in the stimulus sustained period, normalized on a trial-by-trial basis by the mean raw height in the preceding spontaneous period. In *B* and *C*, red dots correspond to action potentials in correct attend trials, and blue dots correspond to action potentials in correct ignore trials.

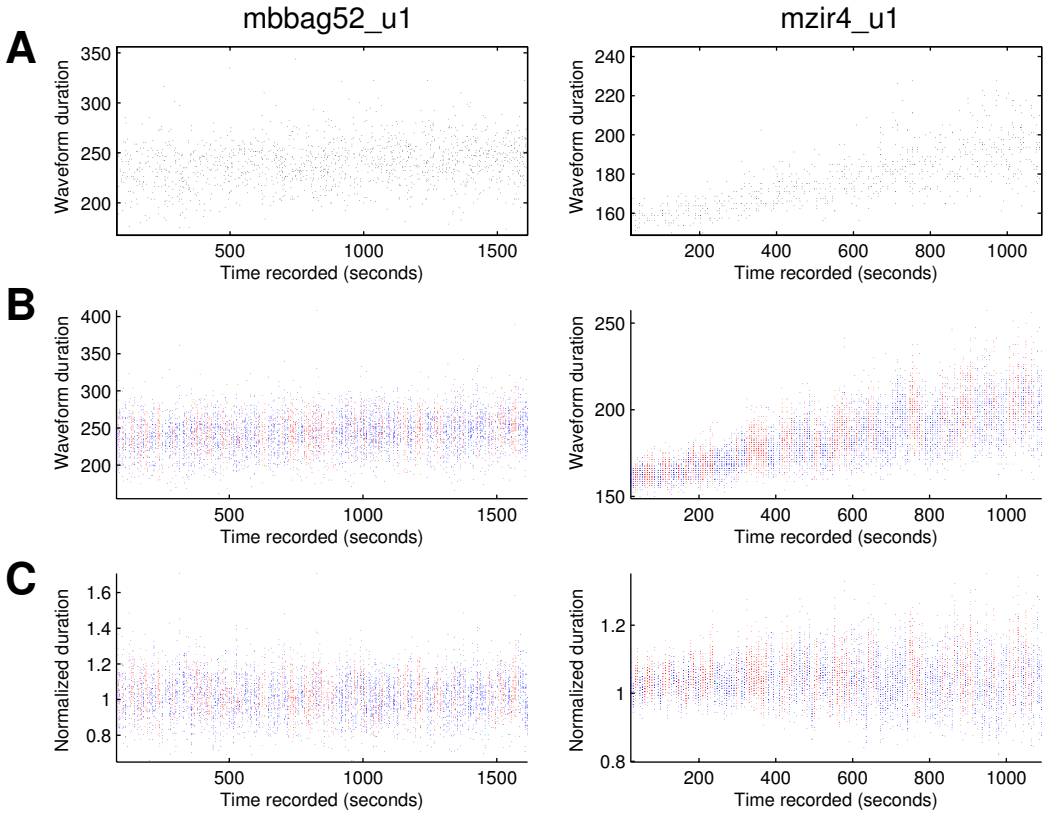

Figure 3.3: Long timescale drift in extracellular duration
First column corresponds to example neuron mbbag52_u1, second column corresponds to example neuron mzir4_u1. *A:* Duration between peak and trough (μs) of spline-interpolated action potentials in the pre-stimulus spontaneous period. *B:* Duration of action potentials in stimulus sustained period. *C:* Duration of action potentials in the stimulus sustained period, normalized on a trial-by-trial basis by the mean duration in the preceding spontaneous period. In *B* and *C*, red dots correspond to action potentials in correct attend trials, and blue dots correspond to action potentials in correct ignore trials.

The position of an extracellular electrode relative to the neuron(s) it records varies over time. To determine whether this positional drift resulted in a long timescale change in action potential shape, I examined whether the height and duration of action potential waveforms varied over time. In general, neurons did show slow changes in action potential height and duration, but for most neurons (such as the first example neuron in Figures 3.2 and 3.3), this drift was modest compared to the variance in action potential height and duration within individual trials. However, some neurons did show pronounced changes in height and duration over time. The second example neuron in Figures 3.2 and 3.3 is one of the most extreme examples of this drift in waveform shape.

I controlled for the effect of this long timescale drift in two ways. First, I normalized the height and duration of the action potential waveforms, on a trial-by-trial basis, by the mean height and duration of the action potential waveforms in the preceding pre-stimulus spontaneous period. The result of this normalization is shown for the two example neurons in the bottom panels of 3.2 and 3.3. Second, I computed height and duration adaptation ratios, where the height or duration of an individual action potential is normalized by that of the preceding action potential. A comparison of the distributions of these normalized metrics with the raw, unnormalized metrics for an example neuron is shown in Figures 3.4 and 3.5. The main pattern of results for this neuron remains the same across the unnormalized and normalized height and duration measures: the neuron exhibits significant reductions in waveform amplitude and significant increases in waveform duration for action potentials with short preISIs compare to those with long preISIs.

To further characterize the dependence of action potential shape on preceding interspike interval, I tested whether there was a significant relationship between interspike interval and the height and duration adaptation ratios. Figure 3.6 shows this relationship for an example neuron, with the mean values of the preISI groups from Figures 3.4 and 3.5 superimposed for comparison. This individual neuron has a highly significant correlation between preISI and height adaptation (Spearman's non-parametric correlation, $p \ll 0.001$, $R_s = 0.54$) as well as a between preISI and duration adaptation ($p \ll 0.001$, $R_s = -0.13$).

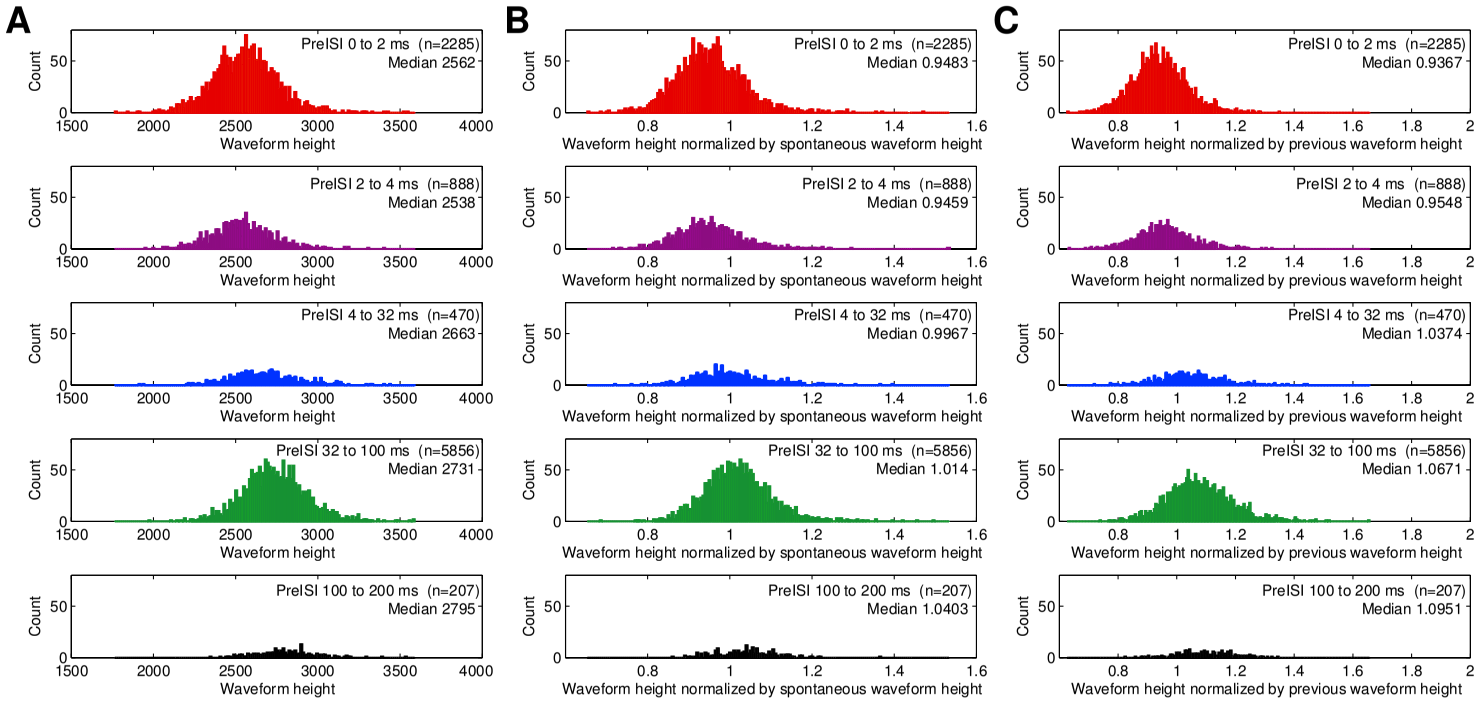

Figure 3.4: Comparison of three spike amplitude metrics applied to example neuron mbbag52_u1
Each row contains the action potentials in the sustained period with a preceding interspike interval within a specified range (same as Figure 3.1). *A:* Distribution of raw waveform heights, computed by taking the maximum raw a/d value minus the minimum raw a/d value. *B:* Distribution of the raw waveform heights normalized, on a trial-by-trial basis, by the mean raw waveform height in the preceding spontaneous period. *C:* Distribution of the raw waveform heights normalized by the raw waveform height of the preceding action potential.

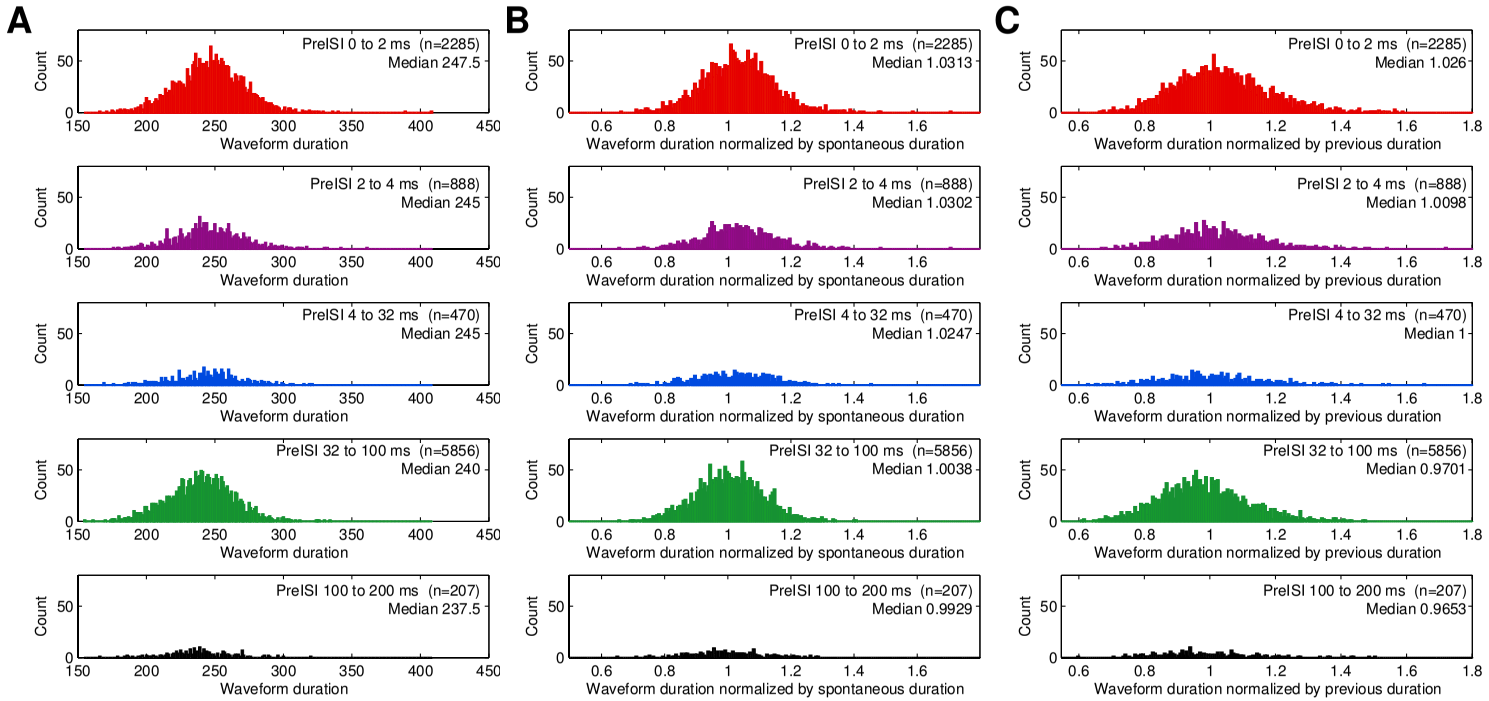

Figure 3.5: Comparison of three spike duration metrics applied to example neuron mbbag52_u1
Each row contains the action potentials in the sustained period with a preceding interspike interval within a specified range (same as Figure 3.1). *A:* Distribution of waveform durations, computed by taking the time between the peak and the trough of the interpolated waveform. *B:* Distribution of the waveform durations normalized, on a trial-by-trial basis, by the mean waveform duration in the preceding spontaneous period. *C:* Distribution of the waveform durations normalized by the waveform duration of the preceding action potential.

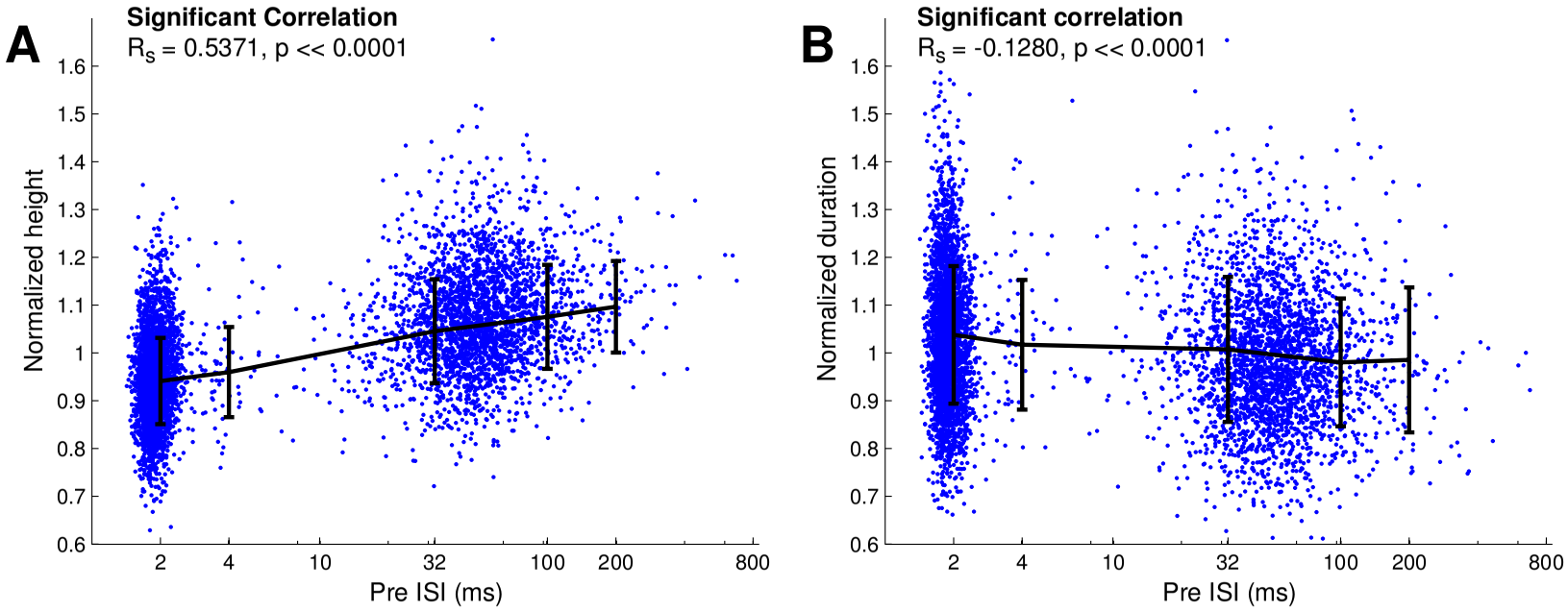

Figure 3.6: Preceding interspike interval predicts waveform amplitude and duration adaptation in example neuron mbbag52_u1

A: Highly significant correlation between preceding interspike interval and action potential height normalized by preceding action potential height (Spearman's non-parametric correlation, $R_s = 0.54$, p « 0.0001). Black points correspond to the mean normalized height from action potentials with preceding interspike intervals with the ranges defined in Figure 3.1. Error bars correspond to +/- 1 STD. *B:* Highly significant correlation between preceding interspike interval and action potential duration normalized by preceding action potential duration (Spearman's non-parametric correlation, R_s = -0.13, p « 0.0001).

Across the entire population, 64 neurons (55.6%) showed a significant correlation between preISI and height adaptation (Spearman's non-parametric correlation, $p < 0.001$). All of these significantly adapting neurons showed a positive correlation (median $R_s = 0.16$), indicating a reduction in height for action potentials with short preISIs. I also found that the distribution of preISI-height R_s values across the entire population was significantly greater than zero (Wilcoxon signed rank test, $p \ll 0.0001$, median $R_s = 0.09$). Similarly, 32 neurons (27.8%) showed a significant correlation between preISI and duration adaptation (Spearman's non-parametric correlation, $p < 0.001$), and that all of but one of these neurons showed a negative correlation (median $R_s = -0.14$), indicating broadening of action potentials with short preISIs. 28 of these neurons (87.5%) also showed significant spike height adaptation. Across the entire population, the distribution of preISI-duration R_s values was significantly less than zero (Wilcoxon signed rank test, $p \ll 0.0001$, median $R_s = -0.04$). Together, these results provide the first evidence that neurons within area V4 of the awake macaque exhibit spike amplitude and spike duration accommodation.

3.4.2 Broad spiking neurons show stronger action potential height adaptation than narrow spiking neurons

Since intracellular studies have reported that fast-spiking inhibitory interneurons show less spike amplitude adaptation than pyramidal neurons, I wondered whether I might also see differences in spike amplitude accommodation between our narrow spiking population (putative fast-spiking interneurons, N=45) and broad spiking population (putative pyramids, $N = 70$). To test this, I first compared the distribution of preISI-height R_s values between the two classes. While both populations have a significant relationship between preISI and height adaptation, broad spiking neurons show a significantly stronger relationship than narrow spiking neurons (Mann-Whitney U test, $p \ll 0.0001$, broad median $R_s = 0.14$, narrow median $R_s = 0.03$). Among broad spiking neurons, 70% ($N = 49$) have a significant preISI-height relationship ($p < 0.001$). In contrast, only a third ($N = 15$) of narrow spiking neurons had significant preISI-height R_s values. Further, as

shown in Figure 3.7, there is also a significant correlation between action potential duration and preISI-height R_s values (Spearman's non-parametric correlation, $p < 0.0001$, $R_s = 0.49$).

In addition to relationship between spike waveform duration and spike height adaptation, there is also a strong relationship between the burstiness of neurons (B.R.I.) and spike height adaptation (Figure 3.8). This was true both when B.R.I. was correlated with the preISI-height R_s values ($p \ll 0.0001$, $R_s = -0.65$), and when B.R.I. was correlated with the mean adaptation ratio of all pairs of spikes with an ISI of 10ms ($p < 0.0001$, $R_s = -0.51$). This relationship between burstiness and spike height adaptation is perhaps unsurprising, given the strong dependence of spike height adaptation on interspike interval. Since the strongest spike height adaptation is seen between spikes with very short ISIs, we would expect to see a great deal of spike height adaptation between spikes within a burst.

Since broad spiking neurons are significantly more bursty than narrow spiking neurons (see Figure 2.3), I wondered whether differences in the burstiness of these populations might account for the difference in height adaptation. However, a significant partial correlation reveals a continued relationship between waveform duration and preISI-dependent height adaptation even after differences in burstiness are taken into consideration (Spearman's partial correlation, $p < 0.0001$, $R_s = 0.36$).

Figure 3.7: Significant correlation between waveform duration and height adaptation

(facing page)

A: Significant correlation between waveform duration and height adaptation (Spearman's non parametric correlation, $p < 0.0001$, R_s = -0.41). The difference between height adaptation among narrow and broad spiking neurons is also significant (Mann U Whitney test, $p < 0.0001$). For each neuron, height adaptation calculated by taking the mean of the ratio of the height between a spike and its predecessor, for all spikes that followed a spike within 10ms. Darker symbols correspond to significant height adapting neurons (neurons with a significant correlation between pre interspike interval and the normalized height ($p < 0.001$)). *B:* Significant correlation between waveform duration and the preISI-height R_s value (Spearman's non-parametric correlation, $p < 0.0001$, $R_s = 0.49$). Height adaptation for each neuron calculated by taking the Spearman R_s value for the non-parametric correlation between pre-interspike interval and the waveform height normalized by the previous spike height. Darker symbols correspond to significant height adapting neurons.

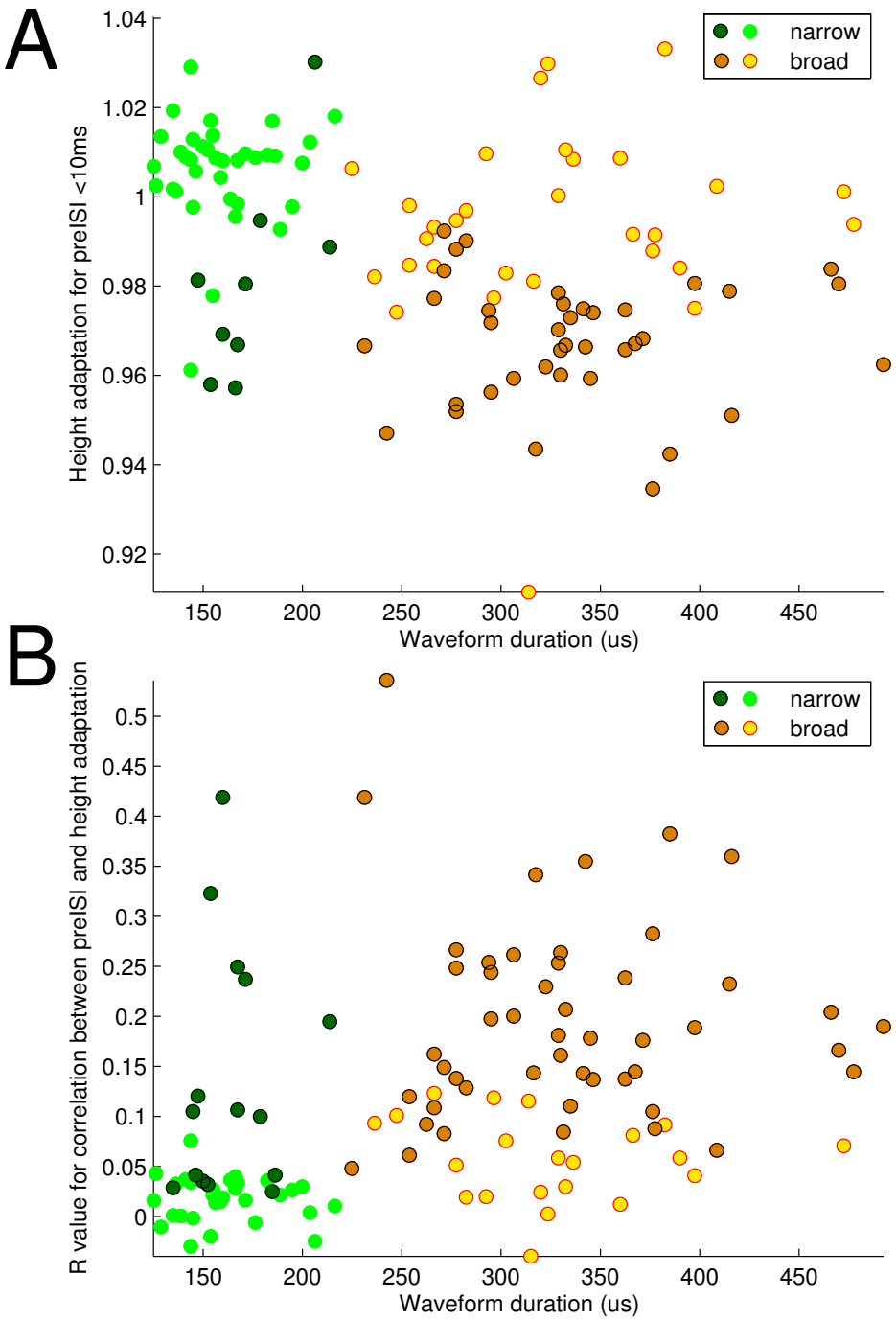
A
narrow
broad
Height adaptation for preISI <10ms
1.04
1.02
1
0.98
0.96
0.94
0.92
150
200
250
300
350
400
450
Waveform duration (us)
B
narrow
broad
R value for correlation between preISI and height adaptation
0.5
0.45
0.4
0.35
0.3
0.25
0.2
0.15
0.1
0.05
0
150
200
250
300
350
400
450
Waveform duration (us)

Figure 3.8: Significant correlation between burstiness (B.R.I.) and height adaptation

(facing page)

A: Significant correlation between burstiness and height adaptation (Spearman's non parametric correlation, $p < 0.0001$, R_s = -0.51). For each neuron, height adaptation calculated by taking the mean of the ratio of the height of a spike and that of its predecessor, for all spikes that followed a spike within 10ms. Darker symbols correspond to neurons with significant height adaptation for all spikes with a preISI < 10ms ($p < 0.001$). *B:* Significant correlation between burstiness the preISI-height R_s value (Spearman's non parametric correlation, p « 0.0001, $R_s = 0.65$). Height adaptation for each neuron calculated by taking the Spearman R_s value for the non-parametric correlation between pre-interspike interval and the waveform height normalized by the previous spike height. Relationship remains significant if median preISI is considered (Spearman's partial correlation, p « 0.0001, $R_s = 0.66$). Darker symbols correspond to neurons with a significant correlation between pre interspike interval and the normalized height ($p < 0.001$).

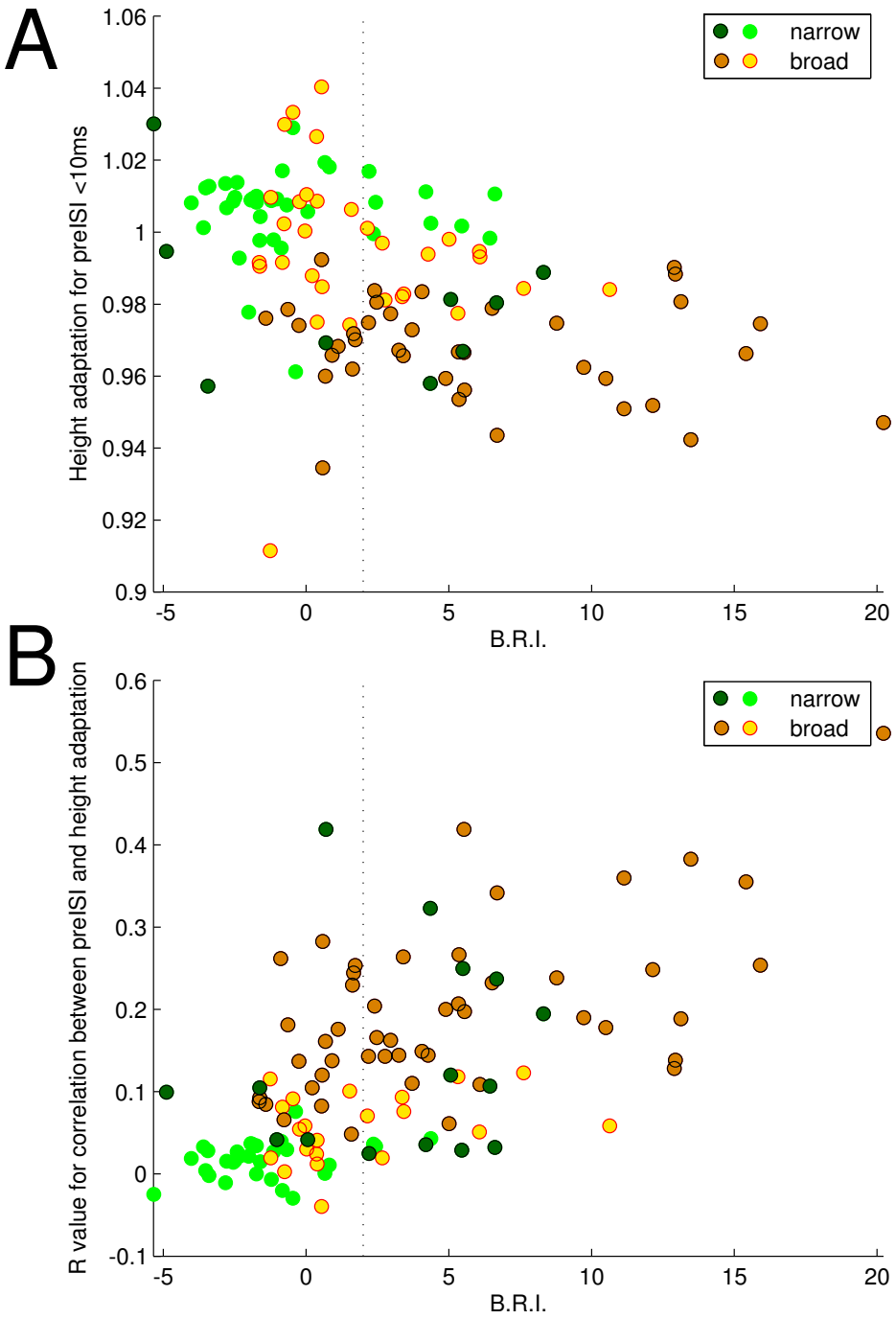
A
narrow
broad
Height adaptation for preISI <10ms
1.06
1.04
1.02
1
0.98
0.96
0.94
0.92
0.9
-5
0
5
10
15
20
B.R.I.
B
narrow
broad
R value for correlation between preISI and height adaptation
0.6
0.5
0.4
0.3
0.2
0.1
0
-0.1
-5
0
5
10
15
20
B.R.I.

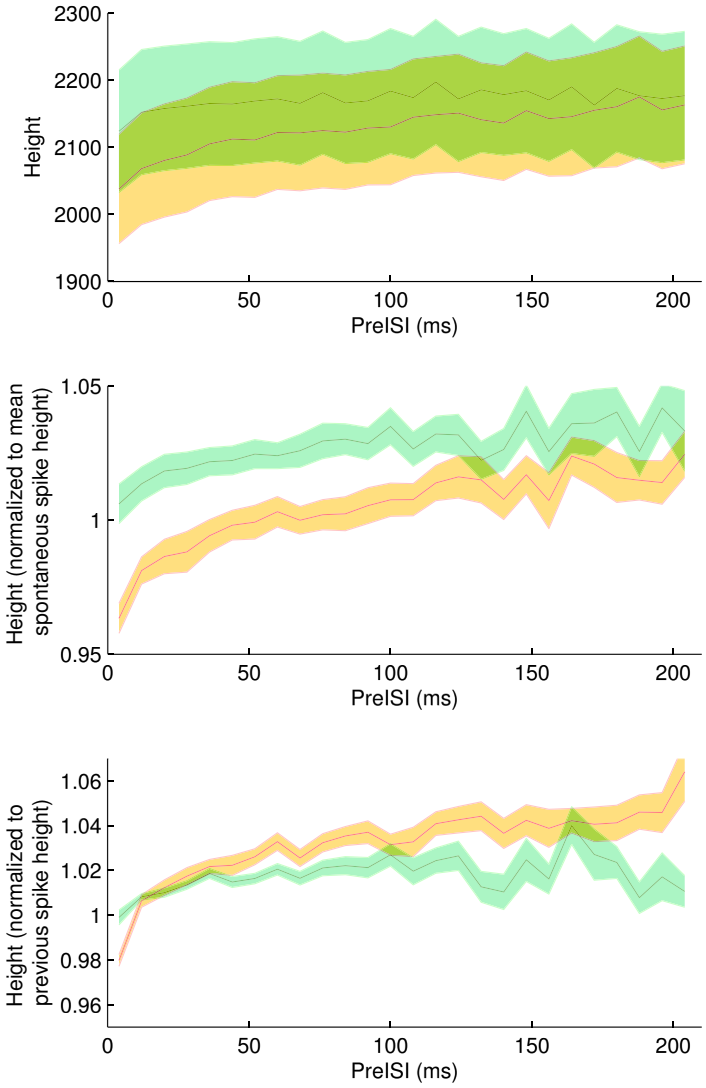

Figure 3.9: Timescale of height adaptation for narrow and broad spiking neurons. Orange traces correspond to the population means of the broad spiking neurons (N=70), green traces correspond to the population means of the narrow spiking neurons (N=45). Shaded regions correspond to +/- 1 SEM. *Top panel:* Unnormalized height (difference between peak and trough) vs. previous pre interspike interval. *Middle panel:* Height normalized, on a trial-by-trial basis, by mean height of action potentials in the spontaneous period. *Bottom panel:* Height normalized by height of preceding action potential.

I next compared height adaptation among broad spiking and narrow spiking neurons as a function of matched preISI bins (discretized to 8ms). This is shown in Figure 3.9, with the raw height shown in the top panel, the height normalized on a trial-by-trial basis by the spontaneous height in the middle panel, and the height normalized by the previous action potential height in the bottom panel.[1] In all three panels, there is a stronger dependence of height on preISI among broad spiking neurons than among narrow spiking neurons. At short duration preISIs (bin 1, 0-8ms), broad spiking neurons exhibit significantly stronger spike height adaptation than narrow spiking neurons (bottom panel, Mann-Whitney U test, $p < 0.0001$; median broad 0.98, median narrow 1.01). Similarly, broad spiking neurons are shorter in normalized height than narrow spiking neurons at short duration preISIs (middle panel; Mann-Whitney U test, $p < 0.01$ for bins 1-6, 0-48ms).

3.4.3 Evidence for spike frequency adaptation among broad spiking neurons

In addition to showing changes in waveform duration and amplitude, many neurons adapt in spike frequency. In intracellular studies, this is typically shown as a decrease in interspike intervals between spikes in a train of action potentials in response to a constant step of depolarizing current. Here, I will present two lines evidence for spike frequency adaptation in an example neuron before turning to population statistics.

The example neuron in Figure 3.10 shows two forms of spike frequency adaptation: an increase in interspike intervals within a burst, and a tendency for bursts of action potentials to be followed by long periods of quiescence. An advantage of this example neuron is the clear separation of burst events from non-burst events (Figure 3.11A), making it possible to consider spike frequency adaptation within bursts independently from transitions between bursting and

[1]Note that in the bottom panel, that when a broad spiking neuron elicits an action potential with a long preISI, the action potential is frequently taller than the preceding action potential. This can be explained by the fact that action potentials with long preISIs are frequently preceded by action potentials with shorter preISIs. Thus, the increase in height relative to the previous action potential reflects a recovery of the neuron from a more adapted state.

quiescence.[2]

The main panels in Figure 3.10 illustrate the first form of spike frequency adaptation, by comparing the first and second interspike intervals of bursts comprised of at least three action potentials. As illustrated in Figure 3.10, the distribution of interspike intervals following the first spike in a burst (top panel) is significantly shorter than those following the second spike in a burst (middle panel)(Wilcoxon signed rank testsi, $p \ll 0.0001$). This intraburst spike frequency adaptation can also be seen in 3.10C, which shows the histogram of the ratio between the second and first interspike intervals within a burst. The distribution of this ratio is significantly greater than zero (Wilcoxon signed rank test, $p \ll 0.0001$), indicating an increase in interspike interval duration between the first and second interspike interval within a burst.

The insets in Figure 3.10 illustrate the second factor can contribute to measures of spike frequency adaptation: a tendency for bursts of action potentials to be followed by periods of quiescence. These insets consider all of the spikes of this neuron, rather than focusing on bursts greater than two spikes (which is particularly important for the case of this particular neuron, as most bursts of action potentials were in fact doublets). We now find a more dramatic difference between the postISI of the first spike in a burst and the second. The top inset shows that unadapted spikes (action potentials following at least 10ms of silence) are almost always followed by an action potential within 10ms, while the middle panel shows that action potentials within a burst (following a spike within 10ms) are frequently followed by a long period of quiesence. This is further quantified in the bottom inset, which compares the percentage of postISIs within 10ms between unadapted action potentials (92.3%) and adapted action potentials (18.4%).

[2]The separation of these two forms of spike frequency adaptation is not meant to imply differences in mechanism. Indeed, both the increase in intraburst interval and the cessation of a burst share common mechanisms (e.g. Kv7/KCNQ/M channel activation; Yue and Yaari, 2004; Gu et al., 2005). Rather, the separation of these two forms of adaptation are meant to illustrate different timescales of the same phenomena, allowing for easier comparison with in vitro cortical data.

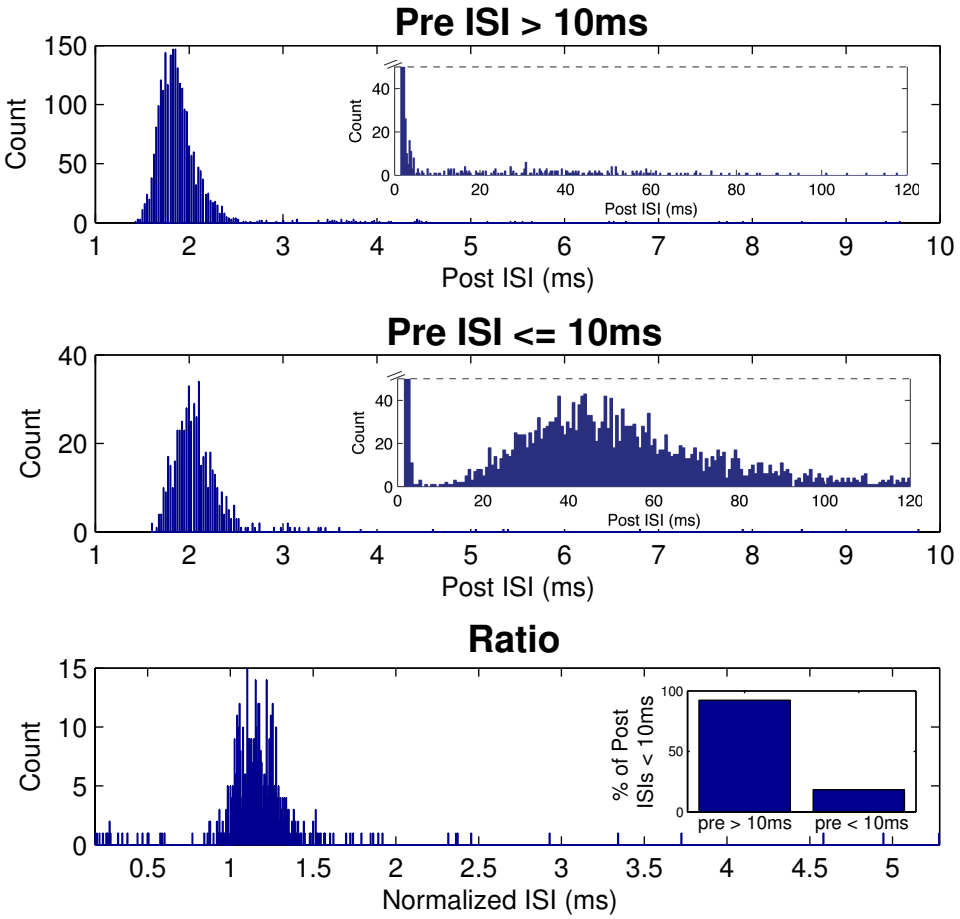

Figure 3.10: Example neuron mbbag52_u1 shows interspike interval (spike frequency) adaptation.
Top panel: Distribution of short post interspike intervals (<10ms) for action with a pre interspike interval greater than 10ms. *Top panel, inset:* Distribution of post interspike intervals for action potentials with with a pre interspike interval greater than 10ms. Top of graph truncated at a count of 50 (top bar > 1000). *Middle panel:* Distribution of short post interspike intervals (<10ms) for action potentials within with a pre interspike interval less than or equal to10ms. *Middle panel, inset:* Distribution of post interspike intervals for action potentials with a pre interspike interval less than or equal to10ms. Top of graph truncated at a count of 50 (top bar > 400). *Bottom panel:* Ratio of short post interspike intervals from the middle panel normalized by the preceding post interspike interval. *Bottom panel, inset:* Percentage of post interspike intervals for action potentials with a pre ISI > 10ms (92.3%) and with a pre ISI <= 10ms (18.4%).

Figure 3.11: Timing of subsequent action potentials depends on preceding interspike interval and action potential height for example neuron mbbag52_u1

(facing page)

A: Interspike interval return map, showing a significant relationship between preISI and postISI (Spearman's non-parametric correlation, p « 0.0001, R_s = -0.65). *B:* Significant relationship between action potential height (normalized on a trial-by-trial basis by the mean spontaneous height) and postISI (Spearman's non-parametric correlation, p « 0.0001, R_s = -0.33). *C:* Mean postISI (discretized into 1ms bins) as a function of preISI. Shaded region indicates +/- 1 SEM. *D:* Mean postISI as a function of spike height, 12 bins. Shaded region indicates +/- 1 SEM. *E:* Probability of firing a subsequent action potential within 4ms depends on preISI. *F:* Probability of firing a subsequent action potential within 4ms depends on the height of the action potential (normalized on a trial-by-trial basis by the mean height in the spontaneous period).

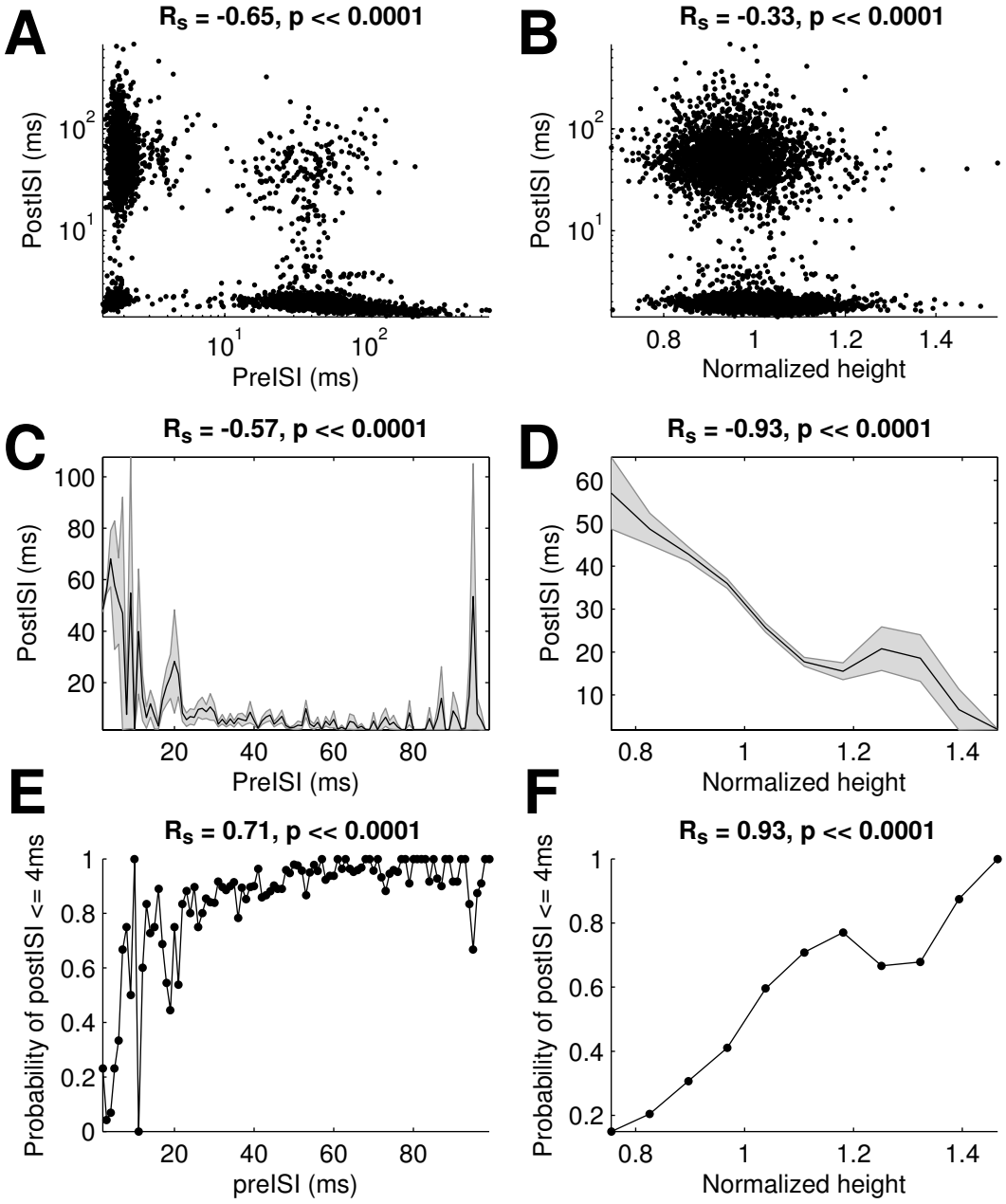
A
R_S = -0.65, p << 0.0001
PostISI (ms)
PreISI (ms)
B
R_S = -0.33, p << 0.0001
PostISI (ms)
Normalized height
C
R_S = -0.57, p << 0.0001
PostISI (ms)
PreISI (ms)
D
R_S = -0.93, p << 0.0001
PostISI (ms)
Normalized height
E
R_S = 0.71, p << 0.0001
Probability of postISI <= 4ms
preISI (ms)
F
R_S = 0.93, p << 0.0001
Probability of postISI <= 4ms
Normalized height

Figure 3.12: Preceding spike interval predicts subsequent spike interval differently for broad and narrow spiking neurons

(facing page)

Top panel: Scatterplot of waveform duration (μs) vs. the relationship between preISI and postISI across the population. The two factors are significantly correlated (Spearman's non-parametric correlation, R_s = -0.45, $p < 0.0001$), with broad spiking neurons showing significantly greater spike frequency adaptation than narrow spiking neurons (Wilcoxon signed rank test, $p < 0.0001$). *Bottom panel*: Scatterplot of burstiness (B.R.I.) vs. the relationship between preISI and postISI across the population. The two factors are significantly correlated with one another (Spearman's non-parametric correlation, R_s = -0.61, p « 0.0001). In both plots, dark colored circles indicate units that showed a significant relationship between preISI and postISI ($p < 0.001$).

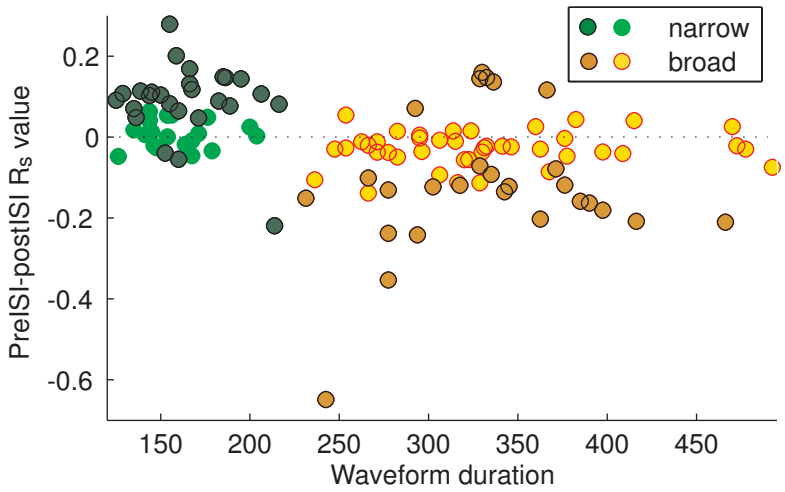
narrow
broad
0.2
0
-0.2
-0.4
-0.6
PreISI-postISI R_s value
150
200
250
300
350
400
450
Waveform duration

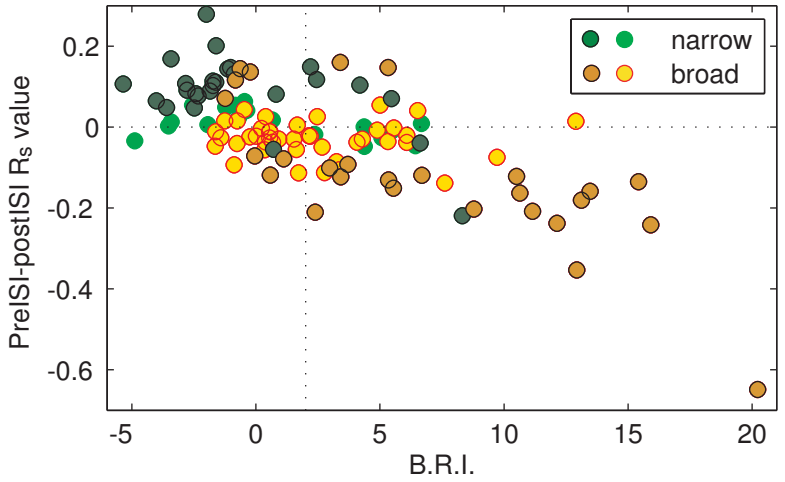
narrow
broad
0.2
0
-0.2
-0.4
-0.6
PreISI-postISI R_s value
-5
0
5
10
15
20
B.R.I.

A more general way to characterize spike frequency adaptation is to determine whether there is a significant (negative) relationship between preISI and postISI. An advantage of this measure is that it does not require the isolation of burst events from non-burst events. As can be seen in Figure 3.11A, there is a significant relationship between preISI and postISI for this example neuron, with action potentials with a short preISI tending to be followed by a longer quiescent period than those with long preISIs (Spearman's non-parametric correlation, $p \ll 0.0001$, R_s = -0.65). Relatedly, this neuron also shows a strong (nonlinear) relationship between preISI and the probability of firing an action potential within 4ms (Spearman's non-parametric correlation, $p \ll 0.0001$, R_s= 0.71). As the time preceding the action potential increases, the neuron rapidly becomes more likely to burst, until a preISI of about 60ms, when the burst probability saturates near 100%.

If action potential height reflects intrinsic properties that underlie the excitability of a neuron (such as sodium channel inactivation), then we would expect that spike height would also predict the subsequent interspike interval. Remarkably, the example neuron in Figure 3.11 has a strong, almost linear, relationship between spike height and the probability of firing a subsequent action potential within 4ms (panel F; Spearman's non-parametric correlation, $p \ll 0.0001$, R_s = 0.93). There is also a highly significant relationship between spike height and postISI (panel B; Spearman's non-parametric correlation, $p \ll 0.0001$, R_s = -0.33). Further, this relationship between height and postISI is not a simple reflection of preceding interspike interval, as the partial correlation remains highly significant (Spearman's non-parametric correlation, $p \ll 0.0001$, R_s = -0.12). This significant partial correlation suggests that spike height can reflect properties beyond the preISI, such as spiking history before the preceding spike, and may be a good indicator of the adaptation state of a neuron at the time of an action potential.[3]

Across the entire population of broad spiking neurons, I continue to find evidence for spike frequency adaptation. As seen in Figure 3.12, the distribution

[3]Indeed, the majority of neurons that significantly adapt in height have exhibit a significant relationship between the "pre-pre" spike interval (the interval between the preceding spike and the spike that preceded it) and the subsequent height adaptation (broad spiking neurons, N = 29 (59% of height adapting neurons); narrow spiking neurons, N = 12 (80% of adapting neurons)).

of preISI-postISI R_s values is significantly less than zero (Mann-Whitney U test, $p < 0.0001$, median R = -0.04), consistent with short ISIs tending to be followed by somewhat longer ISIs. The distribution of height-postISI R_s values is also significantly less than zero ($p < 0.001$, median R = -0.03), consistent with taller (less adapted) spikes being followed by relatively short ISIs and shorter spikes (more adapted) followed by longer ISIs. Both of these factors remained significant when the other was taken into consideration (Mann-Whitney U test, $p < 0.01$, median partial preISI-postISI R_s = -0.04; $p < 0.01$, median partial height-postISI R_s = -0.01), but the distribution of preISI-postISI R_s values was significantly more negative than the distribution of height-postISI R_s values (Mann-Whitney U test, $p < 0.01$). The distribution of the partial correlation R_s values were also significantly less than zero ($p < 0.0001$, preISI-postISI R_s median = -0.04; $p < 0.01$ height-postISI R_s median = -0.01), indicating that across the broad spiking population, the timing of subsequent action potentials depends both on spike height and preceding interspike interval.

3.4.4 Differences in spike frequency adaptation between broad spiking and narrow spiking neurons

One of the classic characteristics of fast-spiking inhibitory interneurons is the fact that they adapt very little in spike frequency. If the narrow spiking neurons largely correspond to FS interneurons, then we would expect to see less adaptation among the narrow spiking neurons compared to the broad spiking neurons. I find that this is indeed the cas*E:* the distributions of preISI-postISI R_s values between the broad and narrow spiking classes are significantly different from one another (Mann U Whitney test, p « 0.0001). I also find a significant relationship between action potential width and this measure of spike frequency adaptation (Figure 3.12; Spearman's non-parametric correlation, R_s = -0.45, $p < 0.0001$). In fact, I find very little evidence of spike frequency adaptation among the narrow spiking population, with only three neurons (6.7%) showing a significantly negative preISI-postISI relationship. Further, while the broad spiking neurons have a significantly negative distribution of preISI-postISI R_s values, consistent with spike frequency

adaptation, the narrow spiking neurons have a significantly positive distribution of preISI-postISI values (Wilcoxon signed rank test, $p < 0.0001$, median $R_s = 0.05$). This positive correlation between preISI and postISI among narrow spiking neurons probably reflects slow, low-frequency oscillations in the firing rate of these neurons during the sustained period (Mitchell et al., 2009).

In addition to the significant relationship between waveform duration and spike frequency adaptation, there is a also a significant relationship between burstiness and spike frequency adaptation (preISI-postISI R_s value and B.R.I.: $R_s = -0.61$, $p \ll 0.0001$.). Again, this is probably not surprising given that the strongest spike frequency adaptation is seen following short interspike intervals commonly found in burst firing. However, differences in burstiness among broad and narrow spiking neurons does not fully account for differences in spike frequency adaptation between broad and narrow spiking neurons, as the partial correlation between duration and spike frequency adaptation (taking B.R.I. into consideration) remained significant ($R_s = -0.31$, $p < 0.001$).

In addition to this difference in the relationship between preISI and postISI between the broad and narrow spiking neurons, narrow spiking neurons also did not show a significant relationship between height and postISI. While the broad spiking neurons showed a significant negative distribution of height-postISI R_s values, the distribution among narrow spiking neurons was not significantly different from zero (Wilcoxon signed rank test, $p > 0.4$, median $R_s = -0.001$). This difference in the distribution of height-postISI R_s values between the two classes is also significant (Mann U Whitney test, $p < 0.001$), and there is a also significant correlation between waveform duration and the relationship between height and postISI ($R_s = -0.35$, $p < 0.001$). Among the subset of narrow spiking neurons that did show significant height adaptation ($N = 15$), I also did not find evidence for spike frequency adaptation: neither the distribution of R_s values between preISI and postISI or the distribution of R_s values between height and postISI were significantly different from zero ($p > 0.3$).

3.5 Discussion

In this chapter, I have presented the first evidence for action potential amplitude, duration, and frequency adaptation in the awake macaque. Further, when I compare neurons with different mean waveform durations, I find significantly greater spike height and spike frequency adaptation among broad spiking neurons compared to narrow spiking neurons. I continued to see differences in spike amplitude adaptation between narrow and broad spiking neurons when I compared conditions matched in preceding interspike interval, suggesting that this difference is not a consequence of the greater measurement sensitivity for spike height adaptation for neurons that fire bursts of action potentials, but instead reflects genuine differences in the adaptation properties of these populations.

3.5.1 Origin of the extracellular signal

The amplitude of the extracellular signal drops off rapidly as the distance from the soma increases, making it difficult to isolate signals originating from an individual neuron beyond a short distance from the soma (Henze et al., 2000). Perhaps due to this isolation-distance relationship, or simply the relatively large size of the soma, well-isolated extracellular recordings are commonly considered to reflect transmembrane currents at the soma of individual neurons. However, an understanding of the origins of extracellular signals is crucial for linking-activity dependent changes in waveform shape to intrinsic neural mechanisms, and thus will be considered further here.

To test the assumption that extracellular recordings reflect somatic activity, Henze et al. (2000) performed simultaneous extracellular and intracellular recordings of hippocampal CA1 pyramidal neurons. They found that the initial deflection of the extracellular action potential is indeed well described by the first derivative of the intracellular action potential measured at the soma. However, the shape of subsequent recovery of the extracellular action potential differed from this prediction. A detailed model of this experimental preparation suggested that the extracellular signal of these pyramidal neurons is dominated by the active perisomatic currents, with almost no contribution from the axon (Gold et al., 2006). In

the model, deviations of extracellular signals from predictions from intracellular recordings at the soma could be explained by differences in the channel distributions between the soma and proximal dendrite.

Based on these results from Henze et al. (2000), it seems reasonable to assume that most of the extracellular recordings presented in this chapter are similarly dominated by signals originating from the perisomatic region. In addition, Henze et al. also found that the position of their extracellular electrode along the somatodendritic axis influenced both the amplitude and the shape of the extracellular signal. Based on this finding, it seems quite likely that the slow drift in action potential amplitude and duration seen in some sessions reflects movement of the electrode away from the soma and towards locations where a greater proportion of the extracellular signal is determined by signals originating from the proximal dendrites. The static properties of this distance-dependent spike attenuation appear to be well controlled by the normalization methods introduced here, but future work should consider potential variability in adaptation estimates across time arising from differences in the adaptive properties of the soma and dendrites.

3.5.2 Extracellular action potential height adaptation likely reflects mechanisms that regulate synaptic integration and burst generation

Many neurons, including neocortical pyramidal neurons, elicit action potentials that adapt in height in response to recent activity. When measured at the soma or the dendrite, spike amplitude adaptation is thought to be largely mediated by the cumulative inactivation of a subset of voltage-gated sodium channels during previous action potentials (Colbert et al., 1997; Jung et al., 1997; Martina and Jonas, 1997; Remy et al., 2009).[4] This inactivation serves an essential role in the regulation of action potential backpropagation from the axon initial segment, which in turn may influence local excitability, synaptic integration, dendritic spik-

[4]Within the dendrite, A-type potassium channels also contribute to spike attenuation, but this attenuation does not appear to have an activity-dependent component. However, the dynamics of these potassium channels further unmask the activity-dependent inactivation of sodium channels (Hoffman et al., 1997; Colbert et al., 1997; Remy et al., 2009).

ing, and burst firing (Williams and Stuart, 1999; Henze and Buzsáki, 2001; Shu et al. 2006a; Remy et al., 2009).

If we assume that the extracellular recordings presented here originate from the soma and/or dendrites of individual neurons, then the spike height adaptation we observe should also reflect local sodium channel inactivation.[5] This would suggest that extracellular spike height adaptation provides a window into the internal state of the neuron that reflects not only recent spiking activity, but other factors such as synaptic inputs or neuromodulators that depolarize the perisomatic region. Further, since sodium inactivation directly influences neural excitability, the ability to monitor spike height adaptation in extracellular recordings can provide a moment-to-moment estimate of the neuron's ability to process future synaptic inputs and generate bursts of action potentials.

3.5.3 Implications of activity-dependent broadening of cortical action potentials

During periods of repetitive activity, the repolarization phase of many neurons slows down, resulting in an apparent broadening of the action potential waveform. This spike duration adaptation is seen across many vertebrate and invertebrate neuron classes, including cortical pyramidal cells and fast-spiking inhibitory neurons (Zhou and Hablitz, 1996; Cauli et al., 1997), and has been observed in the soma, dendrite, and axon (Faber and Sah, 2003). The mechanisms underlying this activity-dependent broadening appears to be the result of cumulative inactivation of voltage-gated and calcium-activated potassium currents (Geiger and Jonas, 2000; Faber and Sah, 2003; Shu et al. 2006b, 2007; Kole et al. 2007). This broadening has been shown to increase the calcium influx at hippocampus mossy

[5]Recently, Shu et al. (2006b) reported that spike amplitude attenuation can also be seen within the axon of pyramidal neurons in response to somatic compartment depolarization. Given the high densities of voltage-gated sodium channels within the axon (Yu et al., 2008; Kole et al., 2008), the mechanism of this attenuation is less clear. Although action potential attenuation would be predicted to reduce neurotransmitter release (Bischofberger et al., 2002), the axonal action potential height attenuation appears to be accompanied by action potential broadening (Shu et al., 2006b), which appears to result in a net increase in neurotransmitter release (Geiger and Jonas, 2000; Shu et al., 2006b, 2007; Kole et al. 2007). However, as discussed in the previous section, it seems less likely that the spike adaptation observe here reflects axonal attenuation than adaptation at the soma or dendrites.

fiber boutons (Geiger and Jonas, 2000), as well as increase the size and delay of the EPSCs of some of the postsynaptic partners of hippocampal and cortical neurons (Geiger and Jonas, 2000; Shu et al. 2006b, 2007; Kole et al. 2007; Boudkkazi et al., 2011). This line of evidence leads to the conclusion that a major consequence of action potential broadening at synaptic terminals is an increase of calcium influx resulting in increased neurotransmitter release.

Taken together, these findings suggest that the activity-dependent broadening observed in the present data could reflect the some of the same mechanisms that directly influence neurotransmitter release. An important consideration, however, is whether extracellular signals reflect signals originating exclusively from the soma and proximal dendrites. Recent evidence from Kole et al. (2007) suggests that axonal action potential broadening may be largely compartmentalized, with somatic action potentials broadening rapidly during burst firing, and axonal action potential duration selectively increased during sustained subthreshold somatic activity.[6] Thus, it is unclear whether the duration adaptation reported here reflects mechanisms that influence neurotransmission directly. Regardless, it seems quite likely that duration adaptation, similar to spike height adaptation, reflects mechanisms that influence synaptic integration and can provide insight into the depolarization state at the soma.

3.5.4 Unexplained variance in spike height and duration

While present results provide evidence for activity-dependent spike height attenuation and broadening in macaque Area V4, there is a great deal of variability in spike height and duration which is not fully explained by preISI or the height of the previous action potential. This can be seen qualitatively for an example neuron in Figure 3.6, and quantitatively from the significant but fairly small R_s values of the correlation between spike shape and preISI. While additional analysis is needed to more fully characterize the spike activity dependence of action potential shape,

[6]Further, differences in pharmacological results across studies could be reconciled if somatic action potential duration adaptation is largely mediated by inactivation of calcium-activated potassium currents (Faber and Sah, 2003; Kole et al., 2007) while cortical axonal duration adaptation is largely mediated by inactivation of Kv1 potassium channels (Shu et al., 2007; Kole et al., 2007).

preliminary results using multiple linear regression suggest that for most broad spiking neurons, only about 20% of the variance in action potential height can be explained by previous action potential height and the ISIs from previous trains of action potentials.

An extensive literature suggests that ongoing synaptic activity provides a critical contribution to the variability in action potential shape observed here. This ongoing activity is known to have a profound impact on the excitability and integrative properties of cortical neurons (Ho and Destexhe, 2000; Chance et al., 2002; Shu et al., 2003). Further, these fluctuations in conductance history have also been shown to reliably influence somatic action potential height and width (de Polavieja et al., 2005; Shu et al. 2006b). This suggests that the variability in action potential shape observed here may also reflect ongoing bombardments of synaptic activity, and may provide insight into the internal state of the cell that cannot be inferred from spiking activity alone. Future work should examine whether extracellular local field potential recordings, which are thought to reflect synaptic activity, could be used to improve predictions of extracellular action potential shape.

3.5.5 Relationship between spike frequency adaptation and burst firing

In addition to action potential height adaptation, most neurons also undergo spike frequency adaptation. As with spike height adaptation, an important source of spike frequency adaptation comes from negative feedback intrinsic to the generation of action potentials within the neuron. The predominant form of this feedback comes from slow and medium timescale afterhyperpolarization (AHP) generating potassium currents. The slow timescale AHP (sAHP) contributes to slow timescale spike frequency adaptation and is probably caused by calcium dependent potassium channels (Madison and Nicholl, 1984). The medium timescale AHP (mAHP), mediated by voltage-dependent Kv7/KCNQ/M channels and an I_h current[7], causes early spike frequency adaptation and suppresses bursting (Madi-

[7]Among cortical pyramidal neurons, SK channels also appear to play a role (Abel et al., 2004).

son and Nicholl, 1984; Yue and Yaari, 2004; Gu et al., 2005; Peters et al., 2005). In addition, the slow recovery of sodium channel inactivation, the adaptation of input neurons, and synaptic depression also contribute to spike frequency adaptation (Fleidervish et al., 1996, Gollisch and Herz, 2004).

The present results show a strong correlation between the burstiness (B.R.I.) of broad spiking neurons and the degree of spike frequency adaptation observed (preISI-postISI R_s value). This relationship should come as no surprise, given that the strongest spike frequency adaptation is seen following short interspike intervals commonly found in burst firing. It is worth noting that both the spike frequency adaptation of individual spikes and of bursts of action potentials are thought to be mediated by common mAHP mechanisms (Yue and Yaari, 2004; Gu et al., 2005). Thus, the strong spike frequency adaptation observed among burst firing neurons does not reflect a different adaptation mechanism, but simply a difference in short-timescale activity.

3.5.6 Differences in spike height and frequency adaptation among cortical neurons

In contrast to pyramidal neurons, fast-spiking inhibitory interneurons exhibit little to no spike height or spike frequency accommodation when measured in vitro (McCormick et al., 1985; Martina and Jonas, 1997; Cauli et al., 1997; Gonzàlez-Burgos et al., 2005) or in anesthetized preparations (Nowak et al., 2003). In fact, some FS neurons actually exhibit spike frequency facilitation/acceleration in response to steps of depolarizing current (Nowak et al., 2003; Izhikevich, 2007). This difference from pyramidal neurons arises from differences in sodium and potassium channel expression, which results in differences in the interaction between the fast and slow dynamics of these channels. In particular, fast spiking inhibitory interneurons recover more rapidly from sodium channel inactivation (Martina and Jonas, 1997). This rapid recovery of sodium channel inactivation is mediated at least in part by the expression of Kv3 potassium channels with fast kinetics, which also serves to reduce the duration of the afterhyperpolarization (Erisir et al., 1999; Carter and Bean, 2009).

Given the evidence for differences in adaptation between fast-spiking inhibitory neurons and other cortical neurons, I hypothesized that if the narrow spiking neurons are FS neurons, then there should be differences in spike height and frequency adaptation between the narrow spiking and broad spiking populations. The results I present here support this hypothesis, providing additional evidence in support of the use of spike waveform duration to infer cortical cell identity. In particular, I found evidence for spike height and frequency adaptation within the broad spiking population, and both forms of adaptation were significantly stronger among broad spiking neurons than narrow spiking neurons.

Within the narrow spiking population, I did find a small subset of neurons that significantly adapted in height (N = 15, 33.3%) and an even smaller number that adapted in frequency (N = 3, 6.7%). A limited amount of spike height and frequency adaptation has been reported among fast-spiking interneurons, which may explain some of the adaptation observed within the the narrow spiking group. However, given the degree of adaptation seen among some of the narrow spiking neurons, it seems likely that not all of the neurons correspond to FS interneurons. For example, the narrow spiking neuron that exhibits the strongest frequency adaptation also elicits action potentials with a duration quite close to the threshold chosen to divide the population into narrow and broad spiking groups (Figure 3.12). It seems plausible that this neuron could belong to different interneuron class, as many interneuron classes adapt in spike frequency and elicit somewhat narrower action potentials on average than pyramidal neurons (Cauli et al., 1997). Further, as shown in Figure 3.8, many of the narrow spiking neurons that exhibited spike amplitude adaptation also exhibited bursty behavior. These neurons may correspond to the so-called chattering neurons, a class of superficial pyramidal neurons that have been described in the cat and the ferret. Such neurons frequently fire in doublets and triplets, and elicit narrow action potentials that show activity-dependent height attenuation (Brumberg et al., 2000; Nowak et al., 2003). Regardless of the specific identity of these adapting narrow spiking neurons, the results presented here emphasize that some narrow spiking neurons may not correspond to fast-spiking inhibitory interneurons, and that spike height and frequency adaptation can provide an additional means to distinguish putative

FS interneurons from other neuronal classes.

Some of the material presented in this chapter and in chapter 4 may be prepared for submission for publication. Anderson EB, Mitchell JF, Reynolds JH. The dissertation author was the primary investigator and author of this material.

3.6 References

Abel HJ, Lee JCF, Callaway JC, Foehring RC (2004) Relationships between intracellular calcium and afterhyperpolarizations in neocortical pyramidal neurons. J Neurophysiol 91:324-335.

Bischofberger J, Jörg R, Geiger P, Jonas P (2002) Timing and efficacy of Ca^{2+} channel activation in hippocampal mossy fiber boutons. J Neurosci 22(24):10593-10602.

Brumberg C, Nowak LG, McCormick DA (2000) Ionic mechanisms underlying repetitive high-frequency burst firing in supragranular cortical neurons. J Neurosci 20(13):4829-4843.

Boudkkazi S, Fronzaroli-Molinieres L, Debanne D (2011) Presynaptic action potential waveform determines cortical synaptic latency. J Physiol 589:1117-1131.

Carter BC, Bean BP (2009) Sodium entry during action potentials of mammalian neurons: incomplete inactivation and reduced metabolic efficiency in fast-spiking neurons. Neuron 64(6):898-909.

Cauli B, Audinat E, Lambolez B, Angulo E, Ropert N, Tsuzuki K, Hestrin S, Rossier J (1997) Molecular and physiological diversity of cortical nonpyramidal cells. J Neurosci 17(10):3894-3906.

Chance FS, Abbott LF, Reyes AD (2002) Gain modulation from background synaptic input. Neuron 35:772-782.

Colbert CM, Magee JC, Hoffman DA, Johnston D (1997) Slow recovery from inactivation of Na^{+} channels underlies the activity-dependent attenuation of dendritic action potentials in hippocampal CA1 pyramidal neurons. J Neurosci 17:6512-6521.

de Polavieja GG, Harsch A, Kleppe I, Robinson HPC, Juusola M (2005) Stimulus history reliably shapes action potential waveforms of cortical neurons. J Neurosci 25:5657-5665.

Erisir A, Lau D, Rudy B, Leonard CS (1999) Function of specific K^+ channels in sustained high-frequency firing of fast-spiking neocortical interneurons. J Neurophysiol 82(5):2476-2489.

Faber ESL, Sah P (2003) Ca^{2+}-activated K^+ (BK) channel inactivation contributes to spike broadening during repetitive firing in the rat lateral amygdala. J Physiol 552(2):483-497.

Fleidervish IA, Friedman A, Gutnick MJ (1996) Slow inactivation of Na^+ current and slow cumulative spike adaptation in mouse and guinea-pig neocortical neurones in slices. J Physiol 493(1):83-97.

Geiger JRP, Jonas P (2000) Dynamic control of presynaptic Ca^{2+} inflow by fast-inactivating K^+ channels in hippocampal mossy fiber boutons. Neuron 28:927-939.

Gold C, Henze DA, Koch C, Buzsáki G (2006) On the origin of the extracellular action potential waveform: a modeling study. J Neurophysiol 95:3113-3128.

Gollisch T, Herz AVM (2004) Input-driven components of spike-frequency adaptation can be unmasked in vivo. J Neurosci 24(34): 7435-7444.

Gonzàlez-Burgos G, Krimer LS, Povysheva NV, Barrionuevo G, Lewis DA (2005) Functional properties of fast spiking interneurons and their synaptic connections with pyramidal cells in primate dorsolateral prefrontal cortex. J Neurophysiol 93(2):942-953.

Gu N, Vervaeke K, Hu H, Storm JF (2005) Kv7/KCNQ/M and HCN/h, but not $K_{Ca}2$/SK channels, contribute to the somatic medium after-hyperpolarization and excitability control in CA1 hippocampal pyramidal cells. J Physiol 566:689-715.

Henze DA, Borhegyi Z, Csicsvari J, Mamiya A, Harris KD, Buzsáki G (2000) Intracellular features predicted by extracellular recordings in the hippocampus in vivo. J Neurophysiol 84:390-400.

Henze DA, Buzsáki G (2001) Action potential threshold of hippocampal pyramidal cells in vivo is increased by recent spiking activity. Neurosci 105(1):121-130.

Ho N, Destexhe A (2000) Synaptic background activity enhances the responsiveness of neocortical pyramidal neurons. J Neurophysiol 84:1488-1496.

Hoffman DA, Magee JC, Colbert CM, Johnston D (1997) K^+ channel regulation of signal propagation in dendrites of hippocampal neurons. Nature 387:869-875.

Izhikevich EM (2007) Dynamical systems in neuroscienc*E:* the geometry of excitability and bursting. The MIT press, Massachusetts

Kole MHP, Ilschner SU, Kampa BM, Williams SR, Ruben PC, Stuart GJ (2008) Action potential generation requires a high sodium channel density in the axon initial segment. Nature Neurosci 11:178-186.

Madison DV, Nicoll RA (1984) Control of the repetitive discharge of rat CA1 pyramidal neurons in vitro. J physiol 354:319-331.

Martina M, Jonas P (1997) Functional differences in Na^+ channel gating between fast-spiking interneurones and principal neurones of rat hippocampus. J Physiol 505(3):593-603.

McCormick DA, Connors BW, Lighthall JW, Prince DA (1985) Comparative electrophysiology of pyramidal and sparsely spiny neurons of the neocortex. J Neurophysiol 54: 782-806.

Mitchell JF, Sundberg KA, Reynolds JH (2007) Differential attention-dependent response modulation across cell classes in macaque visual area V4. Neuron 55:131-141.

Mitchell JF, Sundberg KA, Reynolds JH (2009) Spatial attention decorrelates intrinsic activity fluctuations in macaque area V4. Neuron 63:879-888.

Nowak LG, Azouz R, Sanchez-Vives MV, Gray CM, McCormick DA (2003) Electrophysiological classes of cat primary visual cortical neurons in vivo as revealed by quantitative analyses. J Neurophysiol 89:1541-1566.

Peters HC, Hu H, Pongs O, Storm JF, Isbrandt D (2005) Conditional transgenic suppression of M channels in mouse brain reveals functions in neuronal excitability, resonance, and behavior. Nat Neurosci 8:51-60.

Remy S, Csicvari J, Beck H (2009) Activity-dependent control of neuronal output by local and global dendritic spike attenuation. Neuron 61:906-916.

Shu Y, Hasenstaub A, Badoual M, Bal T, McCormick DA (2003) Barrages of synaptic activity control the gain and sensitivity of cortical neurons. J Neurosci 23:10388-10401.

Shu Y, Duque A, Yu Y, Haider B, McCormick DA (2006) Properties of action-potential initiation in neocortical pyramidal cells: evidence from whole cell axon recordings.

Shu Y, Hasenstaub A, Duque A, Yu Y, McCormick DA (2006) Modulation of intracortical synaptic potentials by presynaptic somatic membrane potential. Nature 441:761-765

Shu Y, Yu Y, Yang J, McCormick DA (2007) Selective control of cortical axonal spikes by a slowly inactivating K^+ current. Proc Nat Acad Sci 104(27): 11453-11458.

Williams SR, Stuart GJ (1999) Mechanisms and consequences of action potential burst firing in rat neocortical pyramidal neurons. J Physiol 521(2):467-482.

Yu Y, Shu Y, McCormick DA (2008) Cortical action potential backpropagation explains spike threshold variability and rapid-onset kinetics. J Neurosci 28(29):7260-7272.

Yue C, Yaari Y (2004) KCNQ/M channels control spike afterdepolarization and burst generation in hippocampal neurons. J Neurosci 24:4614-4624.

Zhou FM, Hablitz JJ (1996) Layer I neurons of rat neocortex. I. Action potential and repetitive firing properties. J Neurophysiol 76(2):651-667.

Chapter 4

Concluding remarks

4.1 Increased spike adaptation may contribute to attention-dependent reductions in variability and burstiness in macaque Area V4

4.1.1 Reduction in variability with attention

As discussed in the Introduction, Area V4 is hypothesized to contribute to attention-dependent improvements in behavioral performance through an improvement in the quality of the signals encoded by populations of V4 neurons. Although classically this improvement in signal quality was thought to arise simply from an increase in firing rate with attention, recent evidence suggests that reductions in variability across trials and reductions in correlated activity may have an even more substantial impact on downstream decoding (Mitchell et al., 2007, 2009; Cohen and Maunsell, 2009).

One way to quantify variability in firing rate across trials is the Fano factor, a metric that normalizes the variance in firing rate across trials by the mean firing rate. The attention-dependent reduction in variability is illustrated in Figure 4.1, which shows the Fano factor as a function of bin size across the two different attention conditions. The four panels in the figure correspond to the bursty and non-bursty broad and narrow spiking groups introduced in chapter 2.

Interestingly, the narrow spiking and bursty broad spiking neurons, which show significant increases in rate with attention, also show a marked reduction in Fano factor across trials. The non-bursty broad spiking group, which did not show a significant change in firing rate with attention, shows a more modest reduction in Fano factor at small bin sizes, and a slight increase in Fano factor at large bin sizes.

4.1.2 Evidence for reduction in burstiness with attention

Recently, Mitchell et al. (2009) suggested that a major component of this reduction in variability among individual neurons reflects a reduction of correlated low-frequency firing rate oscillations within a larger network of neurons. Here, I present preliminary evidence for a second form of variance reduction with attention: a decrease in the burstiness of individual broad spiking neurons with attention.

To examine whether there are differences in burstiness across attention conditions, I first compared the B.R.I. calculated from the unattended trials with the B.R.I. calculated from the attended trials. A scatterplot of this comparison for the broad and narrow spiking neurons is shown in Figure 4.2. As can be seen in this figure, both the broad and narrow spiking neurons tend to fall below the line unity, indicating greater B.R.I. in the unattended condition compared to the attended condition. This difference in B.R.I. across the two attention conditions was significant (Wilcoxon signed rank test, $p < 0.0001$ for all neurons, $p < 0.05$ for broad spiking neurons, and $p < 0.0001$ for narrow spiking neurons).

A disadvantage of comparing the B.R.I. across attention conditions is that a reduction in B.R.I. can reflect an increase in refractoriness rather than a reduction in burst firing per se. In the data presented here, this can be seen for the subset of extremely refractory neurons, which become even more refractory with attention. Although both an increase in refractoriness and a reduction in burst firing could arise from common mechanisms, it would be nice to have a more straightforward metric that more exclusively reflected changes in burst firing with attention.

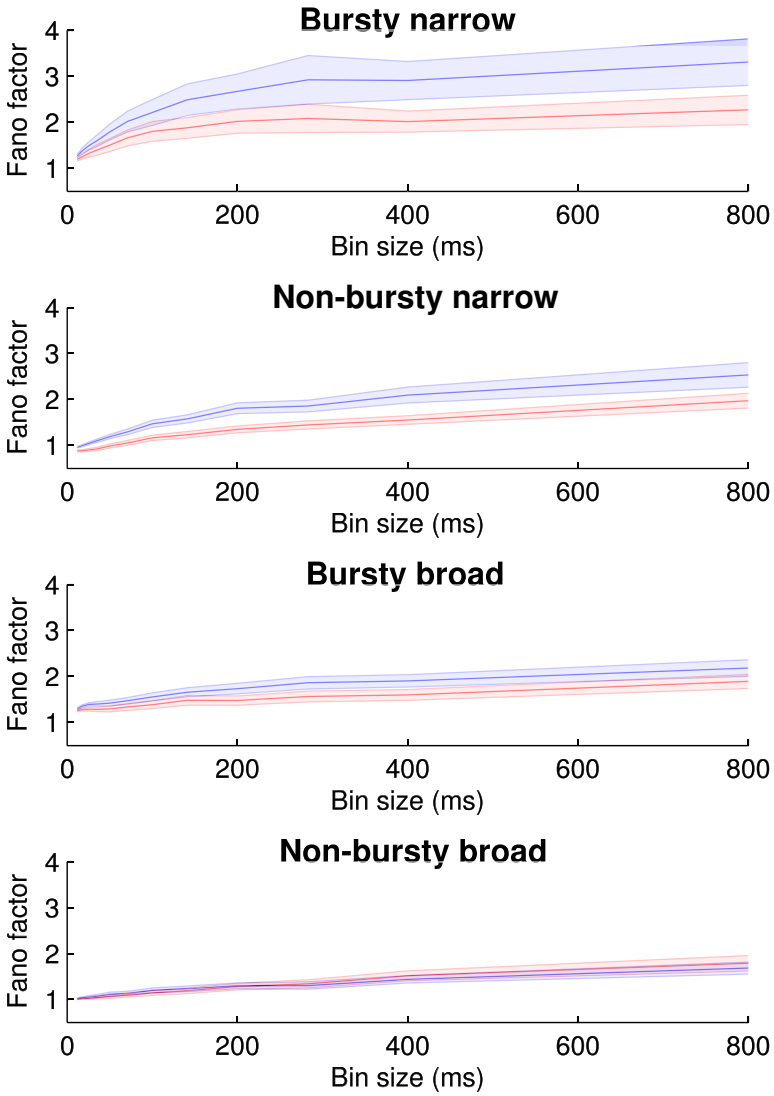

Figure 4.1: Attention-dependent reduction in Fano factor across four groups of V4 neurons
Red lines correspond to mean Fano factor in the attend condition, blue lines correspond to mean Fano factor in the unattend condition. Shaded regions indicate +/- 1 SEM.

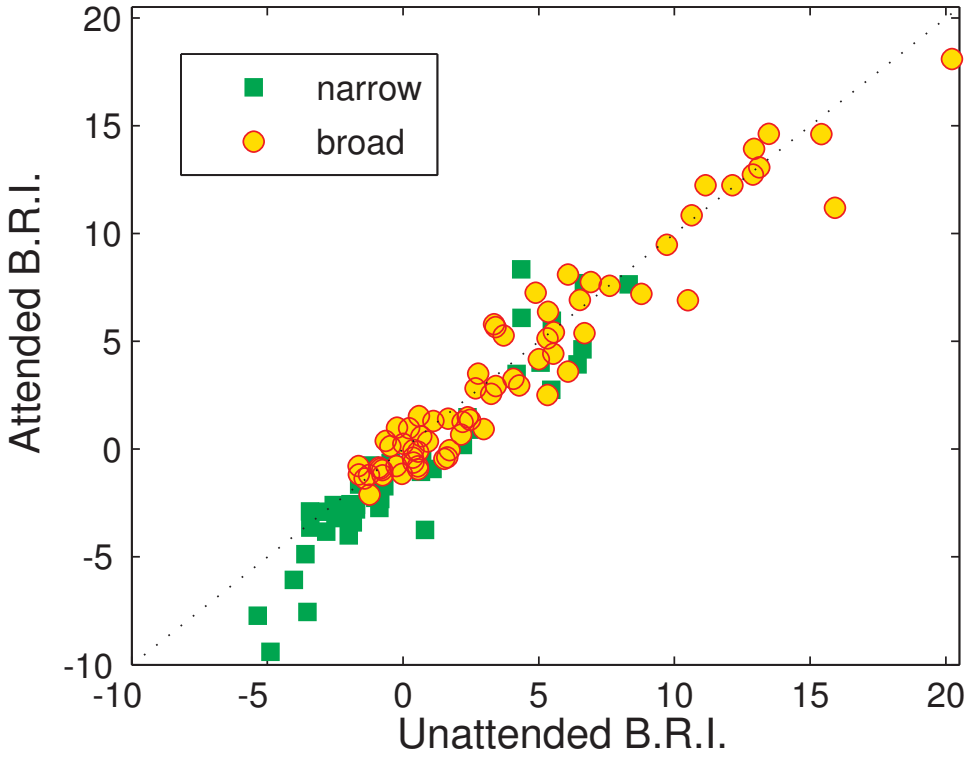

Figure 4.2: Reduction in burstiness (B.R.I.) with attention
Scatterplot of B.R.I. calculated for unattended trials vs. B.R.I. of attended trials. Orange circles correspond to broad spiking neurons, and green squares correspond to narrow spiking neurons. Both groups show significant reductions in B.R.I. across the two attention conditions (Wilcoxon signed rank test, $p < 0.0001$ for all neurons, $p < 0.05$ for broad spiking neurons, and $p < 0.0001$ for narrow spiking neurons).

To better disentangle reductions in burstiness from increases in refractoriness, I developed a second measure of attention-dependent modulation of burst firing. The results of this method are shown in Figure 4.3, which compares the probability of firing two action potentials within 10 ms of one another across the two attention conditions. Panel A shows this comparison for pairs of action potentials where the first spike is unadapted (preISI > 10ms), while panel B shows this comparison when the first spike is more adapted (preISI < 10ms). In both cases, the broad spiking neurons show a greater probability of firing two action potentials in quick succession in the unattended condition compared to the attended condition (Wilcoxon signed rank test, panel *A:* $p < 0.01$, median attend 23.1%, median unattend 24.4%, panel *B:* $p < 0.001$, median attend 18.3%, median unattend 21.1%). In contrast, when the first spike was preceded by a spike within 10ms, narrow spiking neurons show no difference in the probability of firing action potentials within 10ms across the two attention conditions ($p > 0.5$, median attend 30.7%, median unattend 30.8%). When the first spike was preceded by a period of silence 10 ms or greater, the narrow spiking neurons showed a modest increase in the probability of firing an action potential with 10 ms with attention ($p < 0.05$, median attend 29.3%, median unattend 28.6%).

To better compare attention-dependent changes in this second measure of burstiness across narrow and broad spiking neurons, I computed a burstiness attention index for each preISI condition. The burstiness attention indicies are normalized measures of the change in probability of firing action potentials within quick succession, computed as (A-U)/(A+U), where A corresponds to the probability of firing two spikes in quick succession during the attended condition, and U the probability in the unattended condition. The first burstiness attention index (BAI1), was computed over all pairs of spikes where the first spike was preceded by a spike within 10 ms, and the second burstiness attention index (BAI2) was computed over all pairs of spikes where the first spike was preceded by a period of silence lasting at least 10 ms.

Figure 4.3: Attention-dependent reduction in firing action potentials in quick succession among broad, but not narrow, spiking neurons

(facing page)

A: Probability of firing an action potential within 10 ms in the unattended condition vs. the attended condition, for all spikes with a preISI > 10 ms. The distribution among broad spiking neurons is significantly below the line of unity (Wilcoxon signed rank test, $p < 0.01$, median attend 23.1%, median unattend 24.4%). The distribution among narrow spiking neurons is also significant different between the two attention conditions ($p < 0.05$, median attend 29.3%, median unattend 28.6%), but shows an increased probability of firing at short latencies with attention. *B:* Probability of firing an action potential within 10ms in the unattended condition vs the attended condition, for all spikes with a preISI $<=$ 10ms. The distribution among broad spiking neurons is significantly below the line of unity (Wilcoxon signed rank test, $p < 0.001$, median attend 18.3%, median unattend 21.1%). The distribution among narrow spiking neurons is not significantly different between the two attention conditions ($p > 0.5$, median attend 30.7%, median unattend 30.8%). In both panels, orange circles correspond to broad spiking neurons, while green squares correspond to narrow spiking neurons.

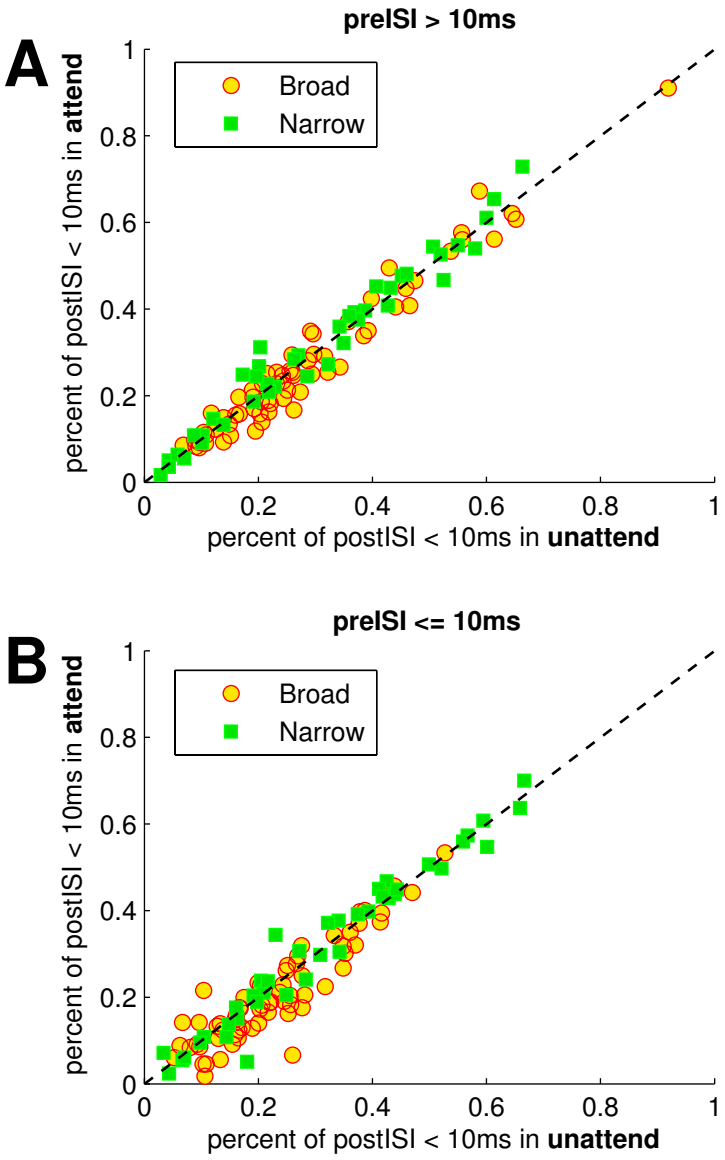
A
preISI > 10ms
Broad
Narrow
percent of postISI < 10ms in attend
percent of postISI < 10ms in unattend
0
0.2
0.4
0.6
0.8
1
B
preISI <= 10ms
Broad
Narrow
percent of postISI < 10ms in attend
percent of postISI < 10ms in unattend
0
0.2
0.4
0.6
0.8
1

Among broad spiking neurons, the distribution of both the BAI1 and BAI2 values were significantly negative, indicating a reduction in burstiness (Wilcoxon signed rank test, BAI1 $p < 0.01$, median BAI1 = -0.02; BAI2 $p < 0.001$, median BAI2 = -0.05). In contrast, among the narrow spiking neurons the distribution of BA1 values was significantly positive ($p < 0.05$, median BAI1 = 0.03) and the distribution of BAI2 values was not significantly different from zero ($p > 0.5$, median BAI2 = 0.01). The distributions of BAI values among broad and narrow spiking populations were significantly different from one another (Mann U Whitney test, BAI1 $p < 0.001$, BAI2 $p < 0.01$).

4.1.3 Reduction in spike height with attention

Future work is needed to establish whether the reduction in burstiness reported here represents an independent component of variability reduction with attention, or whether it reflects previously-reported changes in low-frequency oscillations in firing rate. In particular, reductions in low frequency power would result in a reduction in the peaks of the autocorrelation function, resulting in a reduction in B.R.I.

Alternatively, attention-dependent reductions in burstiness could reflect an overall increase in the depolarization of individual neurons when attention is directed towards their RF. Indeed, it is known that some cortical neurons become less bursty in response to depolarizing current injections, application of neuromodulators such as acetylcholine, or when the animal enters a more aroused state (Steriade et al., 1993, 1998, 2001; Wang and McCormick, 1993).

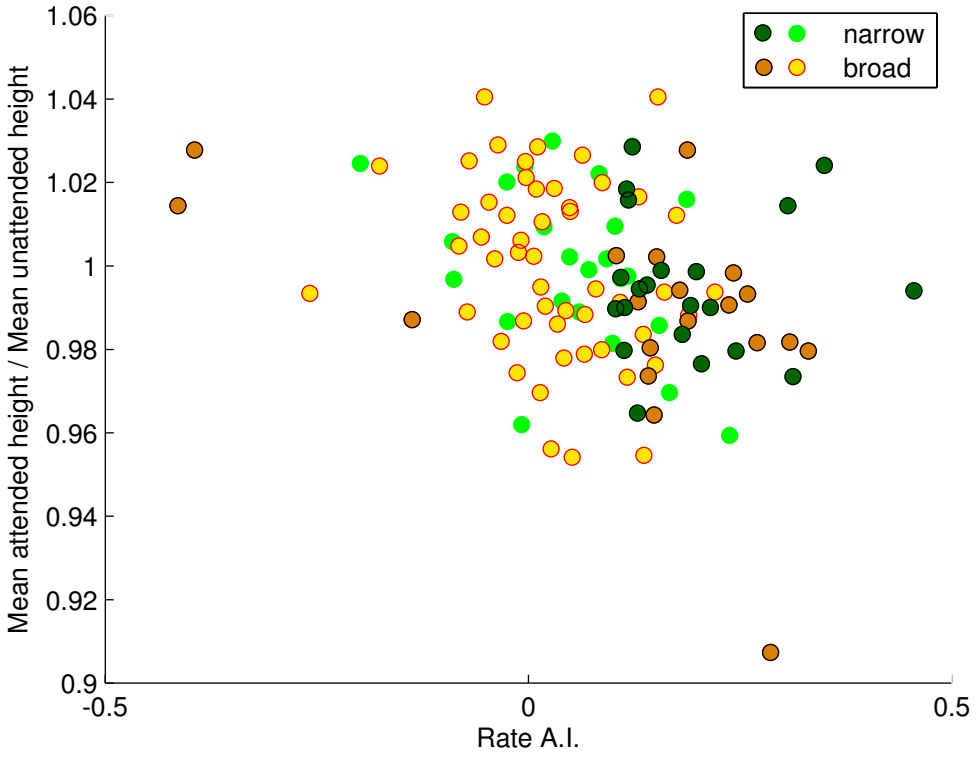

Figure 4.4: Correlation between attention-dependent increases in firing rate and attention-dependent reduction in mean normalized height
Scatterplot of rate A.I. and the ratio of the mean normalized action potential height in the attended condition with the mean normalized action potential height in the unattended condition. Correlation significant among all neurons (Spearman's non-parametric correlation, $p < 0.001$, R_s = -0.33), broad spiking neurons ($p < 0.01$, R_s = -0.36), and marginally among narrow spiking neurons ($p = 0.057$, R_s = -0.30). Orange circles correspond to broad spiking neurons; green circles correspond to narrow spiking neurons. Darker colors are neurons that individually showed significant attention-dependent rate modulation (Mann U Whitney test, $p < 0.001$).

If this reduction in burst firing reflects an increase in somatic or dendritic depolarization, then we would expect that this depolarization would also give rise to a decrease in the height of action potentials in the attended condition. Preliminary evidence suggests that this is indeed the case. Across the population of broad spiking neurons that show a significant increase in rate with attention (N=15), there is a significant reduction in mean normalized action potential height (Wilcoxon signed rank test, $p < 0.0001$, attend median normalized height = 0.979, unattend median normalized height = 0.994). As shown in Figure 4.4, there is also a significant relationship between rate A.I. and the attention-dependent decrease in action potential height among broad spiking neurons and across the entire population (Spearman's non-parametric correlation, all neurons $p < 0.001$, R_s = -0.33, broad spiking neurons $p < 0.01$, R_s = -0.36).

Looking forward, further work is needed to dissect the mechanisms underlying this attention-dependent decrease in action potential height. In particular, an important question will be whether this decrease in height can be fully explained by the increase in spiking activity with attention, or whether additional mechanisms, such as changes in synaptic activity or neuromodulation, are needed. As a starting point, I compared the action potential height in the two attention conditions across matched preISI bins. As can be seen for an example neuron in Figure 4.5, spike height in the unattended condition is consistently taller than in the attended condition, even for matched preISIs. A similar trend is seen across the the population of broad spiking neurons that are significantly modulated by attention, as shown in Figure 4.6. (In future work, I plan to consider the contribution of longer timescale differences in spiking activity. Figure 4.7 illustrates a first glance in that direction, by using the height of the previous action potential as a proxy for the adaptation of the neuron at that previous timepoint.) However, regardless of the source of this increase in spike height adaptation across attention conditions, an increase in the degree of adaptedness could provide a novel mechanism for changes in discharge patterns, such as burst firing, across attentional state.

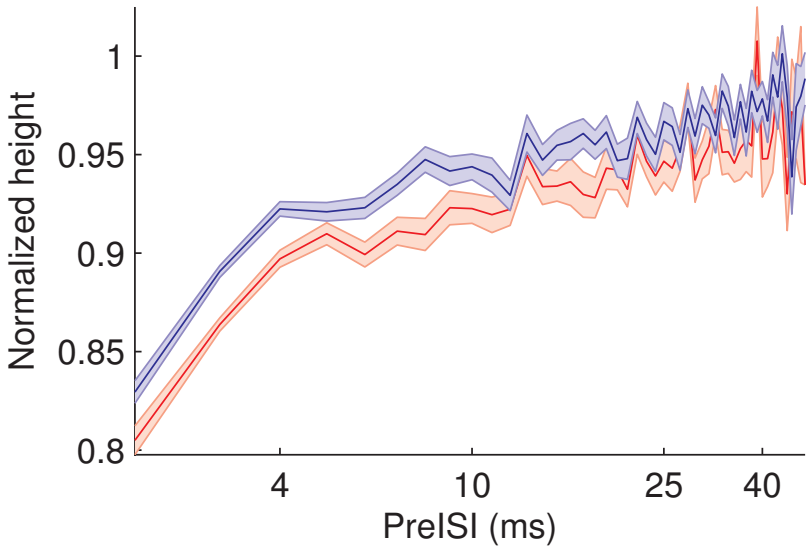

Figure 4.5: Action potentials in the unattended condition are taller than in the attended condition for matched preISIs for example neuron mzir76_u1
Relationship between preISI and action potential height across the two attention conditions for example neuron mzir76_u1. Red lines correspond to the attended condition, blue to the unattended condition. Shaded regions correspond to +/- 1 SEM, binsize 1 ms.

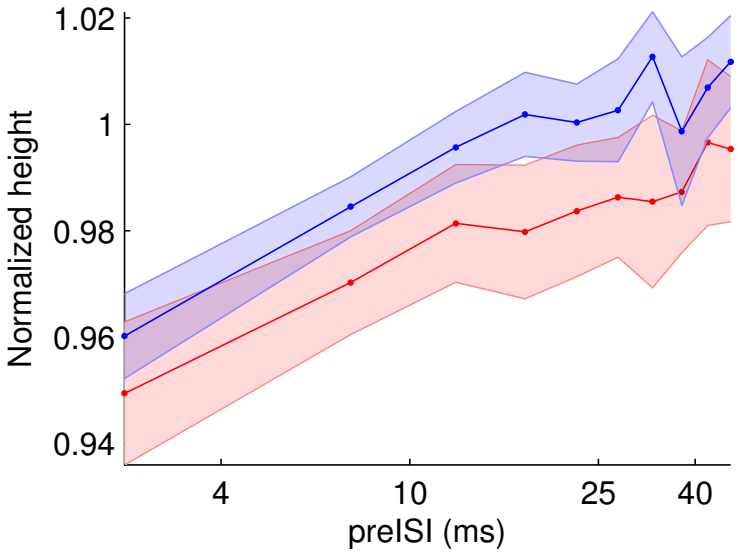

Figure 4.6: Among broad spiking neurons with significant increases in rate with attention, action potentials in the unattended condition are taller than in the attended condition for matched preISIs
Relationship between preISI and action potential height across the two attention conditions, averaged across broad spiking neurons with a significant increase in firing rate with attention. Red lines correspond to the attended condition, blue to the unattended condition. Shaded regions correspond to +/- 1 SEM, binsize 5 ms.

Figure 4.7: Spikes are taller in the unattended condition than attended condition for example neuron mzir76_u1, across conditions matched in preISI and the height of the previous action potential

(facing page)

A: Histogram of the height of preceding action potentials. Dashed lines indicate 1 STD from the mean. Black bars correspond to action potentials shorter than 1 STD of the mean, cyan bars action potentials within 1 STD of the mean, and red bars correspond to action potentials taller than 1 STD of the mean. *B:* Scatterplot of preISI vs the normalized spike height. Red dots correspond to action potentials where the previous action potential was taller than 1 STD of the mean, black dots correspond to action potentials where the previous spike was shorter than 1 STD of the mean. Lines correspond to mean relationship between spike height and preISI for the three groups of previous action potential heights. Error bars correspond to +/- 1 SEM, and bins correspond to those introduced in Figure 3.1. *C:* Spikes are taller in the unattended condition, for conditions matched in preISI and previous spike height. Red lines correspond to action potentials where the previous action potential was taller than 1 STD of the mean, cyan lines correspond to action potentials where the previous action potential was within 1 STD of the mean, and black lines correspond to action potentials where the previous action potential was less than 1 STD of the mean. Solid lines correspond to action potentials elicited in the unattended condition, and dashed lines correspond to action potentials elicited in the attended condition. Error bars correspond to +/- 1 SEM, and bins correspond to those introduced in Figure 3.1.

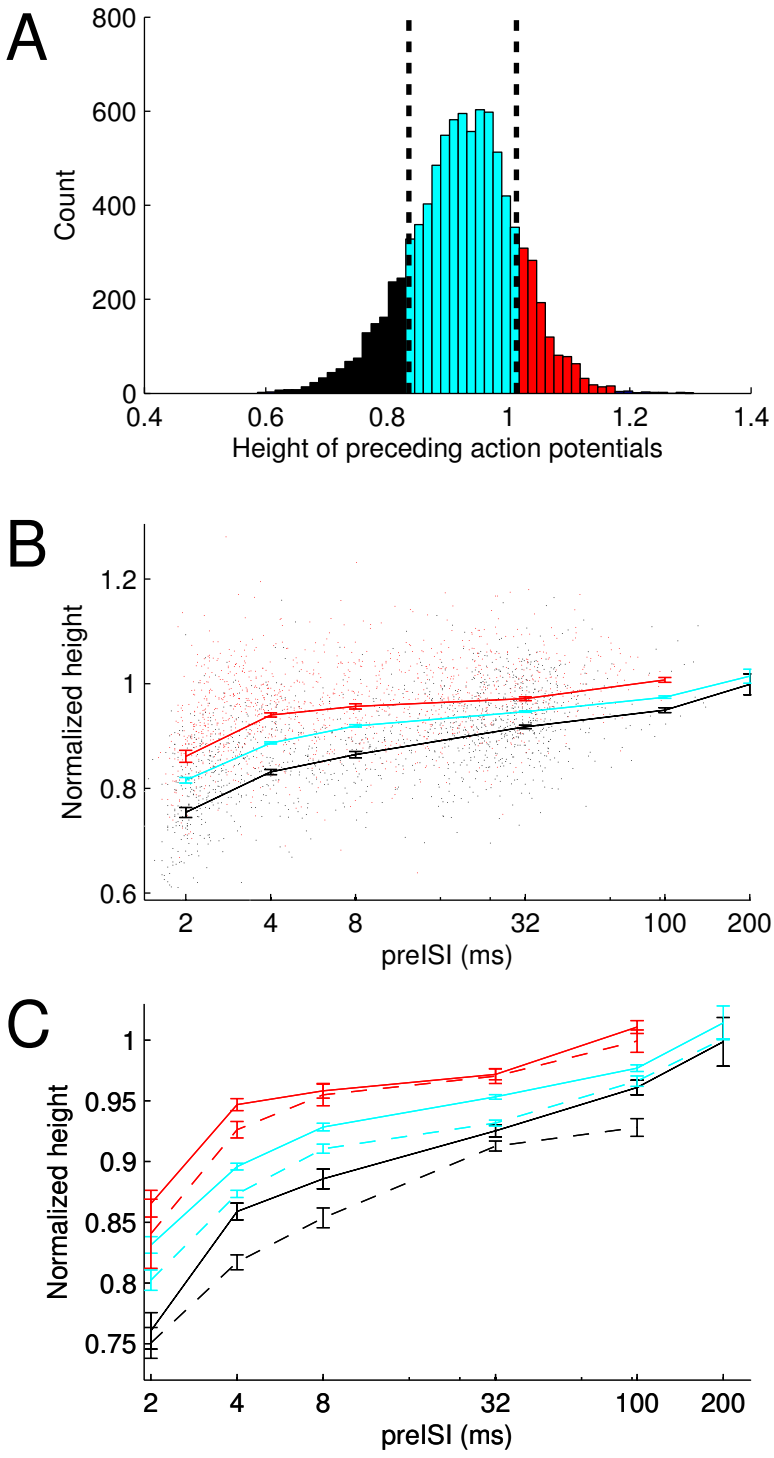
A
800
600
400
200
0
Count
0.4
0.6
0.8
1
1.2
1.4
Height of preceding action potentials
B
1.2
1
0.8
0.6
Normalized height
2
4
8
32
100
200
preISI (ms)
C
1
0.95
0.9
0.85
0.8
0.75
Normalized height
2
4
8
32
100
200
preISI (ms)

4.2 Conclusion

The primary goal of this dissertation was to work towards connecting electrophysiological correlates of attentional state in Area V4 to an understanding at the level of the cortical circuit. A major component of this effort was directed towards linking extracellular signals recorded in Area V4 to specific classes of neurons. To accomplish this goal, I considered aspects of the extracellular signal that are frequently overlooked in primate physiology studies: action potential shape, spike adaptation, and burst firing. Since differences in waveform shape and spiking statistics reflect differences in channel expression across different populations of neurons, characterizing these properties allowed me to make inferences regarding neuron identity and begin to account for heterogeneity in attentional modulation within the population.

In **chapter 2**, my coauthors and I characterized the tendency of neurons in macaque Area V4 to fire bursts of action potentials. We observed considerable variability in burst firing across the population, spanning the gamut of neurons that that fire in a manner similar to a refractory-limited Poisson process to neurons that fire numerous bursts of action potentials. The range of burstiness was particularly pronounced among broad spiking neurons (putative pyramidal neurons), which on average were significantly more bursty than the narrow spiking neurons (putative fast-spiking inhibitory interneurons). We did not, however, find evidence for distinct classes of neurons based on their tendency to fire bursts of action potentials.

We next considered whether this variability in burstiness could help account for the marked heterogenity in attentional modulation of firing rate previously reported in Area V4 (Mitchell et al., 2007). We found that the relationship between burstiness and attentional modulation varied between the narrow and broad spiking neurons. Within the narrow spiking population, burstiness did not vary with attentional modulation, while within the broad spiking population, we found a significant positive correlation between the degree of burstiness and the magnitude of attention-dependent rate modulation. Further, among bursty broad spiking neurons, attention caused a significant median increase in firing rate, as compared to

a non-significant change among non-bursty broad spiking neurons. Among bursty broad spiking neurons, all neurons showing individually significant rate modulation with attention showed increases in mean rate, while among non-bursty broad spiking neurons, attention caused both increases and decreases in mean rate. Across our population, significant decreases in firing rate with attention were thus restricted to non-bursty broad spiking neurons. These results therefore lead to the conclusion that variation in the degree of burstiness helps account for the wider range of attentional modulation among broad-spiking neurons, as compared to narrow-spiking neurons.

In **chapter 3**, I characterized spike amplitude, duration, and frequency adaptation among the broad and narrow spiking populations. To my knowledge, this dissertation presents the first characterization of spike amplitude, duration, and frequency adaptation in vivo in the primate. Consistent with the hypothesis that narrow spiking neurons largely correspond to FS interneurons, I found significantly less spike amplitude and frequency adaptation among these neurons than among the broad spiking population.

In future work, I hope that the ability to characterize spike adaptation extracellularly will provide a means for examining the internal state of individual neurons across behavioral conditions, and ultimately provide insight into the mechanisms that give rise to the electrophysiological correlates of attention. The results presented in **section 4.1** represent an initial effort in that direction. In that section, I present evidence suggesting that one source of attention-dependent reductions in variability is a reduction in the burstiness of broad spiking neurons. Future work is needed to establish whether the reduction in burstiness I observe represents an independent component of variability reduction with attention, or whether it reflects changes in low-frequency oscillations in firing rate. However, I propose that this reduction in burstiness could reflect an overall increase in depolarization with attention. I also present corroborating evidence for an increase in depolarization with attention, in the form of an attention-dependent decrease in spike height.

To conclude, the results presented here provide evidence that differences in the excitability of individual neurons, potentially arising from differences in

channel expression or from differences in synaptic input, can lead to differences in burst firing, spike adaptation, and attentional modulation in macaque Area V4. The more detailed characterization of neuron response properties used here provides a technique for explaining heterogeneity that is often present in extracellular population data, and can provide insight into the identity of individual neurons. Such an approach is especially important in the context of extracellular recordings in the primate cortex, where heterogeneity in population responses is often dismissed as noise. Further work will be needed to uncover the source of the differences in excitability reported here, and to determine the downstream impact of these attention-dependent changes in discharge patterns.

Some of the material presented in this chapter and in chapter 3 may be prepared for submission for publication. Anderson EB, Mitchell JF, Reynolds JH. The dissertation author was the primary investigator and author of this material.

4.3 References

Mitchell JF, Sundberg KA, Reynolds JH (2007) Differential attention-dependent response modulation across cell classes in macaque visual area V4. Neuron 55:131-141.

Mitchell JF, Sundberg KA, Reynolds JH (2009) Spatial attention decorrelates intrinsic activity fluctuations in macaque area V4. Neuron 63:879-888.

Steriade M, Amzica F, Nunez A (1993) Cholinergic and noradrenergic modulation of the slow (approximately 0.3 Hz) oscillation in neocortical cells. J Neurophysiol 70:13850-1400.

Steriade M, Timofeev I, Dürmüller N, Grenier F (1998) Dynamic properties of corticothalamic neurons and local cortical interneurons generating fast rhythmic (30-40 Hz) spike bursts. J Neurophysiol 79:483-490.

Steriade M, Timofeev I, Grenier F (2001) Natural waking and sleep states: a view from inside neocortical neurons. J Neurophysiol 85:1969-1985.

Wang Z, McCormick DA (1993) Control of firing mode of corticotectal and corticopontine layer V burst-generating neurons by norepinephrine, acetylcholine, and 1S,3R-ACPD. J Neurosci 13:2199-2216.